ISOLATION AND CHARACTERIZATION OF DIARYL ESTER CATABOLIZING SOIL FUNGI

by

Volante Moonsamy

Student number: 213506413

Submitted in fulfilment of the academic requirements for the degree of Master of Science in Microbiology

Discipline of Microbiology
School of Life Sciences
College of Agriculture, Engineering and Science
University of KwaZulu-Natal
Pietermaritzburg
South Africa

19 July 2019

Supervisor: Professor Stefan Schmidt

PREFACE

The research contained in this dissertation was completed by the candidate while based in the Discipline of Microbiology, School of Life Sciences, College of Agriculture, Engineering and Science, University of KwaZulu-Natal, Pietermaritzburg, South Africa. The candidate received a bursary from DAAD-NRF.

Signed: Professor S. Schmidt

Date: 19 July 2019

DECLARATION: PLAGIARISM

I, Volante Moonsamy, declare that:

(i) The research reported in this dissertation, except where otherwise indicated or acknowledged, is my original work;

(ii) This dissertation has not been submitted in full or in part for any degree or examination to any other university;

(iii) This dissertation does not contain other persons' data, pictures, graphs or other information, unless specifically acknowledged as being sourced from other persons;

(iv) This dissertation does not contain other persons' writing, unless specifically acknowledged as being sourced from other researchers. Where other written sources have been quoted, then:

a) Their words have been re-written but the general information attributed to them has been referenced;

b) Where their exact words have been used, their writing has been placed inside quotation marks, and referenced;

(v) This dissertation does not contain text, graphics or tables copied and pasted from the Internet, unless specifically acknowledged, and the source being detailed in the dissertation and in the References sections.

Signed: Volante Moonsamy

Date: 19 July 2019

ABSTRACT

Aromatic hydrocarbons are major organic pollutants that can persist in the environment. However, many fungi and yeasts can utilize these compounds as carbon and energy sources under aerobic conditions. Salol and benzyl salicylate are diaryl ester biocides exhibiting endocrine-disrupting properties. Using mineral salts medium containing salol and benzyl salicylate as sole carbon and energy source, aerobic enrichment cultures were established by inoculation with soil samples collected from a local animal farm and Bisley Nature Reserve Pietermaritzburg, KwaZulu-Natal. A salol utilizing fungal isolate and a benzyl salicylate utilizing yeast isolate were selected after enrichment. The fungal and yeast isolate were provisionally assigned to the genus *Fusarium* and *Trichosporon,* based on phenotypic characteristics and the sequence analysis of the ITS1-5.8S rRNA-ITS2 region. Growth kinetics of the fungus were assessed by measuring the dry weight of the biomass over time in batch cultures; the growth of the yeast was assessed via OD_{600} determinations and verified via microscopic cell counts. Appropriate abiotic controls showed that the concentration of tested aromatic pollutants remained stable over time while no biomass formed in biotic controls without added carbon source. Salol and benzyl salicylate utilization was verified by measuring the Chemical Oxygen Demand (COD) and UV-Vis spectra over time. COD measurements and UV spectroscopy indicated that up to 10 mM salol was catabolized completely by *Fusarium* sp. strain VM1 within 10 days while *Trichosporon* sp. strain VM2 catabolized 10 mM benzyl salicylate almost quantitatively. Specific enzyme activity determinations showed that both esterase and catechol-1,2-dioxygenase were induced by growth on salol and benzyl salicylate, indicating that the catabolism of diaryl esters is initiated by hydrolysis of the ester-linkage and the monoaromatic hydrolysis products were further metabolized via catechol and the *ortho*-pathway. These results indicate that members of the genus *Fusarium* and *Trichosporon* present in South African soils have the potential to eliminate diaryl esters and simple monoaromatic pollutants.

Keywords: Aerobic catabolism; Diaryl esters; Soil fungi; Nature reserve; *Ortho*-pathway

ACKNOWLEDGEMENTS

I would like to thank God for His strength and guidance. He has given me the spiritual assistance required to complete my dissertation.

My deepest gratitude is expressed to my supervisor, Professor Stefan Schmidt, for his patience and guidance which has made this research possible.

I would like to thank my fellow colleagues for their support and words of encouragement which helped me persevere. I would also like to thank the Microbiology staff at UKZN for their support.

I would greatly like to thank my parents for their love and patience. My deepest appreciation is expressed to my father for his undying support. You have allowed me the opportunity to come this far in life. No words can express what you have done for me.

My utmost appreciation is conveyed to Nongcebo Memela for her generous contribution to my dissertation and I would like to acknowledge the Deutscher Akademischer Austauschdienst (DAAD) via the National Research Foundation for funding my Master's degree.

LIST OF ABBREVIATIONS USED IN DISSERTATION

- MSM = Mineral Salts Medium
- COD = Chemical Oxygen Demand
- PDA = Potato Dextrose Agar
- NA = Nutrient Agar
- OD_{600} = Optical Density at 600nm
- BSA = Bovine Serum Albumin
- UV-Vis = Ultraviolet-visible
- BCF = Bioconcentration factor
- pH = Pondus hydrogenii

TABLE OF CONTENTS

LIST OF FIGURES

LIST OF TABLES

CHAPTER 1: LITERATURE REVIEW

1.1. Introduction

Aromatic hydrocarbons are major organic pollutants due to their ability to persist in the environment (Daane *et al.,* 2001) and are problematic due to their carcinogenic, toxic and mutagenic properties (Menzie *et al.,* 1992) as well as their ability to bioaccumulate in many aquatic organisms (Lotufo, 1998). However, many bacteria and fungi can utilize these compounds as carbon and energy sources under aerobic conditions (Ghosal *et al.,* 2016; Dagley, 1971). In fact, these microorganisms are therefore of importance to researchers working on the elimination of environmental pollution due to such aromatic pollutants (Van Hamme *et al.,* 2003; Atlas & Cerniglia, 1995). The metabolic pathways for the aerobic catabolism of simple monoaromatic hydrocarbons are well-known for bacteria and fungi (Prenafeta-Boldú *et al.,* 2006; Middelhoven, 1993).

The fate of organic pollutants in the environment is governed by abiotic and biotic factors including bioaccumulation, photooxidation, microbial transformation and volatilization (Ghosal *et al.,* 2016, Golovleva *et al.,* 1990). However, microbial transformation has been reported as the most important factor for the removal of aromatic hydrocarbons (Cerniglia, 1993). One source of pollutant degraders are soil microbes since the rhizosphere soil microbial community comprises of various microorganisms representing different metabolic types that can adapt to environmental changes (Daane *et al.,* 2001). Soil environments such as nature reserves are naturally rich in lignin and due to the added faecal matter from herbivores that comprise of large amounts of plant material that can be broken down further into aromatic compounds such as phenolic acids, polyphenols and tannins serve as an ideal place to isolate pollutant degraders (Song, 2009; Henderson and Farmer, 1955; Henderson, 1961a). Lignin, when catabolized or transformed would result in moieties similar in structure to diaryl esters owing to its complex aromatic nature (Henderson, 1961b). Therefore, lignin rich environments are potential reservoirs for microorganisms with specialized enzymes that can catabolize aromatic hydrocarbons (Kirk *et al*., 1987; Have and Teunissen, 2001).

Benzyl salicylate and phenyl salicylate (also known as salol) have applications in the pharmaceutical industry for their antimicrobial properties (Dongwei *et al.,* 2009). However, these biocides also exhibit endocrine-disrupting properties (Caliman and Gavrilescu, 2009; Ying and Kookana, 2003). Although there is limited research pertaining to the microbial catabolism of these diaryl esters, Clauβen and Schmidt (1999) reported that the simplest diaryl ester, phenyl benzoate, can be mineralized by the hyphomycete, *Scedosporium apiospermum.* These researchers have also reported that the initial point of attack was the ester-linkage in phenyl benzoate. Therefore, due to the structural similarity of the diaryl esters – benzyl salicylate and salol – in comparison to phenyl benzoate, the expected initial point of attack would be the ester-linkage in these diaryl esters (Clauβen and Schmidt, 1999; Göttsching and Schmidt, 2007). The resultant monoaromatic hydrolysis products, phenol, salicylate, benzyl alcohol and benzoate can be further mineralized by diverse microorganisms under aerobic conditions (Clauβen and Schmidt, 1998; Silva *et al.,* 2007; Göttsching and Schmidt, 2007).

1.2. Nature reserves as a reservoir for organic pollutant degraders

Nature reserves are a habitat for mammalian herbivores, which are the most abundant feeding group within the mammals (Kohl *et al*., 2014). They play critical roles in shaping the ecosystem structure and serve as essential resources to humans as game (Kohl *et al*., 2014). The herbivore gut system is stable and at the same time a dynamic environment for microorganisms (Kamra, 2005). This particular ecosystem is stable as it is temperature and pH controlled and can bioconvert feed into volatile fatty acids (Kamra, 2005). In addition, it provides adequate mixing and substrate supply (Kamra, 2005). At the same time, it is dynamic since the microbial population changes considerably with changing diet when adapting to new feed (Steward *et al*., 1992; Odenyo *et al*., 1994). Some of the gut microbes produce antimicrobial compounds, such as gallotannins and polyphenols, many of which are similar in structure to aromatic pollutants such as diaryl esters. These antimicrobial compounds limit the growth of other microbes present in the ecosystem therefore making the herbivore gut highly selective for microorganisms with specialized enzymes that have the potential to catabolize organic pollutants (Steward *et al*., 1992; Odenyo *et al*., 1994).

Tolerance to plant secondary compounds determines the dietary niche of mammalian herbivores (Dearing *et al*., 2000; Moore and Foley, 2005). Since their diet consists of organic polymers with a large percentage of proteins, non-lignin carbohydrates, fats and lignocellulosic plant material (Kamra, 2005), hydrolytic enzymes are essential for the utilization of the organic polymers (cellulose, starch or lignocellulose) as carbon and energy sources (Ndlela and Schmidt, 2016). Hydrolytic enzymes of microbial origin have economical potential since they are biocatalysts that have the ability to break covalent bonds by using water as a co-substrate. Therefore, they can be applied in industrial processes such as biofuel production where cellulosic material can be transformed into glucose, the production of food and beverage and the degradation and recycling of organic waste (Ndlela and Schmidt, 2016). Aside from cellulases, three other major groups of hydrolases – which include esterases, amylases and proteases – are used in industrial processes (Kirk *et al.,* 2002).

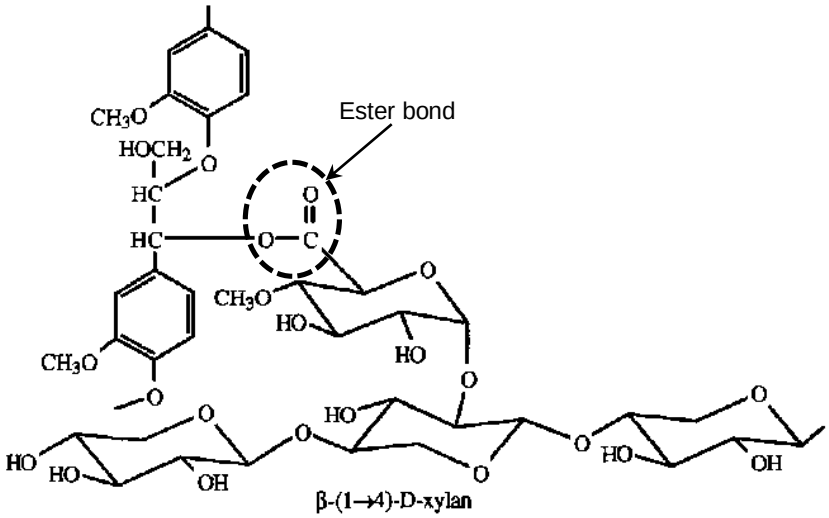

Figure 1.1: Natural ester features related to lignin

Lignin is a complex polymer of aromatic moieties, even sporting ester bonds (Figure 1.1). It is difficult to catabolize since it lacks the standard repeating covalent bond (Song, 2009) and the biological degradation of this polymer is not fully understood (Rodriguez *et al.,* 1997). Fungi play a major role in the biodegradation of lignin due the production of extracellular enzymes such as laccase, lignin peroxidase and manganese peroxidase (Kirk and Farrell, 1987; Have and Teunissen, 2001). These enzymes allow the destabilization of the lignin structure by forming radicals, which

allow the macromolecule to be broken down (Song, 2009). An example of a possible hydrolysis product of lignin is shown in Figure 1.2, which still contains an ester linkage. The catabolism of lignin by bacteria has not been well characterized since they are mostly unable to perform the initial depolymerization step required to biodegrade lignin (Kirk and Farrell 1987). However, bacteria have the ability to utilize aromatic monomers derived from the fungal biodegradation of lignin (Kirk and Farrell, 1987; Wackett and Ellis, 1999).

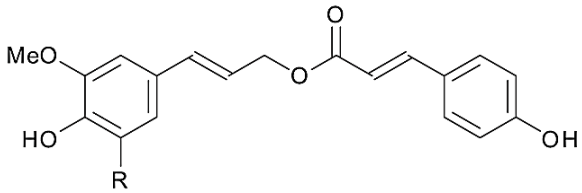

R=H; coniferyl *p*-coumarate
R=OMe; sinapyl *p*-coumarate

Figure 1.2: Lignin sub-structure with an ester bond

Aromatic compounds are not alien in nature. Aromatic amino acids such as phenylalanine and tyrosine are found freely in the environment as well as in herbivore faeces. A study by Khan *et al.* (2002) showed that considerable amounts of phenylpropionic acid, phenyllactic acid and phenylpyruvic acid were produced from rumen bacteria found in goats when the aforementioned amino acids were fermented. Skatole, also known as 3-methylindole, is a mildly toxic organic compound that occurs naturally in faeces since it is produced from tryptophan in the mammalian digestive tract (Brieger, 1878). Therefore, the gut community generates in addition to the simple aromatic compound phenol, a plethora of phenolics. It is therefore possible that nature reserves receiving mammalian herbivore faeces containing large quantities of such compounds can select for soil fungi that can catabolize diaryl esters or similar compounds.

1.3. Diaryl esters as environmental pollutants

Diaryl ester compounds are characterized by two aromatic rings interconnected by an ester linkage. Ester linkages are present in many industrially manufactured organic compounds of environmental concern such as solvents, polymers, pesticides and pharmaceutical compounds (Reich *et al.,* 1999). A large number of

microorganisms with the ability to hydrolyze ester bonds in relevant environmental pollutants have been reported (Golovleva *et al.,* 1990; Cameron *et al.,* 1994; Maloney *et al.,* 1988); however, there is limited information on the microbial catabolism of diaryl esters such as benzyl salicylate and phenyl salicylate (Reich *et al.,* 1999). The following are the uses of the aforementioned diaryl esters:

- Phenyl salicylate: Phenyl salicylate, also known as salol, has an ester linkage connecting the two benzene rings of phenol and salicylic acid (Figure 1.3). It is synthesized by heating phenol and salicylic acid in the presence of a catalyst such as sulfuric acid, hydrochloric acid or sulfonic acid. It is a white crystalline powder with ultra-violet light absorbing properties. It is therefore used in the manufacturing of polymers, lacquers, adhesives waxes, plastics and polishes. Its application extends to medical purposes since it has antibacterial properties. It is also used in detergents, cosmetic and household products (Dongwei et al., 2009).

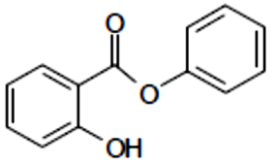

Figure 1.3: Phenyl salicylate (salol)

- Benzyl salicylate: Benzyl salicylate (Figure 1.4) is a diaryl ester with two benzene rings interconnected by an ester linkage. This compound is a clear liquid that is prepared by the esterification of benzyl alcohol and salicylic acid. The balsamic floral scent of this diaryl ester allows for its application in personal care products such as fine fragrances and toiletries (Belsito *et al*., 2007). In addition, its application extends to the use in household products such as detergents and food preservatives. It is also a naturally occurring constituent of essential oils from plants which include *Cananga odorata* (Belsito *et al*., 2007).

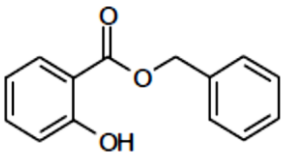

Figure 1.4: Benzyl salicylate

- Phenyl benzoate: Phenyl benzoate (Figure 1.5) is a diaryl ester of benzoic acid that is formed by the reaction between phenol, sodium hydroxide and benzoyl chloride. It is the simplest diaryl ester that is found in industrial effluents since it is used to produce plastics, perfumes and insecticides (Clauβen and Schmidt, 1999). This diaryl ester is produced on an industrial scale since its importance lies in the production of liquid-crystalline polymers for the use in electro-optical devices such as LCD-displays (Krücke *et al.,* 1985). The benzene rings in this thermotropic liquid-crystalline polymer are interconnected by ester linkages (Chang *et al.,* 1996).

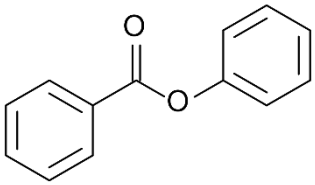

Figure 1.5: Phenyl benzoate

- Phenylacetate: Phenylacetate (Figure 1.6), a phenyl ester, is formed by the reaction between phenol and acetic anhydride. It is a clear colourless liquid that has a fragrant odour therefore it is used to flavour food. This phenyl ester also occurs naturally in mammals since it is an aromatic amino acid metabolite of phenylalanine and exhibits antineoplastic activity (Piscitelli *et al.,* 1995).

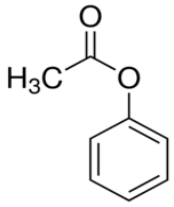

Figure 1.6: Phenylacetate

These man-made pollutants are not per se alien to nature since their chemical structures are similar to those occurring naturally. Hence, microorganisms present in soil, water and sediments will have evolved enzymes to catabolize such pollutants if they have previously been exposed to identical or similar structures (Schmidt, 2002). A review by Schmidt (2002) suggests that there is evidence of diaryl esters of biological origin present in the environment since gallotannins isolated from *Rhus javanica, Haematoxylon campechianum*, and *Ceratonia siliqua* are known to contain diaryl ester structures, which correspond to the simple diaryl ester, phenyl benzoate, and its derivatives. Xanthones are organic phytochemical compounds found in plant families such as *Bonnetiaceae, Clusiaceae* and *Podostemaceae* that contain the phenyl salicylate moiety (Chase and Reveal, 2009). Xanthones are also synthesized by fungi, lichens and bacteria (Masters and Bräse, 2012). Diaryl esters containing the phenyl benzoate moiety are also synthesized by fungi and lichens and these compounds act as herbivore deterrents, a chemical defense for lichens against microbial attack and as chelating agents to acquire micronutrients (Schmidt, 2002).

1.4. Ecotoxicology of salicylate esters

More than 100 000 chemicals exist on the market (Batran, 2014) and a broad range of these chemicals include organic substances (Wu *et al.,* 2000); however as much as these substances are an integral part of the modern life, they also pose a global problem. These organic substances often appear in discharges such as sewage, stormwater and industrial effluents and although their concentrations may be low, their volume is large therefore making it a major source of organic pollutants (Wu et al., 2000). Urban and industrial effluents often lead to soil contamination and contamination of adjacent groundwater and rivers. However, sediment quality is crucial to the health of an aquatic ecosystem (Davoren *et al.,* 2005). As organic pollutants have the ability to physically and chemically bind to sediments, they accumulate and become bioavailable and this has potentially adverse effects on aquatic organisms (De Castro-Catala *et al.,* 2016). Organic pollutants in personal care products have a specific biological activity at low concentrations, which causes a physiological response. Thus, effects including non-desirable activities such as endocrine-disrupting properties are expected even at low concentrations. Therefore,

they are required to undergo regulatory processes before they are made available to the public (Christen *et al.,* 2010).

Phenyl salicylate, also known under the trade name salol, is a known skin irritant but it is not carcinogenic or mutagenic (Fimiani *et al.,* 1990). The ecological toxicity assessment showed that phenyl salicylate has a lethal concentration (LC_{50}) of 0.99 to 1.2 mg/L (96-h) on freshwater fish, *Pimephales promelas* and its acute toxicity indicates that the lethal dose (LD_{50}) is 3.0 g/kg for rats orally and greater than 5.0 g/kg for rats dermally (Belsito *et al.,* 2007). This compound has been shown to be toxic to the reproductive organs of the male rat and causing death of the rat fetus. However, there is no indication that the compound causes cancer, birth defects or reproductive harm to humans (Kristensen *et al.,* 2010).

Benzyl salicylate, like salol, is known to be a skin irritant but does not exhibit carcinogenic and mutagenic properties (Zhanga *et al.,* 2012). However, when the estrogenic potential of benzyl salicylate was tested using an in vitro human estrogen receptor, benzyl salicylate exhibited higher estrogenic activity than bisphenol A (Charles and Darbre, 2009). This compound was also shown to be toxic to the reproductive organs of mice and rats by significantly increasing the uterine weights of immature rodents when treated with ~100 mg/kg/day benzyl salicylate for 3 days (Hashimoto *et al.,* 2003). Ecotoxicity studies indicated that benzyl salicylate has a lethal concentration (LC_{50}) of 2.0 mg/L for zebra fish (*Danio rerio*) (Hashimoto *et al.,* 2003).

Salicylate esters have antibacterial properties and long-term use may lead to less diverse microbial communities or alter the morphology and physiology of microbes leading to increased virulence or even antibiotic resistance of pathogens. Belsito *et al.* (2007) and Lapczynski *et al*. (2007) indicated that phenyl salicylate and benzyl salicylate are similar to other salicylate esters and can be hydrolyzed by carboxyl esterase. The hydrolysis takes place in the intestine under alkaline conditions where the diaryl ester is broken down into phenol and salicylic acid for salol and benzyl alcohol and salicylic acid for benzyl salicylate. However, salicylic acid is metabolized by the liver and conjugated compounds are excreted together with phenol and benzyl alcohol in the urine (Fishbeck *et al.,* 1975; Nair, 2001).

Salicylic acid is toxic to aquatic organisms, inducing morphological and physiological changes by influencing their metabolism and respiratory processes. Salicylic acid has a LC_{50} of 112 mg/L (48-h) for *Daphnia magna* and the half effective concentration (EC_{50}) for algae was greater than 100 mg/L (48-h) (Camacho-Muñoz et al., 2010). In the case of phenol, fish were reported to be the most sensitive with the LC_{50} for guppies (*Poecilia reticulate*) being ony 460 µg/L (96-h) and the water flea, *Ceriodaphnia dubia,* has a LC_{50} of 3.1 mg/L (96-h) (Lepper *et al.*, 2007). Phenol is toxic to humans via oral exposure leading to weight loss, vertigo and anorexia. It is a reproductive toxin that causes increased risk of abortion and low birth weight. The lethal dose is 50 to 500 mg/kg for rats whereas the lethal dose is 300 to 500 mg/kg for dogs and rabbits (Department of Health and Human Services, 2015; World Health Organization and International Programme on Chemical Safety, 1994; EFSA CEF Panel, 2013). Benzyl alcohol is a skin irritant at levels greater or equal to 3% (Nair, 2001). Infant neonates, when exposed to benzyl alcohol, showed gradual neurological deterioration, renal failure, cardiovascular collapse and death (Lebel *et al.*, 1988). Neurological disorders for male and female rats were observed for 800 mg/kg and 200 mg/kg of oral doses of benzyl alcohol respectively (Lebel *et al.*, 1988). The presence of these toxic compounds in the environment therefore poses potential harm to natural ecosystems (Price *et al.,* 2000).

1.5. Abiotic fate of diaryl esters in the environment

Organic pollutants in the environment have a tendency to undergo abiotic processes such as volatilization, photochemical degradation, hydrolysis and bioaccumulation in sediments and animal tissue, which determines their effect on the environment (De Castro-Català *et al.,* 2016).

1.5.1. Volatilization

Volatilization occurs when organic compounds are vaporized; this can be beneficial to the environment since the concentration of the pollutant will be effectively reduced. Spencer and Ciath (1973) determined that the rate of volatilization from soil is controlled by the rate of movement of the organic chemical to the soil surface, by

mass flow in water and by diffusion. Volatilization is related to low aqueous solubility and this process is limited to compounds with high vapour pressure since under normal temperature, they are volatile (Spencer *et al.,* 2009). Phenyl salicylate has a melting point of ~42°C, an approximate water solubility of 0.15 g/L at 20°C and a negligible vapour pressure of 6.27 x 10^{-5} mm Hg at 25°C while benzyl salicylate has a water solubility of ~0.15 mg/L at 20°C and a vapour pressure of less than 10^{-3} mm Hg at 25°C (Belsito *et al.*, 2007). Therefore, volatilization of these compounds is not of concern to the environment (Lapczynski *et al*., 2007) and volatilization will not remove these compounds from polluted environments.

1.5.2. Hydrolysis

Hydrolysis of organic compounds usually occurs in water since it depends on the concentrations of protons or hydroxyl ions or both under suitable pH conditions (Mill and Mabey, 1988). Since terrestrial environments are subjected to varying environmental conditions such as temperature, humidity and rainfall, the water content is not constant. Therefore, this process would be unfavourable in arid environments. However, extremely alkaline soil environments will promote ester hydrolysis (Carey, 1994). Base hydrolysis in soil releases ester-bound material, which represents a significant amount of organic matter and the organic matter that remains after base hydrolysis still contains 10-18% alkyl carbons (Rumpel *et al.,* 2005). Hydrolysis has a major influence on the removal of organic pollutants in aquatic environments (Mill and Mabey, 1988). Salicylate esters such as phenyl salicylate and benzyl salicylate are susceptible to hydrolysis due to the presence of the ester bond (Carey, 1994). Phenyl salicylate was found to have a half-life of 6.6 days at pH 6.3; however, it was stable at pH 4 while benzyl salicylate was found to have a hydrolysis half-life of 1.7 years at pH 7 and 63 days at pH 8 (Lyman *et al*., 1990). These compounds may be subjected to hydrolysis but their building blocks – phenol, benzoate and salicylic acid – are resistant to hydrolysis.

1.5.3. Photodegradation

Photodegradation is a chemical reaction that occurs under the influence of energy-rich photons (ultra-violet light) and takes place in the atmosphere and on the surface

of either soil or water but it does not occur in benthic sediments and deep layers of soil due to shading (Dąbrowska *et al.,* 2004). The majority of UV rays are absorbed in the surface water layer down to 2 meters in depth, allowing for the phototransformation of organic chemicals, photolytic cleavage of chemical bonds or the complete direct or indirect photolysis (Wu *et al.,* 2001). Direct photolysis is a process whereby molecules are oxidized due to excitation by the absorption of a photon but this process is limited to compounds that absorb light in the range of 290-750 nm (Dąbrowska et al., 2004), which is a typical feature of many aromatic compounds. UV radiation causes oxidizing compounds to be formed and reactive oxygen species or oxygen and hydroxyl radicals are capable of degrading organic pollutants (Mill, 1989). Indirect photolysis occurs through reactions with OH-radicals, ozone or nitrate ions. OH-radicals are responsible for the transformation of over 90% of organic compounds occurring in the gaseous phase of the troposphere (Zepp and Schlotzhauer, 1983).

The presence of microorganisms, algae or humic material accelerates photochemical reactions since these have the ability to absorb light (Dąbrowska *et al.,* 2004). Zepp and Schlotzhauer (1983) concluded that the majority of polycyclic aromatic hydrocarbons are photolyzed much faster in the presence of algae. No studies have been done on the photodegradation of salicylate esters but phenyl salicylate and benzyl salicylate are used as UV filter compounds, since they might be photostable (Kunz *et al.,* 2006). However, their constituents – phenol and salicylate – have the ability to undergo photochemical degradation as phenol reacts directly with hydroxyl radicals (Wu *et al.,* 2001). Salicylic acid has a photolysis half-life of 30 to 47 days (Vione *et al.,* 2003) and phenol has a photolysis half-life of 43 to 118 hours (Hwang *et al*., 1987).

1.5.4. Bioaccumulation

Bioaccumulation refers to the uptake and retention of compounds in living tissue usually at levels higher than in the surrounding environment and can lead to the exposure of organisms to high concentrations of potentially toxic compounds (Farré *et al.,* 2008). It occurs when an organism absorbs the contaminant at a faster rate than that at which the substance is metabolized or excreted. Persistent organic

pollutants (POPs) are such compounds that have the ability to bioaccumulate in food chains, exhibiting long-term adverse effects on humans and the environment (Scheringer *et al.,* 2012). It has been reported that POPs accumulate for a longer period in soil and sediment than in water since the adsorption of molecules, due to their affinity to other chemical components of the soil matrix or soil biosphere, protects them from chemical degradation and biodegradation because their bioavailability is reduced (Scheringer *et al.*, 2012). Essentially, the accumulation of pollutants in the soil is related to chemical attraction and bond strength, which is governed by a number of factors – Van der Waals forces, hydrogen bonding, ion exchange, charge transfer mechanisms, lipophilic affinity, entrapment and covalent reactions to humic acids (Wang *et al.,* 2011). In aquatic environments, where polar water molecules predominate, lipophilic pollutants that have an affinity for organic matter will always move to the biosphere or accumulate in sediments rich in organic matter (Connell, 1990).

Bioaccumulation is predominant for compounds with low water solubility, high molecular weight and high lipophilicity (Sharifi and Connell, 2003). A good parameter to evaluate preferential partition of pollutants between the soil and biosphere is to compare octanol/water (K_{ow}) ratios and to compare the bioconcentration factor of the contaminant (BCF) (Steen and Karickhoff, 1981). A BCF exceeding 1000 and a log K_{ow} above 5 indicates the ability of a compound to strongly accumulate in living tissue (Steen and Karickhoff, 1981), while the BCF of phenyl salicylate is 154 and the log K_{ow} 3.82, benzyl salicylate has a BCF of 320 and a log K_{ow} of 4.31 (Steen and Karickhoff, 1981), indicating moderate potential to bioaccumulate. Their constituents, salicylic acid, phenol and benzyl alcohol, have à much lower BCF of 3.16, 5.67 and 1.4 with log K_{ow} values of 2.26, 1.46 and 1.10 respectively (Lapczynski *et al*., 2007; Mackay and Fraser, 2000; Schultz, 1987). This indicates that bioaccumulation is expected even though not to a very large degree.

Organic pollutants are capable of undergoing abiotic removal or degradation but physicochemical processes are slow and the resultant products may be even more harmful to the environment. Therefore, mineralization of organic pollutants by microbial processes is the best option to eliminate such compounds from polluted environments.

1.6. Aerobic catabolism of aromatic compounds

Hydrocarbons are ubiquitous in nature, originating from biogenic and geological processes. Their chemical nature consists of forms ranging from simple alkanes to monoaromatic hydrocarbons and complex polycyclic aromatic hydrocarbons, making them extremely diverse. Stömer (1908) was the first researcher to demonstrate the ability of bacteria to utilize toluene and xylene. Since then, many microorganisms have been isolated with the ability to catabolize organic pollutants as carbon and energy sources. These microorganisms have adapted to mineralize aromatic compounds by means of diverse catabolic pathways (Farré *et al.,* 2008; Hedgespeth *et al.,* 2012).

Bacteria are the most studied microbes in the catabolism of aromatic hydrocarbons and the biodegradation of aromatic compounds by fungi has traditionally been considered to be cometabolic in nature (Dìaz, 2004; Seo *et al.,* 2009). However, studies are available showing that fungi are capable of utilizing simple aromatic hydrocarbons such as benzoate, salicylate and gentisic acids as sole carbon and energy source (Pinedo-Rivilla *et al.,* 2009; Anderson and Dagley, 1980). There are three major modes for the fungal hydrocarbon metabolism: partial transformation reactions, complete biodegradation of hydrocarbons in the presence of a second compatible substrate and independent utilization of hydrocarbons as sole carbon and energy source for growth (Prenafeta-Boldú *et al.,* 2006).

Partial transformation typically results from the activation of dioxygen, with one oxygen atom inserted into the substrate and the second atom reduced to water (Prenafeta-Boldú *et al.,* 2006). This is seen in the transformation of xenobiotics by fungi via the cytochrome-P450 monooxygenase enzyme system, resulting in hydroxylated compounds (Cerniglia *et al.,* 1992; van den Brink *et al.,* 1998). Cometabolic processes catabolized by fungi involve the conversion of aromatic compounds to carbon dioxide and water, which is typically seen in lignin-degrading white-rot fungi (Pinedo-Rivilla *et al.,* 2009). The catabolism of lignin results in generating growth supporting intermediates, cellulose and hemicellulose. Extracellular peroxidases, laccases and P-450 monooxygenases work

simultaneously to further metabolize the intermediates formed (Leonowicz *et al.,* 1999). Although lignin is ultimately mineralized, it does not serve as the sole substrate for the growth of white-rot fungi (Leonowicz *et al.,* 1999). Over the years, the number of fungal strains with the ability to utilize aromatic compounds in closed systems has increased (Jones *et* al., 1993; Pinedo-Rivilla *et al.,* 2009). However, there is currently only limited information available involving the utilization of diaryl esters by fungi as sole carbon and energy source for growth.

In view of complex polycyclic aromatic pollutants, fungal isolates such as *Coriolus versicolor, Trichoderma* sp., *Aspergillus niger* and *Fusarium* sp. were reported to utilize pyrene, while *Fusarium solani* even catabolized phenantrene (Pinedo-Rivilla *et al.,* 2009). Fungal strains also have the ability to utilize simple phenolic compounds such as *p*-cresol, phenol and benzoic acid (Jones *et* al., 1993; Wright, 1993; Henderson, 1961a). *Fusarium* sp. HJ01 utilized 65% of 200 mg/l phenol as the sole carbon and energy source (Sampedro *et al*, 2007) and Cox *et al.* (1993) demonstrated that *Exophiala jeanselmei*, *Clonostachys rosea*, and some *Penicillium* species were able to utilize styrene from biofiltration systems in a closed system. Other examples include the fungus *Panus tigrinus* CBS 557.79, that reduced the polluting load of olive-mill wastewater that had significant amounts of phenolic components (D'Annibale *et al.*, 2006).

1.6.1. Aerobic catabolism of simple aromatic compounds

In the presence of air, oxygenase systems are involved in activating and breaking down aromatic compounds (Hegeman, 1966). Catabolic pathways under aerobic conditions mostly converge at protocatechuate or catechol, which are further degraded via the β-ketoadipate pathway to succinyl-CoA and acetyl-CoA (Figure 1.7) or via meta-cleavage (Harwood and Parales, 1996; Stanier and Ornston, 1973). The oxoadipate pathway is widely distributed in soil bacteria and fungi (Harwood and Parales, 1996; Powlowski *et al*., 1985). Another catabolic sequence, called the gentisate pathway, can be used when aromatic hydrocarbons are converted into gentisate (Dagley, 1971). Some of the aromatic monomers derived from lignin biodegradation include protocatechuate, catechol, hydroquinone, phenylacetate, *p*-hydroxybenzoic acid, gentisate, pyrogallol, gallic acid and resorcinol (Dagley, 1971).

A study on the metabolism of lignin-related aromatic compounds by soil fungi showed that protocatechuic acid is an intermediate in the metabolism of vanillin and ferulic acid by *Pullularia pullulans* (Henderson, 1961a). Henderson and Farmer, (1955) and Henderson, (1960) verified that soil organisms were responsible for the metabolism of aromatic compounds where protocatechuic acid is the intermediate.

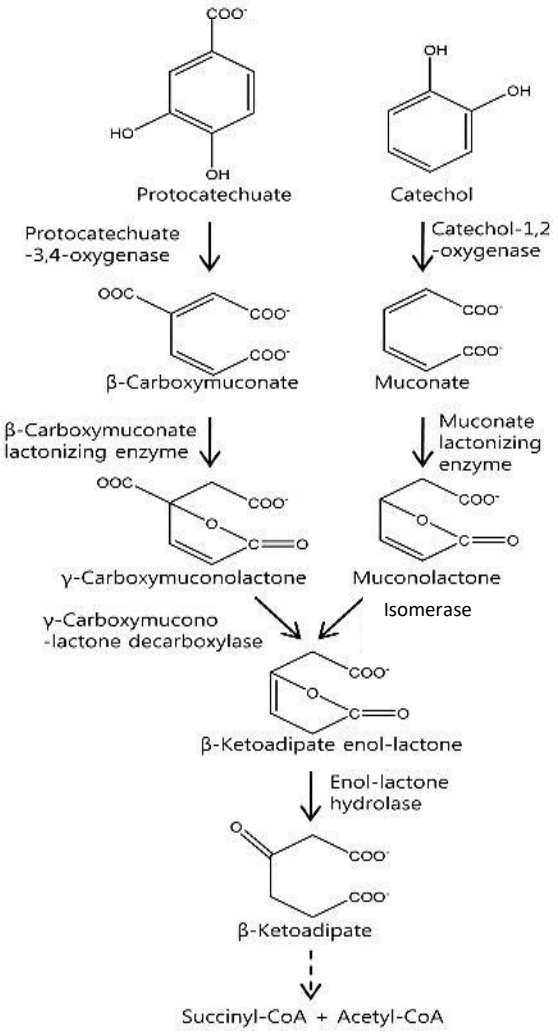

Figure 1.7: The β-ketoadipate pathway (adapted from Song, 2009)

1.6.2. Catabolism of diaryl esters

The simplest diaryl ester, phenyl benzoate, was utilized by a soil fungus (*Scedosporium apiospermum*) as the sole carbon and energy source under aerobic conditions (Clauβen and Schmidt, 1999). An inducible esterase with possible cysteine residues had the ability to cleave the ester-linkage in phenyl benzoate, yielding the metabolites phenol and benzoate (Clauβen and Schmidt, 1999). Another diaryl ester, benzylbenzoate, was hydrolytically cleaved by *Acinetobacter* sp. strain AG1 to yield benzoate and benzylalcohol (Göttsching and Schmidt, 2007). If salol and benzyl salicylate followed the same pathway as the aforementioned diaryl esters, the expected intermediates formed upon hydrolysis of the ester-linkage would be phenol, salicylic acid, and benzyl alcohol which can be further catabolized by fungi (Clauβen and Schmidt, 1998).

The microbial catabolism of salicylic acid was reported to follow typically two routes, the catechol and the gentisate pathway (Filonov *et al.,* 2000). The catechol pathway is initiated by salicylate-1-hydroxylase, decarboxylating salicylic acid to catechol, while the gentisate pathway is initiated by salicylate-5-hydroxylase and gentisic acid is formed from the hydroxylation of salicylic acid at C5 (Ishiyama *et al.,* 2004; Karegoudar and Kim, 2000; Dodge and Wackett, 2005). Phenol was reported to be catabolized by *Scedosporium apiospermum* via two possible routes. The first route involved catechol and 3-oxoadipate while the second route involved hydroquinone, 1,2,4-trihydroxybenzene, maleylacetate and 3-oxoadipate (Clauβen and Schmidt, 1998). Benzyl alcohol is further catabolized via benzaldehyde to yield benzoate, which is finally catabolized with aiding enzymes from the ortho-pathway via 3-oxoadipate (Göttsching and Schmidt, 2007).

1.7. Factors affecting the microbial catabolism of diaryl esters in the environment

The rate of biodegradation of organic pollutants in the environment is affected by a number of factors, which include environmental conditions and molecular properties of the compound. This, in turn, has an effect on the microorganisms involved in

biodegradation. Therefore, suitable factors are required to support the microbial activity responsible for biodegradation (Boopathy, 2000).

1.7.1. Molecular properties of the compound

The target molecule's physiochemical properties determine its potential to undergo microbial catabolism as well as the degree and rate of transformation according to the number, position and type of substituents present in the hydrocarbon. Leahy and Colwell (1990) reported that the rate of aerobic biodegradation is usually affected when the number of substituents is increased since this leads to a more complex hydrocarbon owing to the increased molecular weight. Electron drawing and electron donating substituents also affect the rate of biodegradation since they can inhibit or support an initial oxygenase attack. Cycloalkenes and aliphatic hydrocarbons with long chain lengths exceeding C20 are reported to be resistant to biodegradation (Baek *et al.,* 2006) and only a restricted number of microorganisms has the ability to mineralize these compounds. The aromatic ring system plays an important role in the biodegradability of organic compounds. The number of aromatic rings when increased adds to the molecular weight and hydrophobicity, which reduces the solubility of the compound thus reducing the bioavailability to the microorganism's metabolism (Colombo *et al.,* 1996). While simple haloaromatics such as 4-chlorobenzene or chlorophenol can undergo biodegradation under aerobic conditions, polyhalogenated aromatic compounds commonly undergo dehalogenation under anaerobic conditions since the increase in the number of halogens typically reduces the rate of aerobic biodegradation (Wackett *et al*., 1994). Wang *et al.* (1988) also reported that the position of the substituent attached to aromatic compounds affects the rate of biodegradation.

1.7.2. Environmental conditions

Environmental factors play an important role in the rate of biodegradation and affect the activity of microorganisms responsible of biodegradation. These factors include pH, oxygen content and temperature.

pH

The pH of soil is variable throughout the world; however, soil pH is a crucial determinant of the composition of the microbial community in soil (Zhang *et al.,* 2016). Pawar (2015) observed biodegradation of PAH's (anthracene, pyrene and phenanthrene) between soil pH ranging from 5 to 8. However, a soil pH of 7.5 was most suitable for the bacterial biodegradation, since 50% of all PAH's were catabolized in 3 days at pH 7.5 while this was not the case at lower or higher pH values. However, in the same study *Penicillium* species were prevalent at acidic conditions (pH 5), while *Aspergillus* species were prevalent at a neutral pH (Pawar, 2015). Maddela *et al*. (2015) reported that a pH of 5 was adequate for the fungal biodegradation of diverse petroleum hydrocarbons and Cookson (1995) also noted that the rate of fungal biodegradation increased in acidic conditions since the pH influences functional groups that can be ionized but not aliphatic substituents.

Oxygen content

Microorganisms that catabolize hydrocarbons under aerobic conditions or use aerobic pathways are generally considered faster than those anaerobic microbes that catabolize aromatic pollutants (Leahy and Colwell, 1990). During the aerobic catabolism of aromatic compounds, oxygen acts as a terminal electron acceptor and co-substrate for oxygenases, which allows for initiation and subsequent cleavage of the aromatic ring. The initial hydroxylation is catalyzed by oxygenases in bacteria and fungi (Schmidt and Kirby, 2001; Gaal and Neujahr, 1980). The oxygen content in soil depends on the soil porosity and water content. Even in well aerated soil, anaerobic zones can be present due to micro-aggregates that limit oxygen diffusion. Flooded soil environments also have limited oxygen supply since oxygen diffuses approximately 10000 times slower through water than through air (Sylvia, 2005). However, even under anoxic conditions, hydrolases can tackle diaryl esters.

Temperature

Temperature affects the physical state of the organic pollutant and enzyme activities, thus affecting the rate of biodegradation by microbial activity (Margesin and Schinner, 2001). Mesophilic temperatures between 10°C to 40°C had no significant

impact on the rate of biodegradation of petroleum pollutants by bacteria and fungi; however, temperatures below 10°C reduced the rate of biodegradation while temperatures above 40°C would not allow for biodegradation by mesophilic microorganisms (Margesin and Schinner, 2001). Das and Chandran (2010) also reported that these temperatures are adequate for microbial biodegradation of various petroleum hydrocarbons; however, the highest degradation rates were observed at 30-40°C for soil environments, 20-30°C for freshwater environments and 15-20°C for marine environments. The temperatures of soil environments vary according to the local climate. South Africa has an average temperature of 30°C in summer (November – March) while the average temperature in winter (June – August) is 20°C (Jury, 2013). These temperatures are appropriate for fungal biodegradation of organic pollutants.

Temperature additionally affects the substrate's viscosity, solubility, sorption, reactivity and volatilization. It was reported that organic compounds in water had a higher level of solubility at increased temperatures, since the solubility of salicylic acid was 1.8 g/L at 20°C, 3.7 g/L at 40°C and 20.5 g/L at 80°C (Nordström and Rasmuson, 2006). Similarly, temperature can affect the viscosity of organic compounds, since the viscosity of salol was 8.3 Pa.s at 43°C and 7.2 Pa.s at 50°C and that of benzyl salicylate was 7.5 Pa.s at 59°C and 7.0 Pa.s at 62°C (Iqbal and Chaudhry, 2008; Yang and Li, 2006). Therefore, temperature influences the rate of biodegradation of organic pollutants in the environment (Margesin and Schinner, 2001).

1.8. Aim of the dissertation

For South Africa and specifically KwaZulu-Natal, data on the fungal catabolism of diaryl ester pollutants are scarce. The aim of this study was therefore to isolate and characterize diaryl ester utilizing soil fungi from a local nature reserve and a local farm in Pietermaritzburg, KwaZulu-Natal.

The main objectives of this study were:

- To isolate and characterize fungi from soil samples collected from Bisley Nature Reserve and Crafty Duck Farm in Pietermaritzburg, KwaZulu-Natal, able to utilize selected diaryl esters as sole carbon and energy source by selective aerobic enrichment using mineral salts medium.

- To determine the growth kinetics of the isolated strains utilizing salol and benzyl salicylate and to establish the degree of substrate utilization using COD analysis and UV-Vis spectroscopy.

- To determine the ability of the selected isolated to utilize selected products of hydrolysis of the diaryl esters tested.

- To determine the specific activity of selected key enzymes potentially involved in the utilization of the diaryl esters analysed in this study.

CHAPTER 2: MATERIALS AND METHODS

2.1. Media preparation

2.1.1. Mineral Salts Medium (MSM)

The MSM contained per litre of distilled water 2.8 g Na_2HPO_4, 1 g KH_2PO_4, 0.5 g $(NH_4)_2SO_4$, 0.1 g $MgCl_2$ x $6H_2O$ and 50 mg $Ca(NO_3)_2$ x $4H_2O$ and 0.5 ml of a trace elements solution containing per litre 5 g EDTA, 3 g $Fe(II)SO_4$ x $7H_2O$, 30 mg $MnCl_2$ x $4H_2O$, 50 mg $Co(II)Cl_2$ x $6H_2O$, 10 mg $CuCl_2$ x $2H_2O$, 20 mg $NiCl_2$ x $6H_2O$, 30 mg Na_2MoO_2 x $2H_2O$, 50 mg $ZnSO_4$ x $7H_2O$ and 20 mg H_3BO_3 (Göttsching and Schmidt, 2007). The pH of the medium was adjusted to 7.5 using HCl and autoclaved at 121°C (2 atm) for 15 minutes. For solid media, 12 g/l of bacteriological agar (Biolab, Merck) was added.

2.1.2. Addition of carbon source

Phenyl salicylate (salol), benzyl salicylate and phenylacetate (purity > 99%) were purchased from Sigma-Aldrich (South Africa). The hydrolysis intermediates benzyl alcohol, phenol, salicylate and acetate of the aforementioned aromatic esters were also purchased from Sigma-Aldrich (South Africa). Salol, benzyl salicylate, phenylacetate and benzyl alcohol were added directly to the still hot medium. However, in the case of phenol, sodium salicylate and sodium acetate, 200 mM stock solutions were prepared and sterile filtered (Millex® GS Filter unit, 0.22 µm) into sterilized Schott bottles. All of these compounds were used as the sole carbon and energy source and added aseptically to the still hot sterile medium (~50°C) to the desired concentrations.

2.2. Isolation of aerobic soil fungi

2.2.1. Sample collection

Soil samples were collected from Crafty Duck Farm (S 29°56’22”, E 30°44’64”) and Bisley Nature Reserve in Pietermaritzburg, KwaZulu-Natal (S29°39’44”, E30°23’25”) using sterile Schott bottles and stored at 4°C. The samples were analysed in the laboratory on the same day within 2 hours after collection.

2.2.2. Enrichment and isolation

Phenyl salicylate utilizing microorganisms were isolated from soil samples by selective enrichment using 20 ml of MSM in 100 ml Erlenmeyer flasks containing the target compound, 10 mM phenyl salicylate, as the only carbon and energy source. These flasks were inoculated with 1 ml soil solution (prepared by homogenizing 1 g of soil in 9 ml of sterile 0.85% (*w/v*) saline solution) and incubated on a rotary shaker at 25°C and 100 rpm in the dark. After 7 days of incubation, 1 ml of enrichment cultures was transferred to fresh medium. This was repeated 5 times to allow for selection of phenyl salicylate utilizing microorganisms and after the last transfer, culture samples were streaked onto solid MSM containing the target compound as well as onto Nutrient Agar (Biolab, Merck). After successive sub-culturing, pure cultures were established by using single colonies. The two selected fungal cultures, an isolated fungus obtained from the soil from Bisley Nature Reserve and a yeast isolate obtained from the soil from a local farm, were routinely streaked on Nutrient agar and analysed by microscopy to determine their purity.

These two isolates were also grown on the aromatic esters, benzyl salicylate and phenylacetate at 10 mM and on phenol, benzyl alcohol, sodium salicylate and sodium acetate at 5 mM, respectively, as the sole energy and carbon source.

To verify the viability of the conidia produced by the fungus, the germination rate was tested by diluting a conidial suspension of 1 x 10^6 conidia per ml 10000 fold with sterile saline solution. 100 µl of the diluted suspension was then spread plated onto Nutrient agar and grown at ambient temperature in the light for a week.

The fungal culture and the yeast isolate were preserved by growing them in MSM with 10 mM phenyl salicylate for 3 days and then storing samples thereof in 20 % (v/v) glycerol by adding 800 µl liquid culture to 200 µl glycerol with storage at -20°C. In addition, the fungal conidial suspension of 1 x 10^6 conidia per ml of sterile saline solution was stored at -80°C.

The fungal strain, designated as VM1, and the yeast strain, designated as VM2, with the ability to grow on the target compounds as sole carbon and energy source were further characterized by routine microbiological methods.

2.3. Characterization of the fungus and the yeast

The characterization of the two isolates was performed by examining colony characteristics and the cell morphology. Additional classification and identification (i.e. analysis of the ITS1-5.8S rRNA-ITS2 region) was carried out to verify the identity of the isolated strains.

2.3.1. Morphological characteristics

- Colony characteristics

Strain VM1 and strain VM2 were streaked onto Nutrient Agar (NA) and incubated for a week at ambient temperature in the light. The colony characteristics of strain VM1 were further analysed on Potato Dextrose Agar (PDA) using the same conditions. The colonies of the aforementioned strains were assessed for colour and morphology.

- Mycelium and yeast cells characteristics

Light microscopy

Wet mounts of strain VM1 were prepared by using colony material from PDA and NA plates and from liquid cultures (MSM and 10 mM phenyl salicylate) and isolated conidia. Wet mounts of strain VM2 were prepared by embedding washed yeast cells (grown in liquid MSM supplemented with 8 mM sodium acetate for 3 days at 25°C and 100 rpm, collected by centrifugation [8000x *g* for 5 minutes (Heal force® Neofuge 13)]) in 20% (*w/v*) gelatine. The prepared wet mounts of strain VM1 and VM2 were then examined using bright field and phase contrast microscopy (Zeiss, AXIO Scope.A1).

Scanning electron microscopy

Fungal mycelium and yeast cells grown in liquid MSM supplemented with phenyl salicylate for 3 days at the aforementioned culture conditions were collected by centrifugation, washed twice with sterile saline solution and subsequent centrifuging at 8000x *g* for 5 minutes (Heal force® Neofuge 13). After the samples were air-dried on filter paper (Whatman No. 2, 0.2 mm), they were mounted on aluminium stubs and coated with gold using an Eiko IB-3 ion coater. These samples were then examined using a Zeiss EVOLS15 Scanning Electron Microscope.

Transmission electron microscopy

Fungal mycelium grown in liquid MSM supplemented with phenyl salicylate for 3 days at the aforementioned culture conditions was collected by centrifugation, washed twice with sterile saline solution and subsequent centrifuging at 8000x *g* for 5 minutes (Heal force® Neofuge 13). The biomass was then suspended in sterile water and fixed using 3% glutaraldehyde. Thereafter, the biomass was washed twice using 50 mM sodium cacodylate (pH= 7.4) and post-fixed in 2% osmium tetroxide, dehydrated using an ethanol series of 10%, 30%, 50%, 70%, 90% and 100%, followed by 100% propylene oxide. The pellet was then embedded in 50:50 Spurr resin (Spurr, 1969). An ultra-microtome (EM UC7: Leica Microsystems) was used to section the samples. The sections were then stained with 2% uranyl acetate and examined using a JEOL 1400 Transmission Electron Microscope (Jeol, Japan).

2.3.2. Analysis of the ITS1-5.8S rRNA-ITS2 region sequence

- DNA extraction

Genomic DNA of the fungal and the yeast isolate was extracted from 20 mg mycelium (wet weight) and 20 mg yeast cells (wet weight) respectively from a 3 day culture grown in MSM and 10 mM phenyl salicylate using the ZR Fungal/Bacterial DNA MicroPrep™ kit as per manufacturer's instructions.

- Amplification of the ITS1-5.8S rRNA-ITS2 region

A set of established primers designed for amplifying the ITS1-5.8S rRNA-ITS2 region was used (White *et al*., 1990). These primers are:

Forward primer = ITS5 (5'-GGAAGTAAAAGTCGTAACAAGG-3')

Reverse primer = ITS4 (5'-TCCTCCGCTTATTGATATGC-3')

PCR was done according to White *et al*. (1990).

- Sequencing

The sequences for strain VM1 and strain VM2 of the PCR amplified ITS1-5.8S rRNA-ITS2 region (Appendix I and II) were generated by Ms Nongcebo Memela, Sasri, Durban, South Africa. They were compared with those published in Genbank using the Basic Local Alignment Search Tool (BLAST) on the NCBI Homepage (www.ncbi.nlm.nih.gov).

- Phylogenetic analysis

The internal transcribed spacer (ITS) region of the isolated strains was aligned with the sequences of the ITS region of type strains obtained from GenBank. The sequence alignment was performed using ClustalW with MEGA version 7 (Tamura *et al.,* 2016). A phylogenetic tree was generated using the neighbour-joining algorithm with resampling for 1000 replicates. The ITS region of *Aspergillus bisporus* isolate NRRL 3690 (accession number EF661206.1) was used as the out-group for strain VM1 and the ITS region of *Saccharomyces cerevisiae* (accession number HQ171815.1) was used as the out-group for strain VM2. The tree topology was verified by using the Maximum Likelihood algorithm.

2.4. Growth of the isolated strains and utilization of the target compounds

2.4.1. Growth of strain VM1

The fungus was grown in MSM supplemented with 10 mM of the diaryl esters (salol and benzyl salicylate) and phenylacetate respectively, as sole carbon and energy source at 25°C and 100 rpm in batch cultures over a period of 10 days. However, in the case of the potential hydrolysis intermediates (phenol, benzyl alcohol, salicylate

and acetate), a 5 mM concentration was used and the culture period was 5 days. The strain was pre-grown on Nutrient Agar plates over a 3 day period at ambient temperature in the dark. These plates were then washed with sterile saline solution as follows to collect the conidia for inoculation: 5 ml of saline solution together with a sterile spatula was used to scrape the conidia from the plates; this suspension was centrifuged at 10 000x *g* for 10 minutes and washed twice with sterile saline solution. The harvested conidia were re-suspended to a conidial stock solution (2 x 10^{10} conidia per ml) in sterile saline and used to inoculate 75 ml MSM in 250 ml Erlenmeyer flasks so that each flask contained 2 x 10^{6} conidia per ml (counted using a THOMA counting chamber, Marienfield, Germany). Two sets of controls were employed. The first control was medium that contained the aforementioned carbon sources and conidia that were heat inactivated in a heating block set at 90°C for 1 hour. The second biotic control was inoculated medium that contained no carbon source. To determine the effect of different concentrations of the diaryl esters on the growth of strain VM1, concentrations from 0 mM to 25 mM of the diaryl esters were employed and the cultures were grown for 5 days in the dark at 25°C and 100 rpm. However, the concentration of the intermediates tested ranged from 0 mM to 10 mM and the culture conditions remained the same except for phenol, which required 10 days to reach stationary phase.

2.4.2. Growth of strain VM2

The yeast was grown in MSM supplemented with 10 mM of the diaryl esters (salol and benzyl salicylate) and phenylacetate respectively, as sole carbon and energy source at 25°C and 100 rpm over a period of 8 days. However, in the case of the potential hydrolysis intermediates (phenol, benzyl alcohol, salicylate and acetate), a 5 mM concentration was used. The strain was pre-grown on Nutrient Agar plates over a 3 day period at ambient temperature in the dark. These plates were then washed with sterile saline solution as follows to collect the yeast cells for inoculation purposes, 5 ml of saline solution together with a sterile spatula was used to scrape cells from the plate; this suspension was centrifuged at 10 000x *g* for 10 minutes and washed twice with sterile saline. The harvested yeast cells were re-suspended to a cell stock solution (2 x 10^{10} yeast cells per ml) in sterile saline and used to inoculate

75 ml MSM in 250 ml Erlenmeyer flasks so that each flask contained 2 x 10^6 yeast cells per ml (counted using a THOMA counting chamber, Marienfield, Germany). The re-suspended pellet was also used to inoculate 75 ml MSM to an OD_{600} of 0.1. Two sets of controls were employed. The first control was medium that contained the aforementioned carbon sources and yeast cells that were heat inactivated in a heating block set at 90°C for 1 hour. The second biotic control was inoculated medium that contained no carbon source. To determine the effect of different concentrations of the diaryl esters on the growth of strain VM2, concentrations from 0 mM to 25 mM of the diaryl esters were employed and the cultures were grown for 8 days in the dark at 25°C and 100 rpm. However, in the case of the intermediates, the concentrations tested ranged from 0 mM to 10 mM.

2.5. Growth measurements

2.5.1. Growth of strain VM1

Mycelium was harvested from cultures by vacuum filtration using pre-dried and pre-weighed filter paper (Whatman no. 1, 55 mm). The mycelium was washed twice with distilled water to remove salts and dried overnight at 105°C. The biomass yield was established by weighing the dried filters and was always compared to the controls. The weight of the fungal biomass was measured every 24 hours and at the same time 1 ml of culture supernatant (including the controls) was collected in triplicates using a pipette and centrifuged at 10 000x *g* for 10 minutes. The cell-free supernatant was stored at -20°C for further analysis (i.e. COD and UV-Vis analysis).

2.5.2. Growth of strain VM2

The growth of the yeast was monitored by measuring the optical density and establishing total cell counts. Every 24 hours the optical density of 1 ml samples of cultures was measured at 600nm using a UV-Vis spectrophotometer (SHIMADZU, UVmini-1240) and uninoculated medium was used as the blank. Subsequently, the cell concentration was determined by counting the total yeast cells using a counting chamber (THOMA counting chamber, Marienfield, Germany). 1ml of the culture was collected in triplicates at the same time point and centrifuged at 10 000x *g* for 10

minutes; the supernatant was separated and stored at -20°C for further analysis (i.e. COD and UV-Vis analysis).

2.6. Analysis of substrate utilization

Substrate utilization was analysed via Chemical Oxygen Demand measurements (COD Cell Test, Merck) and UV-Vis Spectroscopy.

2.6.1. COD measurement

Strain VM1 and strain VM2 were grown in replicate test tubes with 3 ml MSM and 10 mM of the aromatic esters (salol, benzyl salicylate or phenylacetate) for 10 days and 8 days at 25°C and 100 rpm with the initial inoculum being 2 x 10^6 conidia per ml and 2 x 10^6 yeast cells per ml respectively. However, in the case of the potential intermediates (phenol, benzyl alcohol, salicylate and acetate), strain VM1 and strain VM2 were grown with 5 mM of the intermediates and 2 ml MSM for 5 days and 8 days respectively at the aforementioned culture conditions.

The substrate utilization was analysed every 24 hours by measuring the COD in COD reaction cells. The content of the reaction cell was mixed vigorously and heated at 150°C in a preheated COD reactor for 120 minutes. The reaction cell was then removed from the COD reactor and let to cool for 10 minutes. Thereafter, it was shaken and allowed to cool to room temperature (~30 minutes). The reaction cell was then placed in a Spectroquant® NOVA 60 photometer to measure the COD, as previously reported (Ndlela and Schmidt, 2016).

2.6.2. UV-Vis Spectroscopy

The cell-free frozen supernatants obtained during the growth experiments were thawed and used to assess the utilization of the aforementioned substrates during the growth of the isolated fungal and yeast strain in MSM. Each sample, including the control, was routinely diluted 5-fold (200 µl of the sample and 800 µl of distilled water) and subjected to a spectral scan between the wavelengths of 200 and 400 nm. MSM that was diluted 5-fold with distilled water was used as the blank.

2.7. Utilization of other compounds

Both strains were grown in MSM and in the presence of various organic compounds (typically 2.5 mM) as sole carbon source to determine whether they had the ability to utilize these compounds. These compounds included the aromatic compounds benzoic acid and 4-methylbenzoate and the non-aromatic compounds glucose, succinic acid and citric acid. Stock solutions (200mM) of these compounds were prepared and sterile filtered (Millex® GS Filter unit, 0.22 µm) into sterilized Schott bottles.

The concentration of the tested substrates was 2.5 mM in 25 ml of MSM in 100 ml Erlenmeyer flasks inoculated to contain 2 x 10^6 conidia per ml and 2 x 10^6 yeast cells per ml for strain VM1 and strain VM2 respectively. The flasks were incubated on a rotatory shaker at 25°C and 100 rpm in the dark. The control was inoculated with conidia and yeast cells respectively but without a carbon source. These cultures were then examined after a week for visible growth.

2.8. Specific enzyme activities

2.8.1. Preparation of crude extracts

Batch cultures of the two strains were carried out in 1 l Erlenmeyer flasks with a working volume of 400 ml MSM supplemented with 10 mM of the aromatic esters (salol, benzyl salicylate or phenylacetate) and 5 mM of the intermediates (phenol, salicylate or benzyl alcohol). The strains were pre-grown on Nutrient Agar plates over a 3 day period at ambient temperature in the dark. These plates were then washed with sterile saline to collect the conidia or yeast cells (as described under 2.4) to inoculate 400 ml MSM to 2 x 10^6 conidia per ml for strain VM1 or an OD_{600} of 0.1 for strain VM2. The flasks were incubated in a rotary shaker at 25°C and 100 rpm in the dark. For the non-induced cells, the washed conidia or yeast cells were used to inoculate 400 ml MSM supplemented with 5 mM acetate at the aforementioned culture conditions. Strain VM1 and strain VM2 grown to the exponential phase were harvested via centrifugation at 10 000x *g* for 10 minutes at 4°C (BECKMAN, Avanti, J-26 XPI), washed three times with phosphate buffer (20mM, pH 7.4) and the pellet was separated from the supernatant. The method described by McIlwain (1948) was

used to prepare the crude extracts. The harvested mycelia or yeast cells (about 1–2 g wet weight) and an equivalent amount of aluminium oxide and 7 ml of phosphate buffer (20 mM, pH 7.4) was transferred to a pre-cooled mortar (-80°). Liquid nitrogen was then added intermittently and the biomass was ground with a pre-cooled pestle. After 20 minutes of grinding, the solution was collected in 10 ml centrifuge tubes and centrifuged at 10 000x *g* for 10 minutes at 4°C to remove debris. Thereafter, the solution was further centrifuged at 40 000x *g* for 1 hour at 4°C, yielding a clear supernatant, which was used for all enzyme assays. The amount of protein in the cell-free extracts was determined according to Bradford (1976).

2.8.2. Protein quantification

According to Bradford (1976), a calibration curve was constructed using standard protein solutions ranging from 0 to 45 µg/ml of Bovine Serum Albumin from a stock solution of 1 mg/ml Bovine Serum Albumin (BSA) Fraction V (Roche) in phosphate buffer (20 mM, pH 7.4). 100 µl of the standard protein solutions were added to 900 µl of Bradford reagent (Sigma-Aldrich) and incubated at room temperature for 5 minutes; this was prepared in triplicates. Thereafter, the absorbance of the dye-protein complex was recorded at 595 nm (Bradford, 1976). Protein quantification for the crude extracts followed the same procedure; 100 µl of the crude extract or appropriate dilutions were added to 900 µl Bradford reagent and the recorded absorbance at 595 nm was used to extrapolate the protein concentration of the crude extracts from the calibration curve (Appendix III).

2.8.3. Enzyme assays

Enzyme activities involving the catabolism of aromatic compounds were measured in quartz cuvettes (1-cm light path) at 25°C using a SHIMADZU, UVmini-1240 spectrophotometer. Specific enzyme activities were expressed as nmol per minute per mg protein at 25°C.

Catechol-1,2-dioxygenase activity was measured by following the formation of *cis,cis*-muconic acid at 260nm for 5 minutes at 10 second intervals. The molar extinction coefficients (ε) used are as reported: ε = 16 800 L x mol^{-1} x cm^{-1} for

muconic acid from catechol and ε = 13 900 L x mol^{-1} x cm^{-1} for methyl muconic acid from methylated catechol (Dorn and Knackmuss, 1978a). Additionally, catechol-2,3-dioxygenase activity was measured at 375nm based on the formation of 2-hydroxymuconic semialdehyde (ε = 33 000 L x mol^{-1} x cm^{-1}) (Kaschabek et al., 1998).

Catechol-1,2-dioxygenase and catechol-2,3-dioxygenase activity was assessed in an assay system of 1 ml containing phosphate buffer (20 mM, pH 7.4), crude extract and the reaction was initiated by the addition of 5 µl of substrate solution in ethanol. Non-induced and induced crude extracts were added to the reaction mixture in varied quantities (10 – 100 µg protein). For the reference cuvette, 5 µl ethanol was added to the reaction mixture instead of the substrate. Substrates that were tested included: 50 mM catechol, 20 mM 3-methylcatechol and 20 mM 4-methylcatechol dissolved in ethanol. Additionally, spectral scans of the reaction mixture were recorded between 200nm and 400nm to monitor the change in absorbance so that the turnover of catechol to the cleavage product could be confirmed.

General esterase activity was determined spectroscopically at 405nm by monitoring the release of *p*-nitrophenol (ε = 18 500 L x mol^{-1} x cm^{-1}) from the assay substrate *p*-nitrophenylacetate (Clauβen and Schmidt, 1999). Esterase activity was assessed in an assay system of 1 ml containing phosphate buffer (20 mM, pH 7.4), crude extract and the reaction was initiated by the addition of 20 µl of 20 mM *p*-nitrophenylacetate dissolved in ethanol. The aforementioned crude extract quantities were used. Additional spectral scans of the reaction mixture were recorded between 250nm and 500nm to monitor the change in absorbance so that the release of *p*-nitrophenol could be confirmed.

CHAPTER 3: RESULTS

3.1. Characterization of the isolated strains

After enrichment using mineral salts medium (MSM) containing salol (phenyl salicylate) as sole carbon and energy source and inoculation with soil samples from a local animal farm and Bisley Nature Reserve, two morphologically different isolates – designated isolates VM1 and VM2 – were selected for further analysis.

3.1.1. Morphological characteristics

- Isolate VM1

Preliminary characterization of the two isolates selected included analysis of colony morphology after growth on solid medium and the cell morphology determined by light microscopy and scanning electron microscopy.

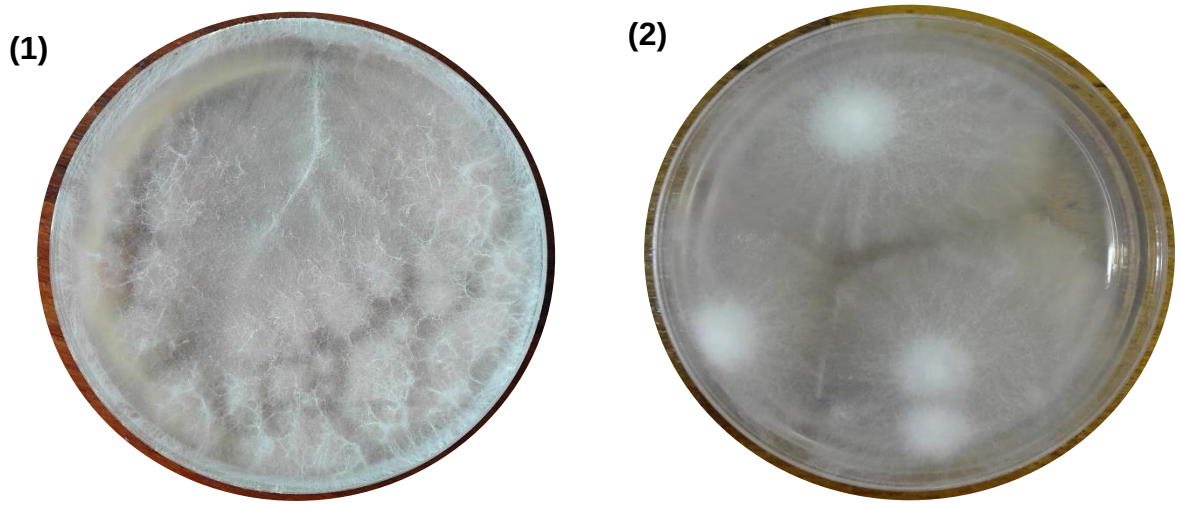

Figure 3.1: The colony appearance of fungal strain VM1 when grown on PDA (1) and NA (2) for 1 week at ambient temperature in the light.

The appearance of strain VM1 differs in colour when grown on PDA and NA (Figure 3.1). When grown on PDA, the fungal strain VM1 produces a light pink pigmentation with cottony aerial mycelium. However, when the strain is grown on NA, there is no visible pigment formation.

Figure 3.2: Hyphae structure of fungal strain VM1 grown in MSM and 10 mM phenyl salicylate for 3 days at 25°C and 100 rpm analysed by phase contrast microscopy. (1) Vacuole; (2) Conidiophore; (3) Septum.

Figure 3.2 shows that the fungal strain VM1 is a septate hyphae-forming ascomycete. It forms conidiophores and produces vacuoles.

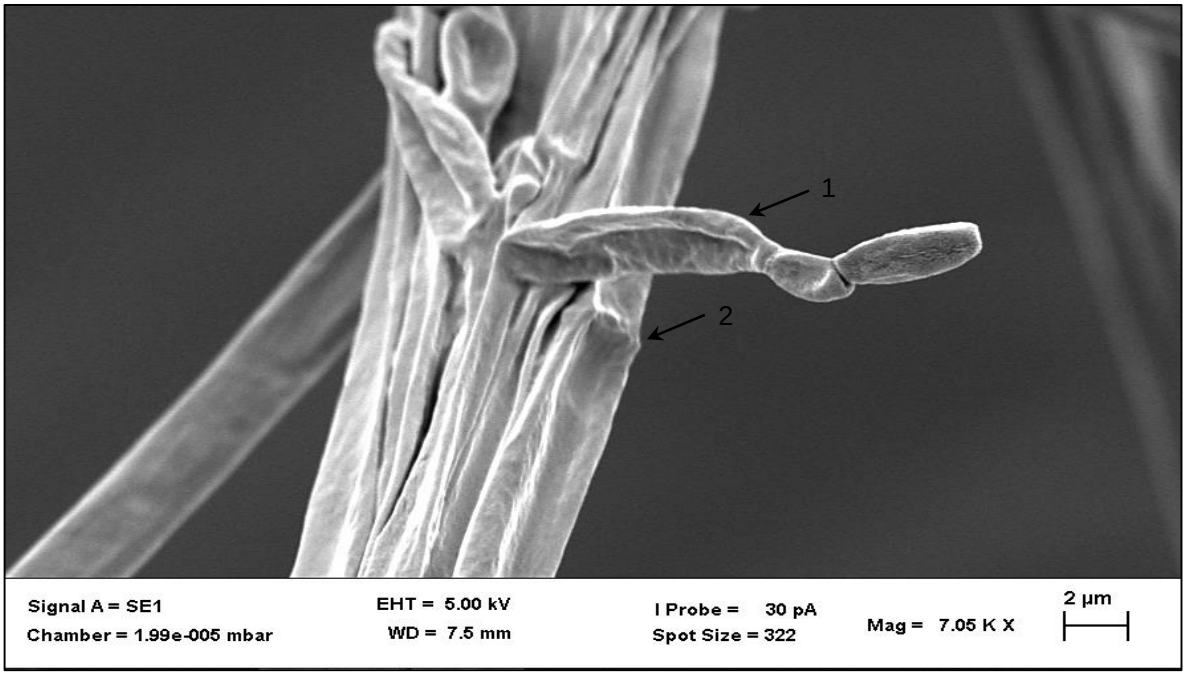

Figure 3.3: Hyphae structure of fungal strain VM1 grown in MSM and 10 mM phenyl salicylate for 3 days at 25°C and 100 rpm analysed by scanning electron microscopy. (1) Conidiophore; (2) Septum.

Analysis of mycelia samples by scanning electron microscopy confirmed that strain VM1 produced conidiophores and that the hyphae were septated (Figure 3.3).

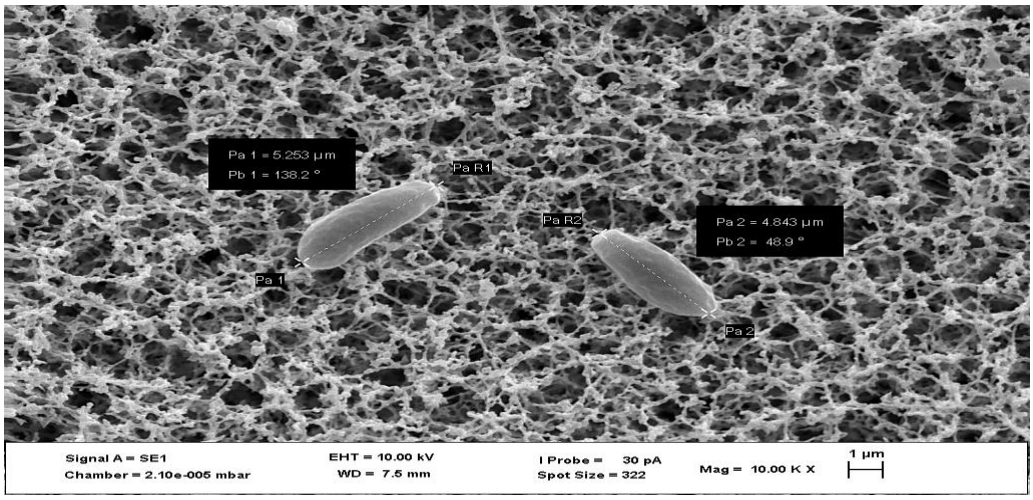

Figure 3.4: Size and shape of microconidia formed by strain VM1 when grown on NA plates for 1 week at ambient temperature in the light and analysed by scanning electron microscopy.

Strain VM1 is able to produce ovoid microconidia (Figure 3.4) that were used as the inoculum in the growth and substrate utilization experiments. These conidial cells typically range from 4 µm to 5 µm in length. The viability of the conidia was tested by a 10000 fold dilution (with saline) of 1 x 10^6 conidia per ml suspension. 100 µl of the diluted suspension was spread plated onto NA and grown at ambient temperature in the light for 1 week. After replicating the procedure 3 times, the germination rate of the conidia was found to be 60%.

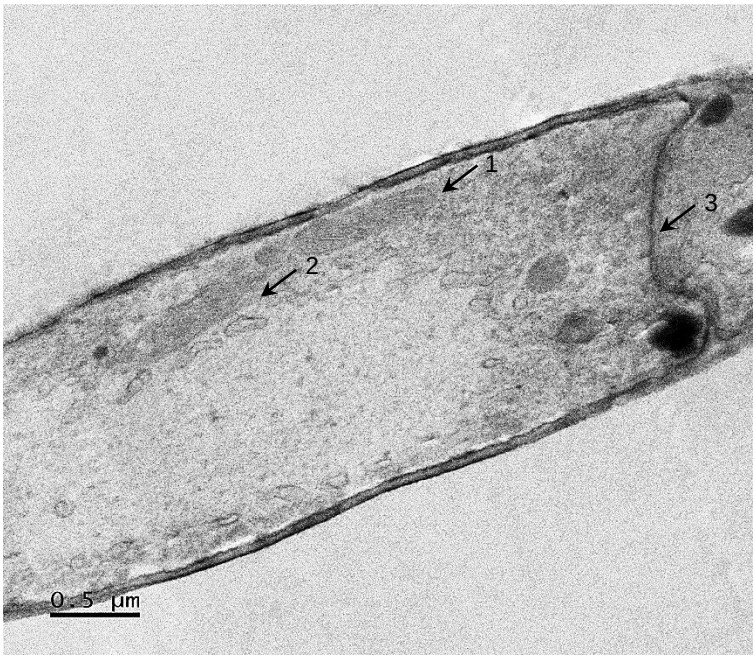

Figure 3.5: Ultrastructural analysis of fungal hyphae of strain VM1 when grown in MSM and 10 mM phenyl salicylate for 3 days at 25°C and 100 rpm and analysed by transmission electron microscopy. (1 & 2) Mitochondria; (3) Septum.

Ultrastructural analysis of thin sections of *Fusarium* sp. strain VM1 by transmission electron microscopy showed that the fungal hyphae contained mitochondria with cristae and a septum (Figure 3.5).

- Isolate VM2

Figure 3.6: The colony appearance of yeast strain VM2 when grown on NA for 1 week at ambient temperature in the light.

Strain VM2, when grown on NA, produced circular colonies with radial furrows that are cream in colour, have an umbonate elevation and a dull appearance (Figure 3.6).

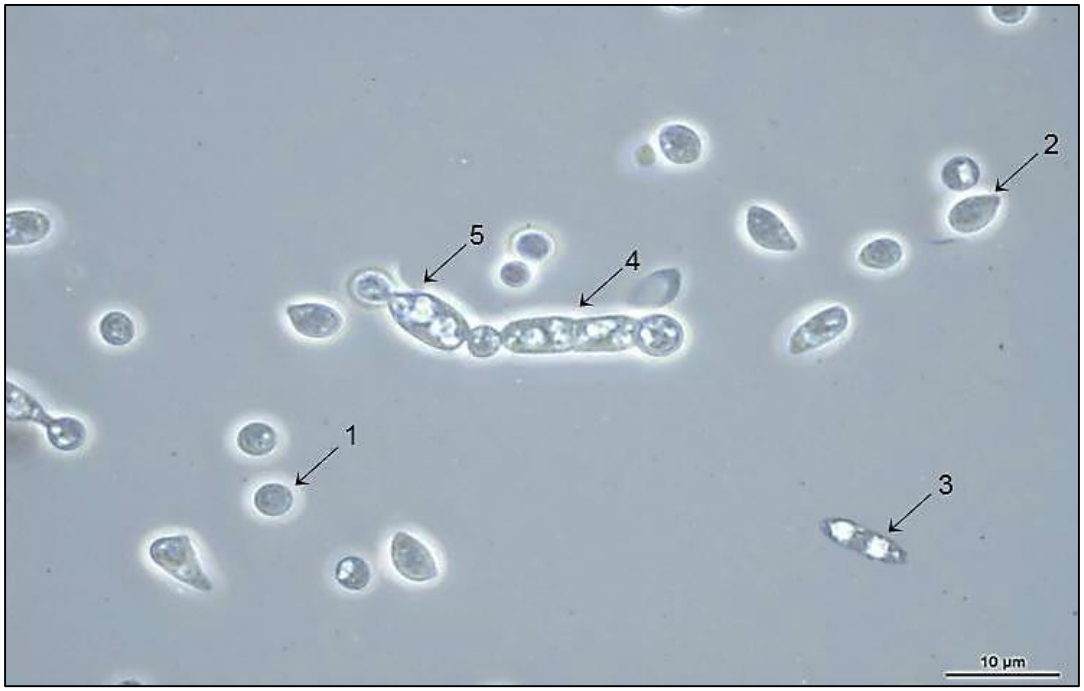

Figure 3.7: Cell structure of yeast strain VM2 grown in MSM and 8 mM acetate for 3 days at 25°C and 100 rpm, embedded in 20 % (*w*/v) gelatine and analysed by phase contrast microscopy. (1) Circular blastoconidia; (2) Ovoid blastoconidia; (3) Vacuole; (4) Septum; (5) Budding.

Yeast strain VM2 has highly variable cell structures, forming circular blastoconidia, ovoid conidia and pseudohyphal buds with arthroconidia (Figure 3.7). It also forms septa and vacuoles.

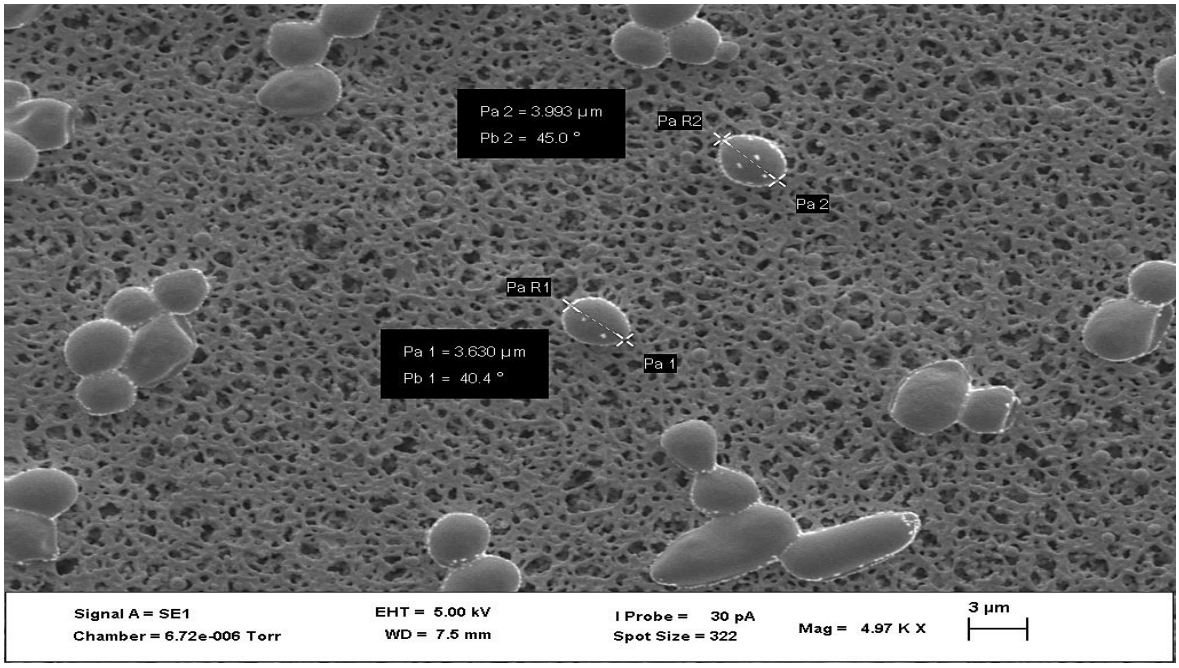

Figure 3.8: Size and shape of strain VM2 cells grown in MSM and 10 mM phenyl salicylate for 3 days at 25°C and 100 rpm analysed by scanning electron microscopy.

Strain VM2 produced a large proportion of blastoconidia (Figure 3.8) when grown in MSM and 8 mM acetate for 3 days at 25°C and 100 rpm. These blastoconidia were typically ~3 µm in diameter.

3.1.2. Analysis of the sequence for the ITS1-5.8S rRNA-ITS2 region

The sequencing of the amplified ITS1-5.8S rRNA-ITS2 region resulted in sequences of 563 bases for strain VM1 and 521 bases for strain VM2. The sequences were then compared to those deposited in Genbank using the Basic Local Alignment Search Tool (BLAST, www.ncbi.nim.nih.gov). The best matches based on the sequence similarities and the E-values from the database are listed in the Tables 3.1 and 3.2:

Table 3.1: Best matching sequences in the NCBI database for the ITS1-5.8S rRNA-ITS2 region of strain VM1

Accession	Description	Max score	E value	Identity*
KU872849.1	*Fusarium oxysporum* isolate AFIC15 18S ribosomal RNA gene, partial sequence	1040	0.0	100%
KJ150718.1	Fungal sp. FNBR LK5 18S ribosomal RNA gene, partial sequence	1040	0.0	100%
KU872814.1	*Fusarium oxysporum* isolate AFIC3 18S ribosomal RNA gene, partial sequence	1020	0.0	99%
KC119203.1	*Fusarium oxysporum* strain KAML01 18S rRNA gene, partial sequence	1007	0.0	99%
KU680361.1	*Fusarium oxysporum* isolate CBS F327 18S ribosomal RNA, partial sequence	1002	0.0	99%

*Based on NCBI Blast search performed on June 22, 2019.

Comparison of the ITS1-5.8S rRNA-ITS2 sequence of the isolated fungal strain VM1 to the sequences contained in Genbank gave best matches at a similarity level of ≥99% to sequences of environmental and type strains of *Fusarium* species (Table 3.1). This similarity level is adequate to assign the isolate VM1 to genus level (Janda and Abbott, 2007). Thus, isolate VM1 can be assigned to the genus *Fusarium*. To further analyse the phylogenetic relationship of strain VM1, its ITS1-5.8S rRNA-ITS2 sequence was used to generate phylogenetic trees (Figures 3.9 and 3.10).

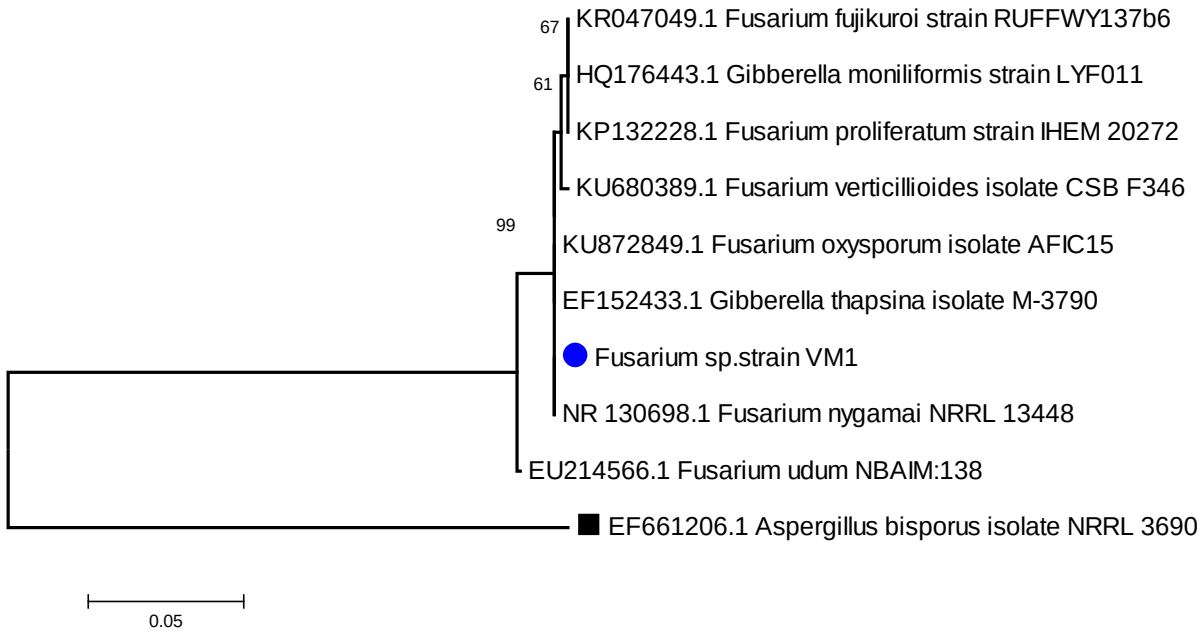

Figure 3.9: Phylogenetic assignment of strain VM1 (●) using the neighbour-joining method based on its ITS1-5.8S rRNA-ITS2 region in comparison with the ITS region of selected environmental and type strains of *Fusarium* and its teleomorph, *Gibberella*. The ITS region of *A. bisporus* (■) was used as the out-group. The scale bar represents 5 estimated changes per 100 nucleotides.

The phylogenetic analysis revealed that strain VM1 was closely related to species of the genus *Fusarium* and its teleomorph, *Gibberella* (Figure 3.9), clustering closely with *Fusarium oxysporum* and *Fusarium nygamai* and *Gibberella thapsina*, the teleomorph of *Fusarium thapsina*. The tree topology was confirmed by the maximum likelihood method (Figure 3.10).

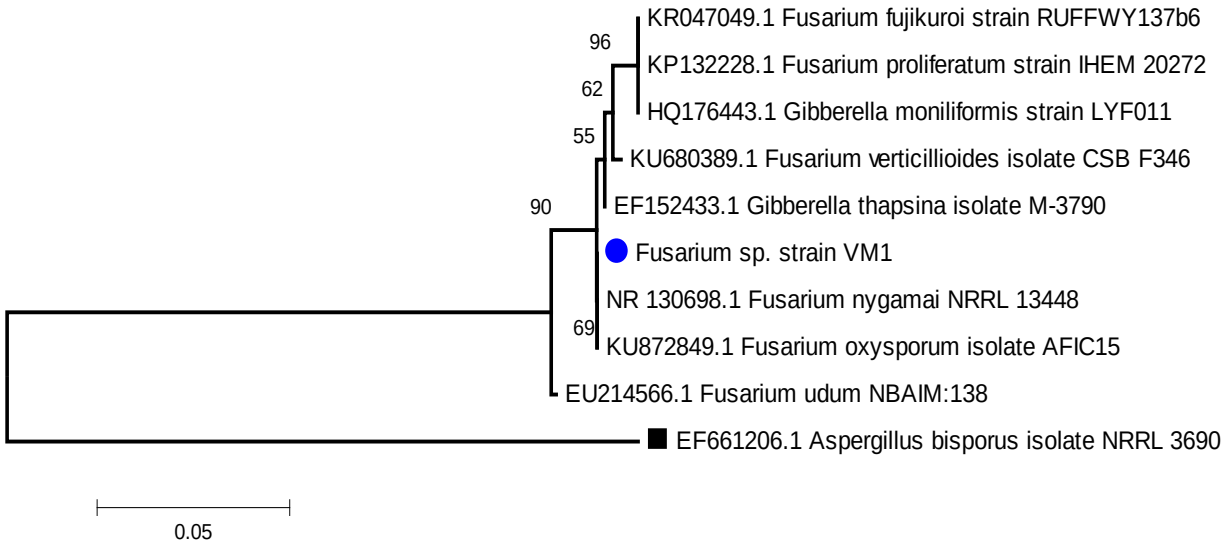

Figure 3.10: Phylogenetic assignment of strain VM1 (●) using the maximum likelihood method based on its ITS1-5.8S rRNA-ITS2 region in comparison with the ITS region of selected environmental and type strains of *Fusarium* and its teleomorph, *Gibberella*. The ITS region of *A. bisporus* (■) was used as the out-group. The scale bar represents 5 estimated changes per 100 nucleotides.

The phylogenetic analysis of the same sequences but using the maximum likelihood method confirmed the tree topology established using the neighbour-joining method and that strain VM1 was closely related to species of the genus *Fusarium* and its teleomorph, *Gibberella* (Figure 3.10), closely grouping with *Fusarium oxysporum* and *Fusarium nygamai* as seen in the previous Figure 3.9.

Table 3.2: Best matching sequences in the NCBI database for the ITS1-5.8S rRNA-ITS2 region of strain VM2

Accession	Description	Max score	E value	Identity*
KY103036.1	*Cutaneotrichosporon terricola* culture CBS:8498 small subunit ribosomal RNA gene, partial sequence	905	0.0	99%
EU551190.1	*Trichosporon sp.* P5 18S ribosomal RNA gene, partial sequence	880	0.0	99%
KY103033.1	*Cutaneotrichosporon terricola* culture CBS:8497 small subunit ribosomal RNA gene, partial sequence	876	0.0	99%
AB031517.1	*Trichosporon terricola* genes for ITS1, 5.8S rRNA, ITS2, partial and complete sequence	782	0.0	99%
NR 136947.1	*Cutaneotrichosporon terricola* JCM 11688 ITS region; from TYPE material	795	0.0	98%

*Based on NCBI Blast search performed on June 22, 2019.

The amplified ITS1-5.8S rRNA-ITS2 sequence of strain VM2, when compared to sequences contained in Genbank, gave highest similarity levels ≥98% to sequences of environmental and type strains of *Trichosporon* (*Cutaneotrichosporon*) species (Table 3.2). According to Janda and Abbott, (2007), these levels are sufficient to assign the isolated yeast strain to genus level therefore, strain VM2 can be assigned to the genus *Trichosporon* (*Cutaneotrichosporon).* As for isolate VM1, phylogenetic assignment was performed to further assess the relationship of *Trichosporon* sp. strain VM2 to other members of this fungal genus (Figures 3.11 and 3.12).

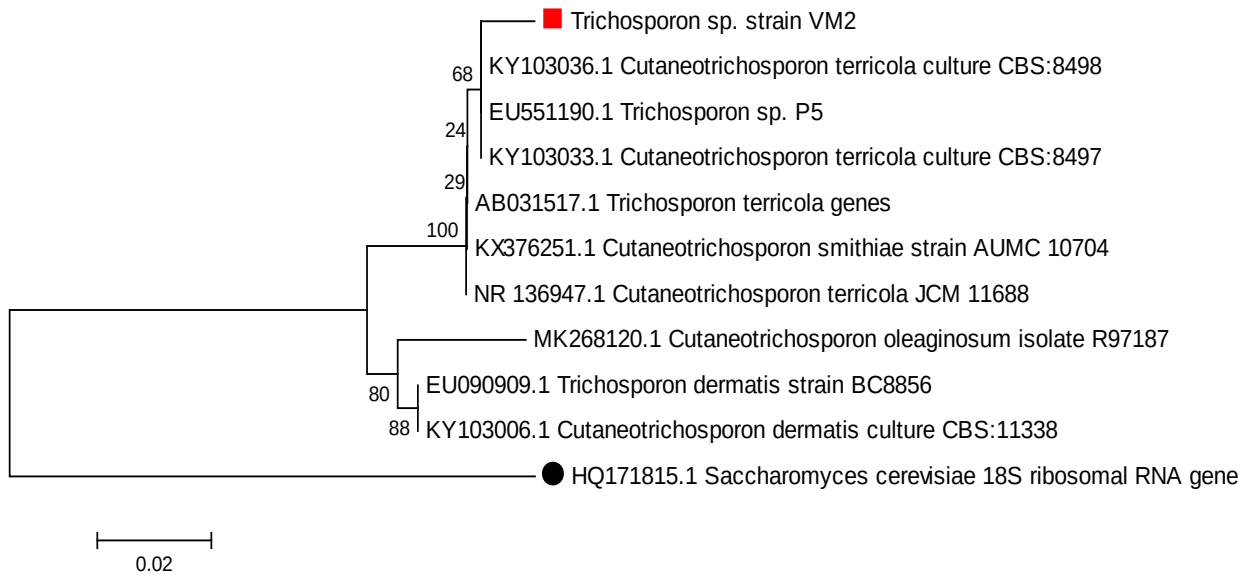

Figure 3.11: Phylogenetic assignment of strain VM2 (■) using the neighbour-joining method based on its ITS1-5.8S rRNA-ITS2 region in comparison with the ITS region of selected type strains and environmental isolates of *Cutaneotrichosporon* and *Trichosporon*. The ITS region of *S. cerevisiae* (●) was used as the out-group. The scale bar represents 2 estimated changes per 100 nucleotides.

Figure 3.11 illustrates the phylogenetic relationship of strain VM2 to that of selected environmental and type strains of the same genus. The phylogenetic analysis revealed that isolate VM2 closely clusters with members of the genus *Trichosporon* (*Cutaneotrichosporon*), most closely grouping with *Cutaneotrichosporon terricola.* Again, the maximum likelihood method was used to confirm the tree topology (Figure 3.12).

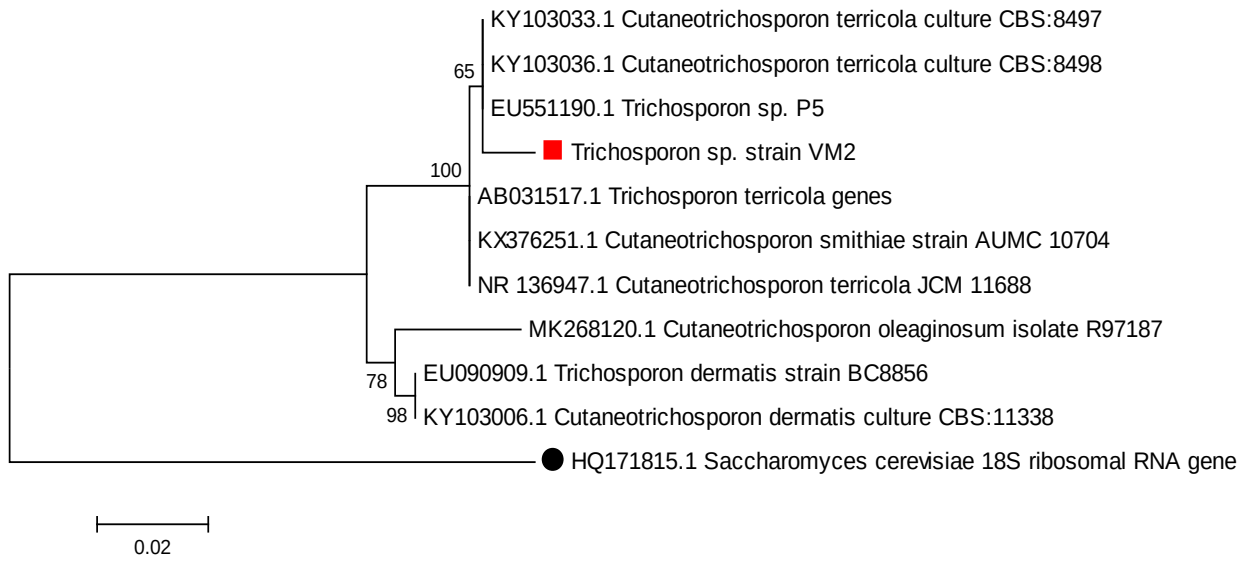

Figure 3.12: Phylogenetic assignment of strain VM2 (■) using the maximum likelihood method based on its ITS1-5.8S rRNA-ITS2 region in comparison with the ITS region of selected environmental and type strains of *Cutaneotrichosporon* and *Trichosporon*. The ITS region of *S. cerevisiae* (●) was used as the out-group. The scale bar represents 2 estimated changes per 100 nucleotides.

Figure 3.12 confirms the tree topology established using the neighbour-joining method. Furthermore, it shows that strain VM2 can be assigned to the genus *Trichosporon* (*Cutaneotrichosporon*), forming a close relationship to *Cutaneotrichosporon terricola* as shown in the previous Figure 3.11.

Based on the cell structure, colony morphology and the ITS1-5.8s rRNA-ITS2 sequence, the two isolates were provisionally assigned as *Fusarium* sp. strain VM1 and *Trichosporon* sp. strain VM2.

3.2. Growth of *Fusarium* sp. strain VM1 and utilization of target compounds

To determine whether salol, benzyl salicylate, phenylacetate, phenol, salicylate, benzyl alcohol or acetate served as a carbon and energy sources for the growth of the isolated fungus, strain VM1 was initially grown with 10 mM of the diaryl esters and 5 mM of the intermediates as the sole carbon source. The growth was analysed over time by measuring the dry weight of the fungal biomass and the substrate utilization was analysed by measuring the Chemical Oxygen Demand and verified via UV-Vis spectroscopy.

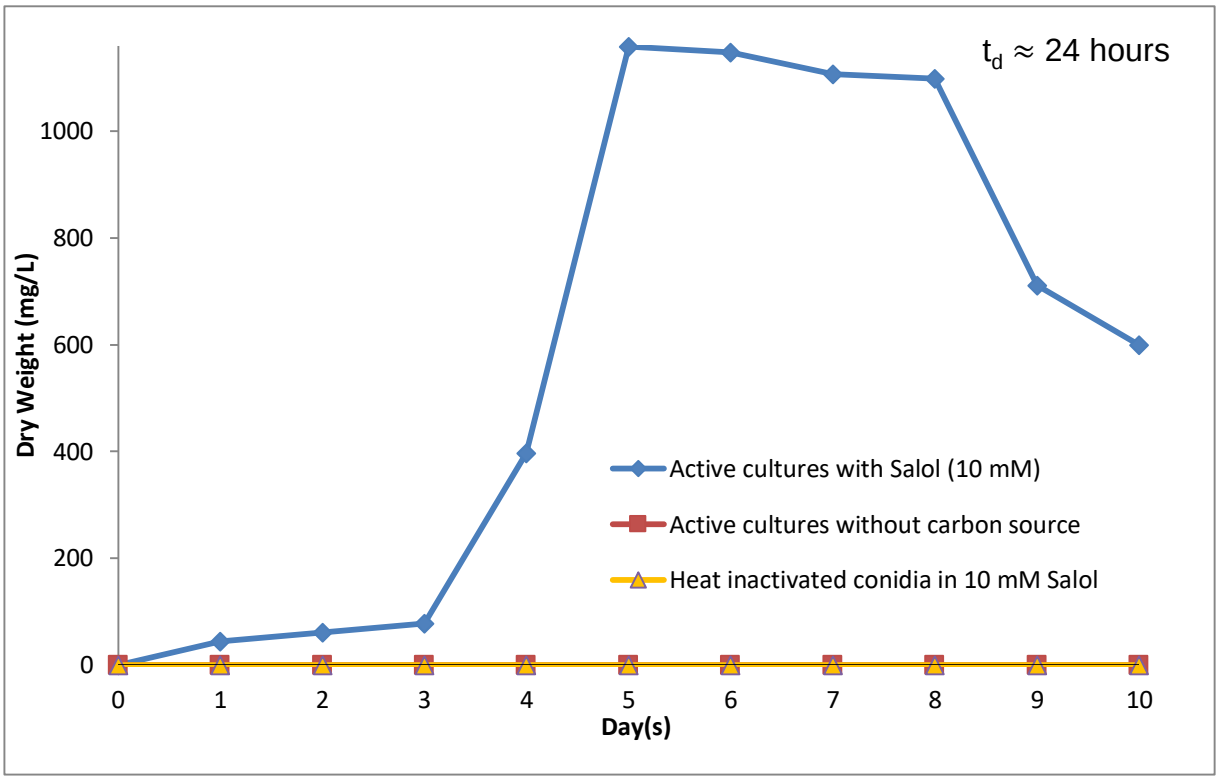

Figure 3.13: Growth of *Fusarium* sp. strain VM1 with 10 mM salol as the sole carbon source in MSM at 25°C and 100 rpm. Flasks were inoculated with 2 x 10^6 conidia per ml.

Figure 3.13 shows a typical growth curve when *Fusarium* sp. strain VM1 was grown in MSM supplemented with 10 mM salol as sole source of carbon and energy. The initial lag phase lasted up to 3 days, thereafter an exponential phase followed until day 5, followed by the stationary phase lasting from day 5 to day 8. The final phase was the death phase, which occurred from day 8 to day 10 with a rapid decrease in

biomass. No growth was observed in the absence of the substrate and with heat inactivated conidia in the presence of 10 mM salol. The doubling time (t_d) under the specified growth conditions was established as ~24 hours.

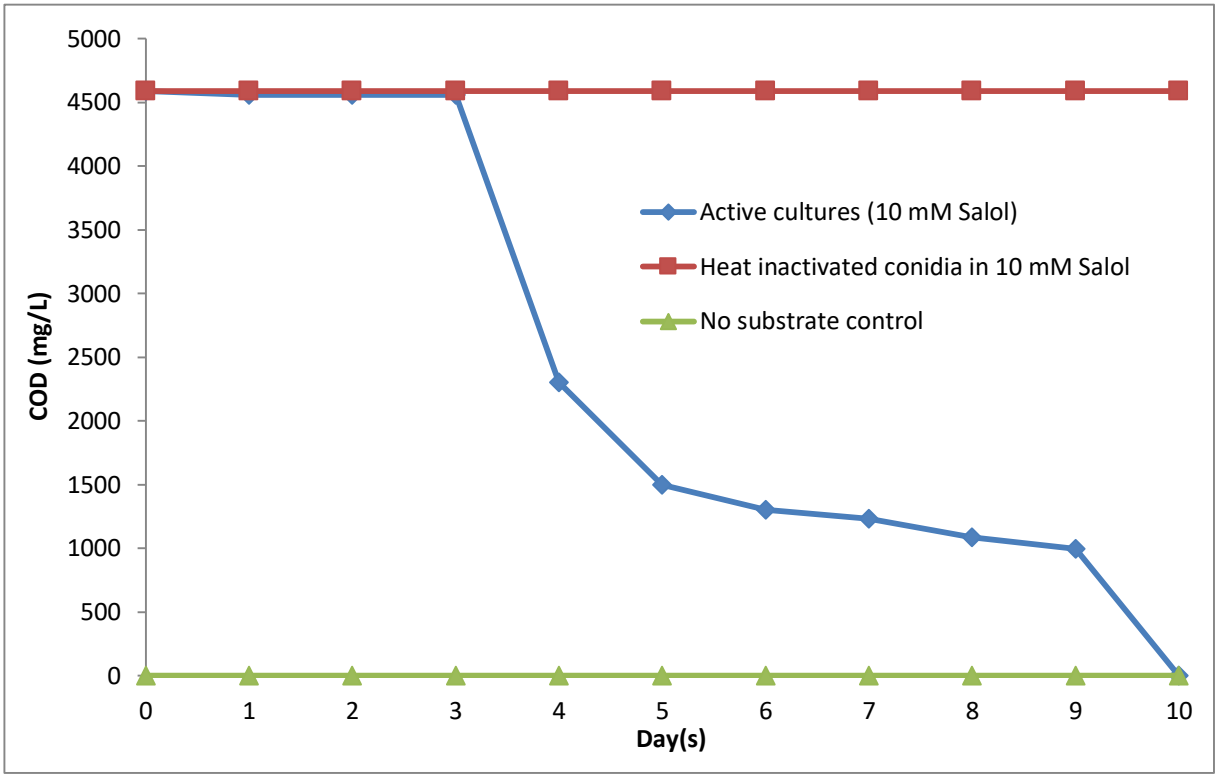

Figure 3.14: COD analysis of *Fusarium* sp. strain VM1 cultures grown with 10 mM salol as the sole carbon source in MSM at 25°C and 100 rpm. Flasks were inoculated with 2 x 10^6 conidia per ml.

The COD analysis of cultures of *Fusarium* sp. strain VM1 in the presence of 10 mM salol as the sole carbon source showed that the substrate concentration decreased over time (Figure 3.14). The substrate concentration determined as the COD remained fairly stable up to day 3, which perfectly matched the growth curve pattern for the lag phase (Figure 3.13). Thereafter, the substrate concentration decreased rapidly (day 3-5) until 10 mM phenyl salicylate had been catabolized quantitatively – judged by the COD – by *Fusarium* sp. strain VM1 at day 10, again matching the growth curve pattern shown in Figure 3.13. The controls with heat inactivated conidia indicated that the substrate concentration remained stable at a COD of ~4500 mg/l, close to the theoretical COD of 10 mM salol (4480 mg O_2) and the controls without substrate added show that there was no measureable COD unless salol was

present. The highest molar biomass yield under the specified growth conditions was established as ~138 g dry weight /M substrate consumed.

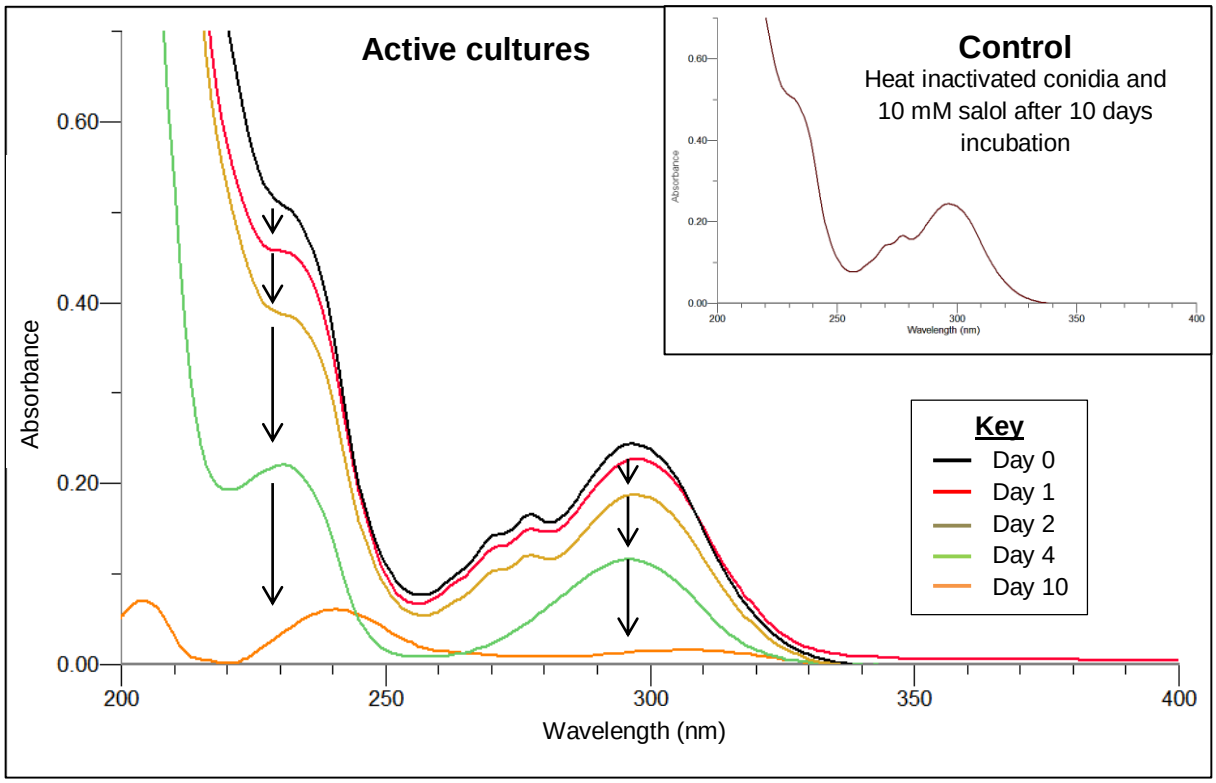

Figure 3.15: UV-Vis spectral analysis of the catabolism of 10 mM salol in MSM in the presence of *Fusarium* sp. strain VM1 in cultures incubated at 25°C and 100 rpm from day 0 to day 10. The insert graph shows the UV-Vis spectrum for the abiotic control after 10 days.

The UV-Vis analysis of culture supernatants over time demonstrated that only in the presence of active cultures the aromatic body of phenyl salicylate – showing an absorbance maximum at ~290 nm – was catabolised over time (Figure 3.15). Specifically, the additional decrease in the absorbance in the region of 210 nm to 260 nm indicates that the diaryl ester, phenyl salicylate, was catabolized by *Fusarium* sp. strain VM1. The abiotic control (heat inactivated conidia and the substrate) shows that the aromatic body of phenyl salicylate remained stable over the 10 day period. Therefore, active cultures were solely responsible for the disappearance of phenyl salicylate in the medium. The water solubility of phenyl salicylate is 0.15 g/L at 20°C. The UV-Vis spectrum for phenyl salicylate at Day 0

therefore matches the amount of compound that is soluble in water based on the molar extinction coefficient at 290 nm.

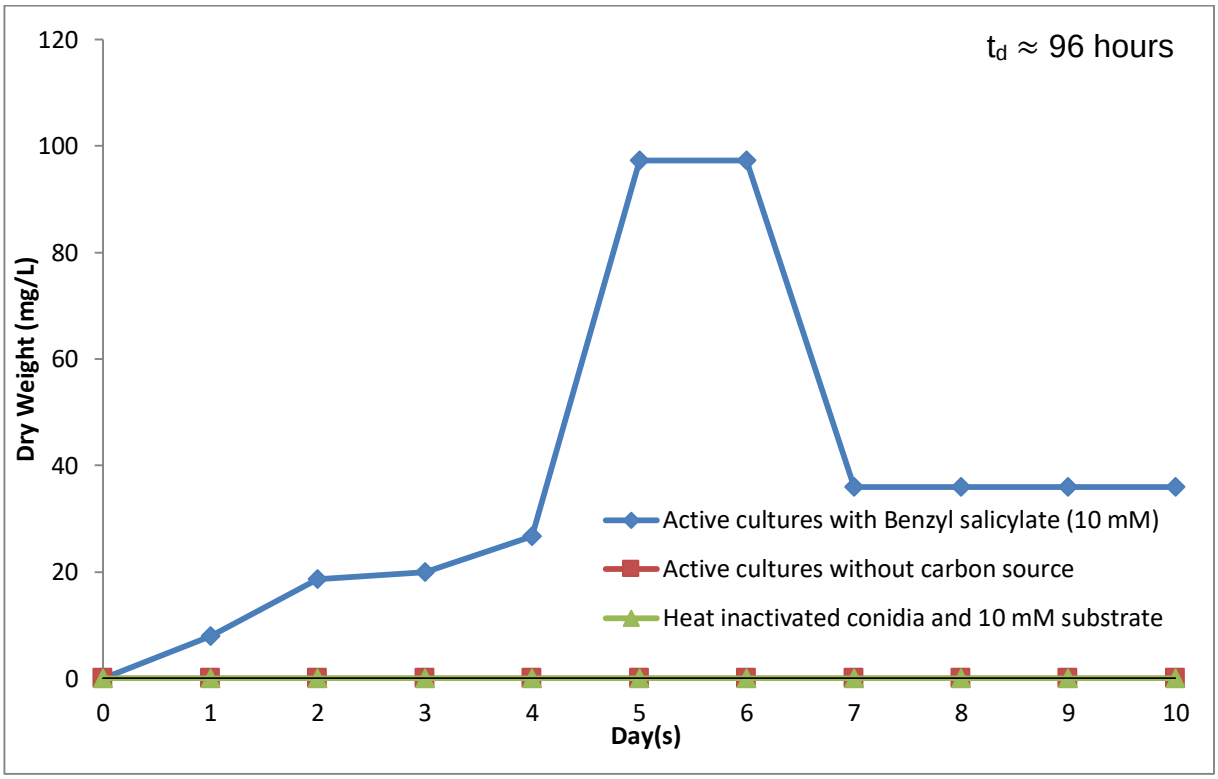

Figure 3.16: Growth of *Fusarium* sp. strain VM1 with 10 mM benzyl salicylate as the sole carbon source in MSM at 25°C and 100 rpm. Flasks were inoculated with 2 x 10^6 conidia per ml.

Figure 3.16 shows the growth curve of the fungal isolate VM1 when grown in MSM and 10 mM benzyl salicylate as sole carbon source. A 4 day lag phase was followed by a short exponential phase from day 4 to day 5. The stationary phase occurred from day 5 to day 6 followed by the death phase until day 10. No growth was observed in the absence of the substrate and when heat inactivated conidia were incubated in the presence of 10 mM substrate. The doubling time (t_d) under the specified growth conditions was established as ~96 hours. The biomass yield for benzyl salicylate was one tenth to that of the biomass yield for salol.

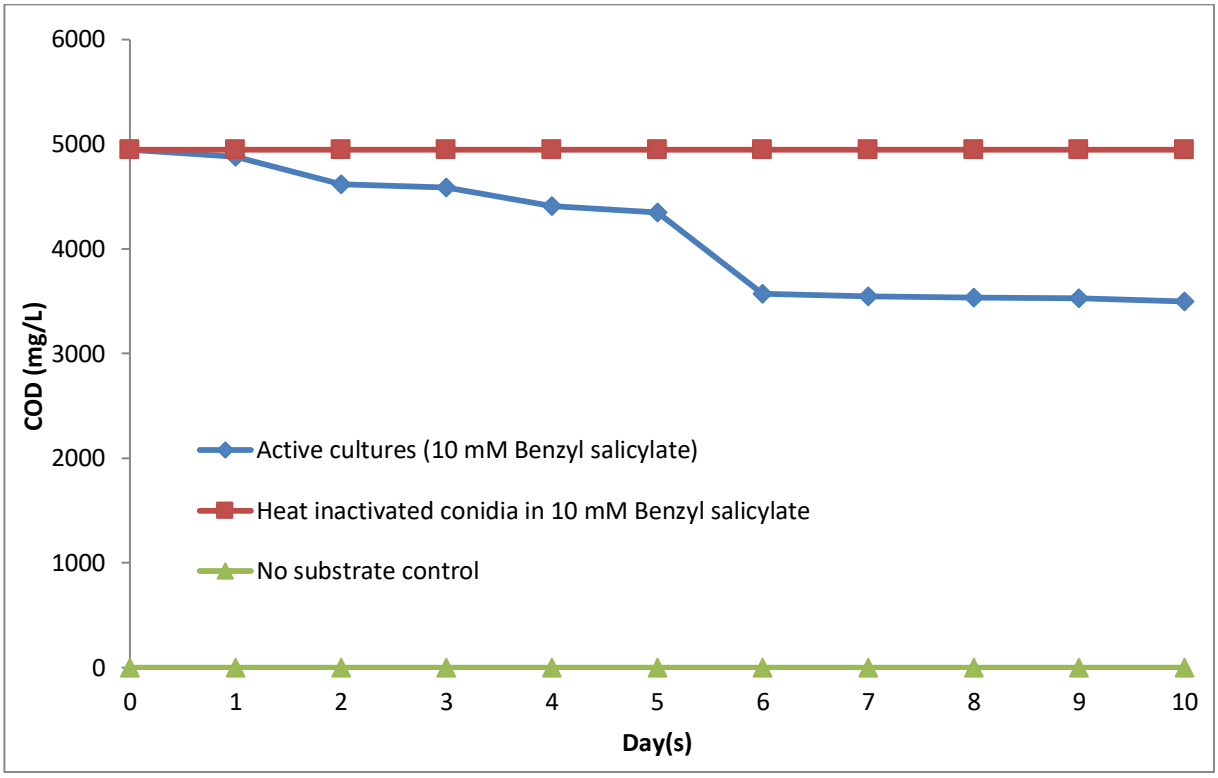

Figure 3.17: COD analysis of *Fusarium* sp. strain VM1 cultures grown with 10 mM benzyl salicylate as the sole carbon source in MSM at 25°C and 100 rpm. Flasks were inoculated with 2 x 10^6 conidia per ml.

The COD analysis of cultures of strain VM1 grown in the presence of 10 mM benzyl salicylate showed a slow decline in substrate concentration over time (Figure 3.17). The substrate concentration determined as the COD gradually decreased from day 0 to day 6, which is in accordance with the growth pattern for the exponential phase (Figure 3.16). Thereafter, the substrate concentration did not decrease further and stabilized at ~30% of 10 mM benzyl salicylate catabolized by the fungus at day 10. The controls with heat inactivated conidia indicated that the substrate concentration remained stable at ~4950 COD mg/L, close to the theoretical COD of 10 mM benzyl salicylate (4960 mg O_2) and the controls without benzyl salicylate added show that there was no measureable COD unless the substrate was present. The highest molar biomass yield under the specified growth conditions was established as ~13.8 g dry weight /M substrate consumed.

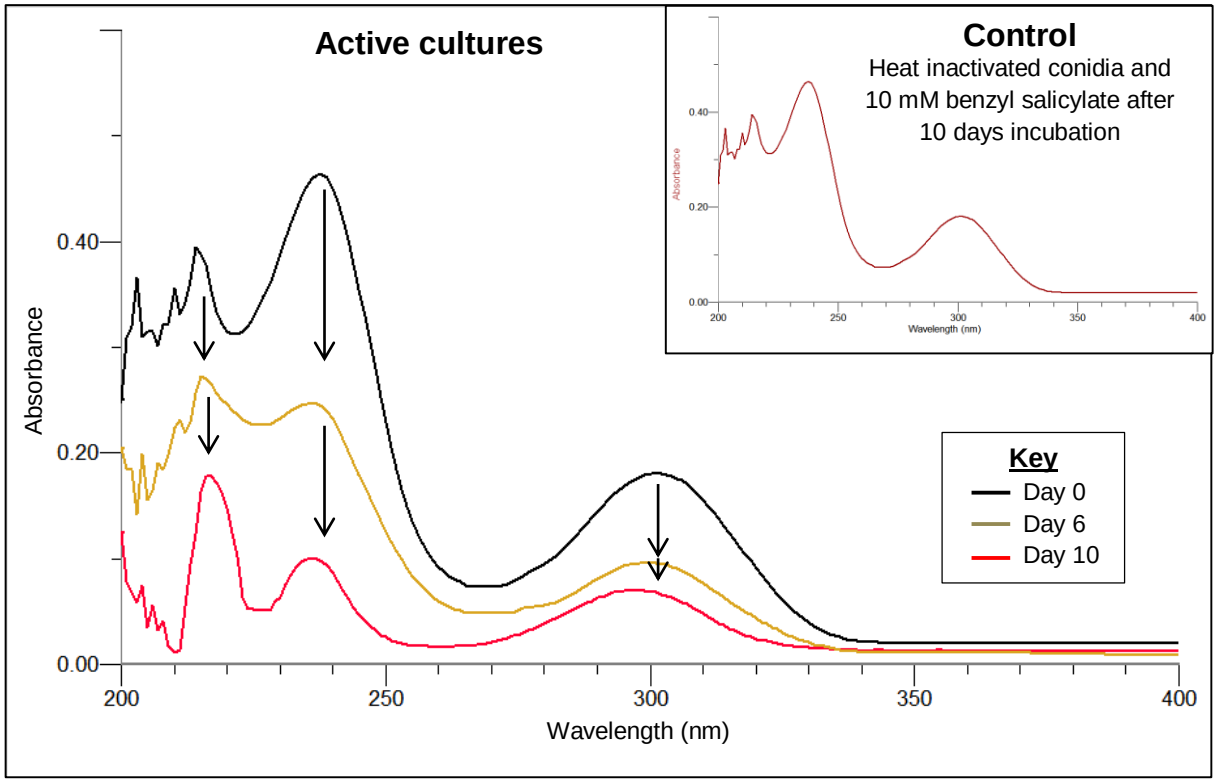

Figure 3.18: UV-Vis spectral analysis of the catabolism of 10 mM benzyl salicylate in MSM in the presence of *Fusarium* sp. strain VM1 in cultures incubated at 25°C and 100 rpm from day 0 to day 10. The insert graph shows the UV-Vis spectrum for the abiotic control after 10 days.

According to the insert graph, there was no observable change in the spectrum of benzyl salicylate with heat inactivated conidia indicating that the aromatic body remained intact throughout the 10 day period. However, the culture supernatants, when analysed by UV-Vis spectroscopy demonstrated that even when active cultures were present, the aromatic body of benzyl salicylate was not completely eliminated within the incubation period (Figure 3.18), thereby matching the COD data.

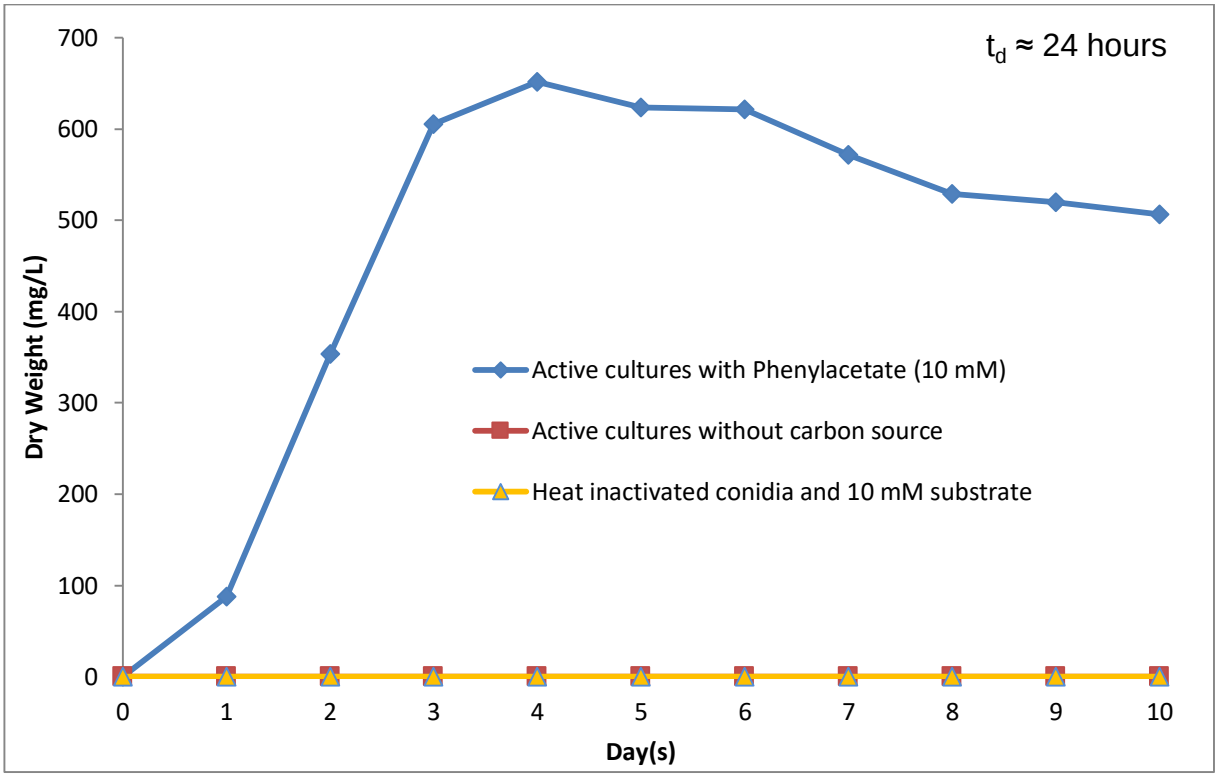

Figure 3.19: Growth of *Fusarium* sp. strain VM1 with 10 mM phenylacetate as the sole carbon source in MSM at 25°C and 100 rpm. Flasks were inoculated with 2 x 10^6 conidia per ml.

Figure 3.19 shows a typical growth curve when *Fusarium* sp. strain VM1 was grown in MSM with 10 mM phenylacetate as sole carbon source. A slight lag phase that lasted for 1 day was observed, thereafter an exponential phase followed till day 3, and the stationary phase lasted from day 3 to day 6. There was a decline in biomass from day 6 to day 10, indicating that this was the death phase. No growth was observed in the absence of the substrate and with heat inactivated conidia in the presence of 10 mM substrate. The doubling time (t_d) under the specified growth conditions was established as ~24 hours.

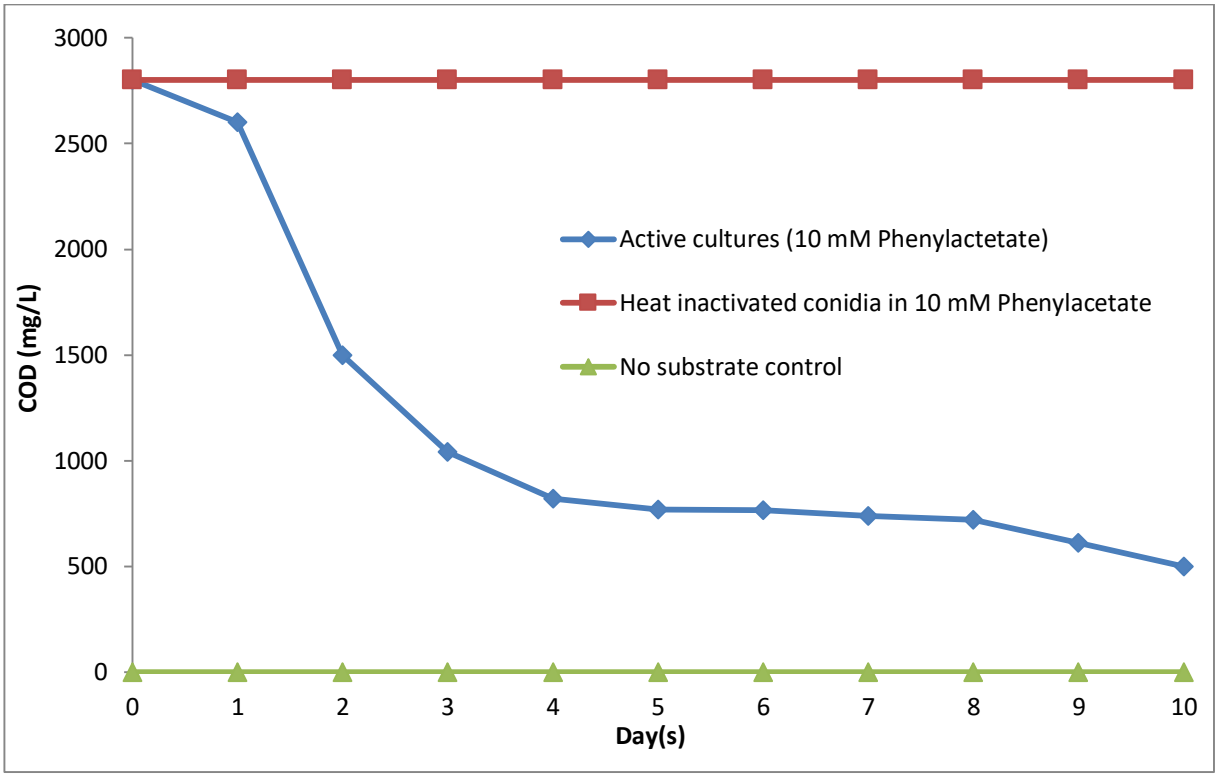

Figure 3.20: COD analysis of *Fusarium* sp. strain VM1 cultures grown with 10 mM phenylacetate as the sole carbon source in MSM at 25°C and 100 rpm. Flasks were inoculated with 2 x 10^6 conidia per ml.

Cultures of *Fusarium* sp. strain VM1 when grown in the presence of 10 mM phenylacetate showed that the substrate concentration decreased over time as indicated by the decreasing COD values (Figure 3.20). The substrate concentration as the COD decreased rapidly from day 0 to day 4, which is in accordance with the exponential growth phase established (Figure 3.19). Thereafter, the substrate concentration slowly declined until ~87% of 10 mM phenylacetate was catabolized by *Fusarium* sp. strain VM1 at day 10, matching the growth curve pattern for the stationary and death phase (Figure 3.19). The controls with heat inactivated conidia indicated that the substrate concentration remained stable at ~2800 COD mg/L, close to the theoretical COD of 10 mM phenylacetate (2880 mg O_2) and the controls without substrate added show that there was no measureable COD unless phenylacetate was present. The highest molar biomass yield under the specified growth conditions was established as ~96 g dry weight/M substrate consumed

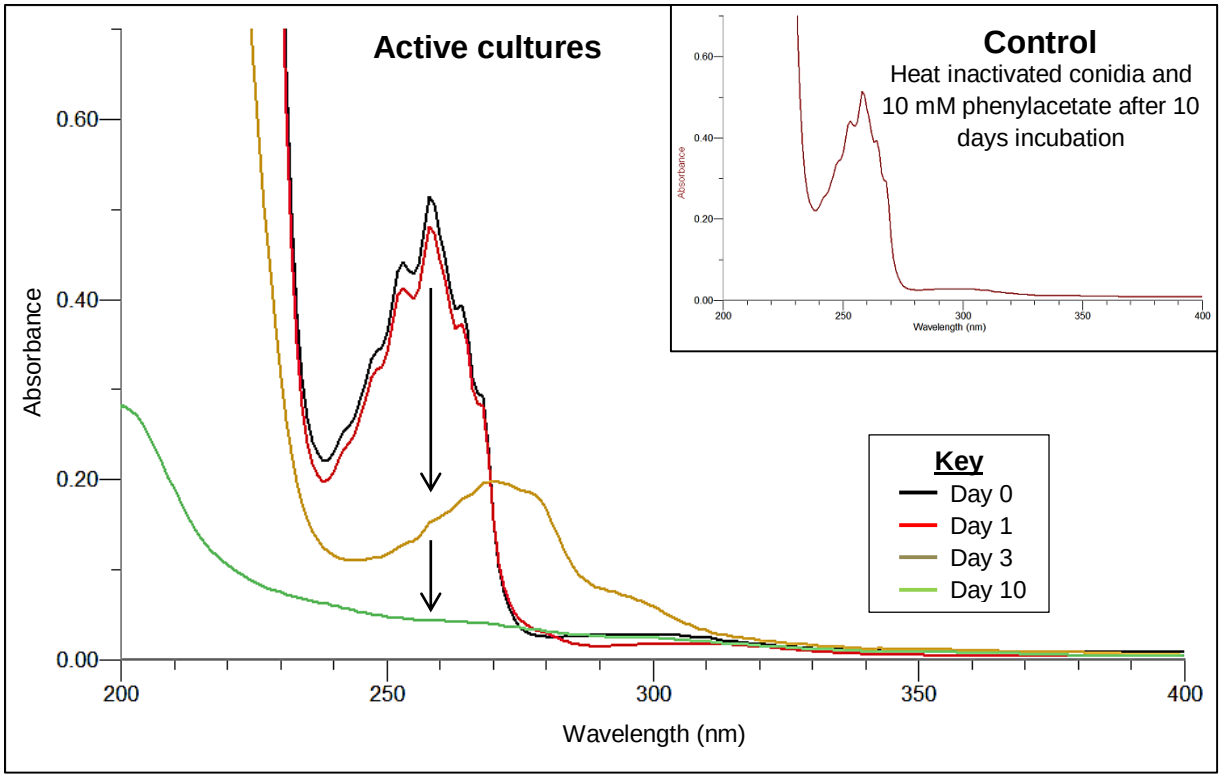

Figure 3.21: UV-Vis spectral analysis of the catabolism of 10 mM phenylacetate in MSM in the presence of *Fusarium* sp. strain VM1 in cultures incubated at 25°C and 100 rpm from day 0 to day 10. The insert graph shows the UV-Vis spectrum for the abiotic control after 10 days.

The UV-Vis analysis of culture supernatants obtained from phenylacetate grown cultures over time demonstrated that only in the presence of active cultures the aromatic substrate was catabolized (Figure 3.21). Interestingly, at day 3 the recorded UV-Vis spectrum indicated the transient formation of phenol, which is a known intermediate upon cleavage of the ester bond. The decrease of the absorbance maximum at ~260nm indicates that the aromatic body of phenylacetate was catabolized by *Fusarium* sp. strain VM1. No change in the spectrum of phenylacetate was observed with heat inactivated conidia and the substrate, indicating that the aromatic body remained intact over the 10 day period. Therefore, active cultures are solely responsible for the elimination of phenylacetate in the medium.

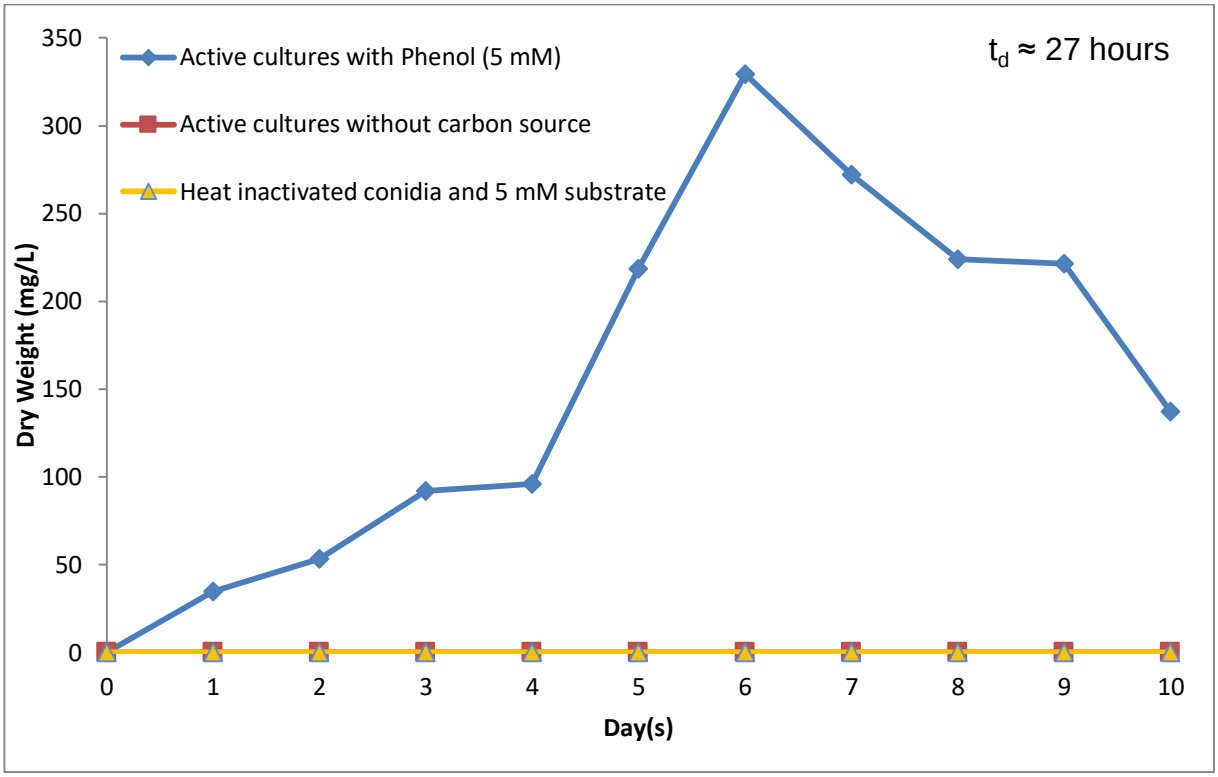

Figure 3.22: Growth of *Fusarium* sp. strain VM1 with 5 mM phenol as the sole carbon source in MSM at 25°C and 100 rpm. Flasks were inoculated with 2 x 10^6 conidia per ml.

The growth curve obtained when *Fusarium* sp. strain VM1 was grown in MSM and 5 mM phenol as sole carbon source for 10 days is shown in Figure 3.22. The initial lag phase lasted for 4 days, followed by an exponential phase from day 4 to day 6. No growth was observed in the absence of the substrate and when using heat inactivated conidia in the presence of 5 mM phenol. The doubling time (t_d) under the specified growth conditions was established as ~27 hours.

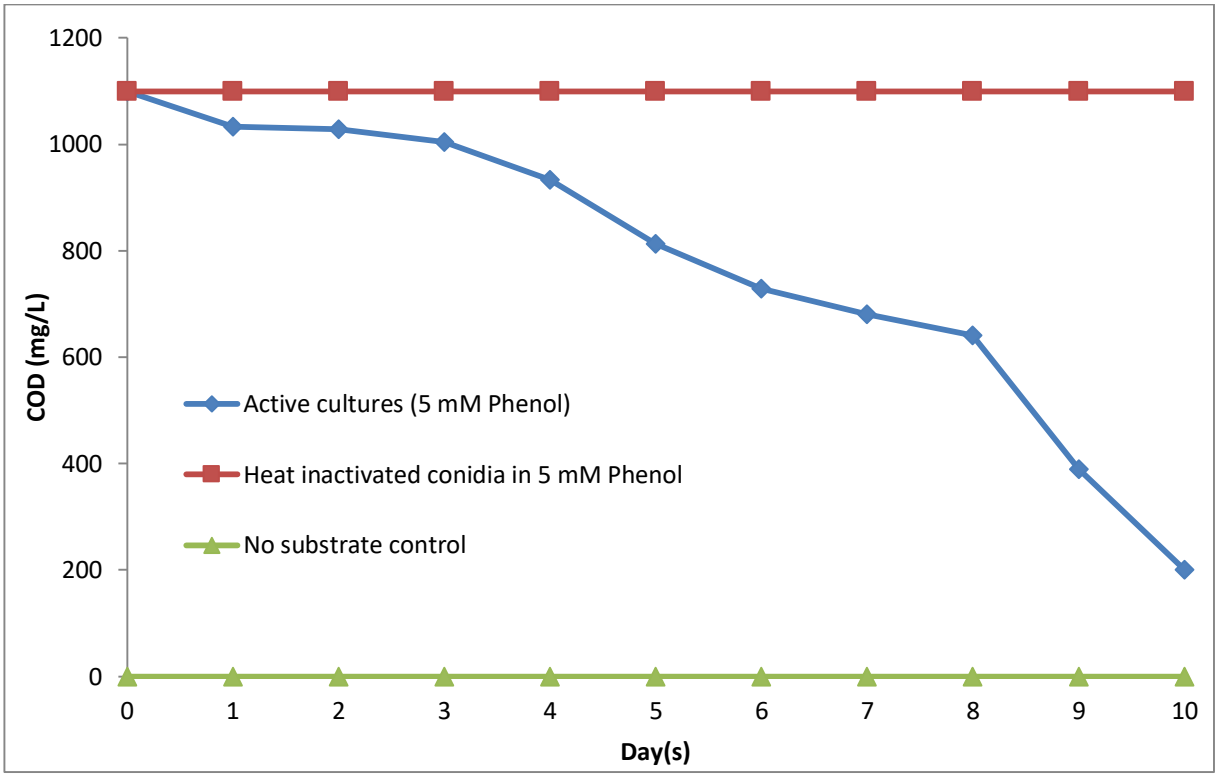

Figure 3.23: COD analysis of *Fusarium* sp. strain VM1 cultures grown with 5 mM phenol as the sole carbon source in MSM at 25°C and 100 rpm. Flasks were inoculated with 2 x 10^6 conidia per ml.

The COD analysis of cultures of *Fusarium* sp. strain VM1 grown in the presence of 5 mM phenol showed that the substrate concentration decreased over time only in active cultures (Figure 3.23). The substrate concentration determined as the COD gradually decreased from day 0 to day 4. Thereafter, a rapid decline in substrate concentration took place, which is in accordance with the initial growth phases observed in the matching growth curve (Figure 3.22). *Fusarium* sp. strain VM1 had the ability to utilize ~82% of 5 mM phenol by day 10. The controls with heat inactivated conidia indicated that the phenol concentration remained stable at a COD of ~1100 mg/L, close to the theoretical COD of 5 mM phenol (1120 mg O_2) and the controls without substrate added show that there was no measureable COD unless phenol was present. The highest molar biomass yield under the specified growth conditions was established as ~49 g dry weight/M substrate consumed.

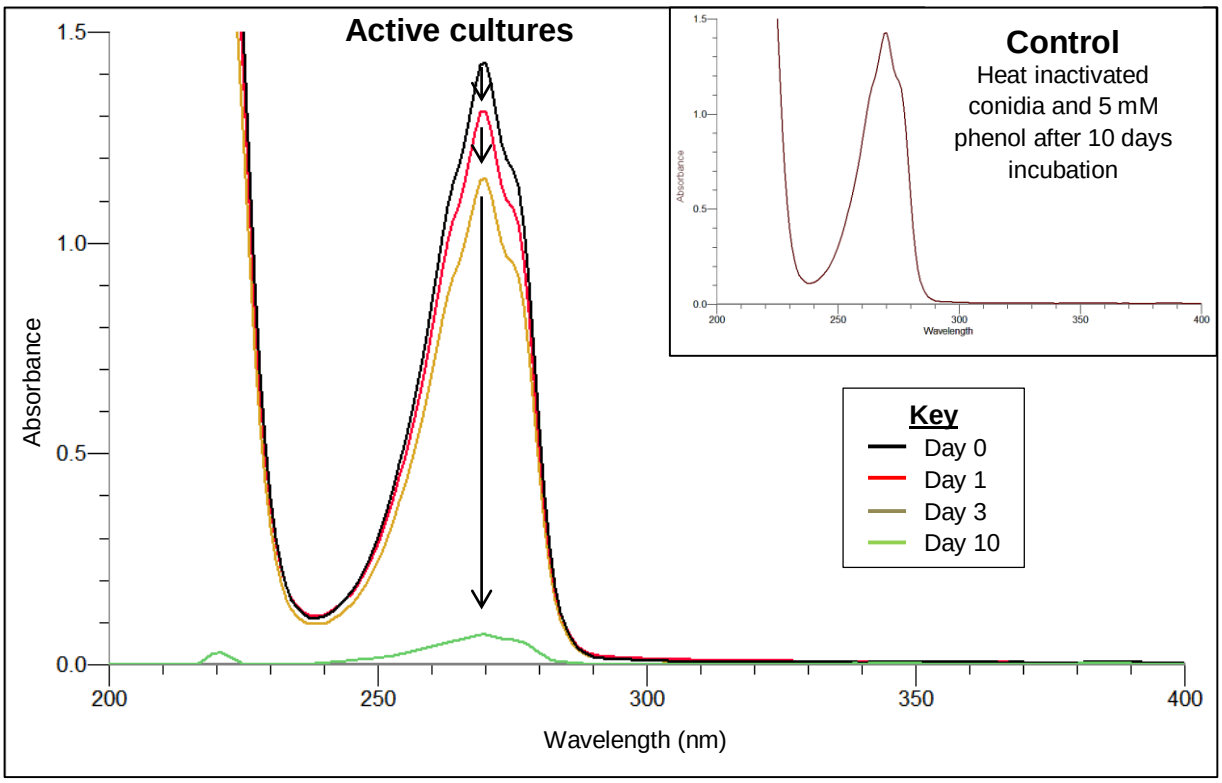

Figure 3.24: UV-Vis spectral analysis of the catabolism of 5 mM phenol in MSM in the presence of *Fusarium* sp. strain VM1 in cultures incubated at 25°C and 100 rpm from day 0 to day 10. The insert graph shows the UV-Vis spectrum for the abiotic control after 10 days.

Culture supernatants analysed by UV-Vis spectroscopy demonstrated that active cultures were responsible for the catabolism of phenol over time (Figure 3.24). The decrease in the absorbance at 270nm indicates that the aromatic compound was catabolised by *Fusarium* sp. strain VM1. However, the aromatic body had not been completely catabolized by strain VM1 since about ~18% of phenol was still in solution on day 10, which is in accordance with the COD analysis in Figure 3.23. Based on the molar extinction coefficient of phenol at 270nm (ε = 1700 L x mol^{-1} x cm^{-1}) (Mach *et al*., 1992), the concentration of phenol at day 0, 1, 3 and 10 had decreased to 10%, 24%, 40% and 96% of the initial concentration respectively. Therefore, about 86% phenol was utilized by the fungus by day 10, matching the COD analysis (Figure 3.22). The abiotic control (with heat inactivated conidia and the substrate) shows that the aromatic body of phenol remained stable over the 10 day period. Therefore, only in the presence of active cultures phenol was eliminated from the medium.

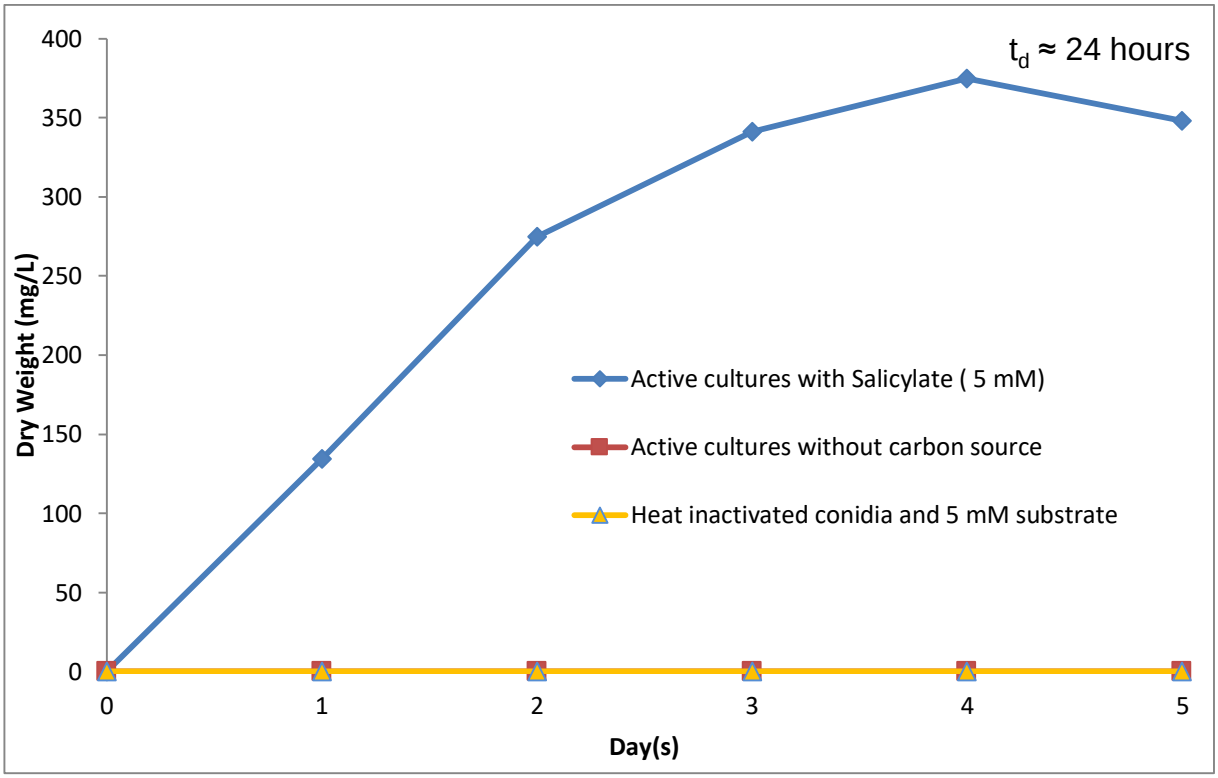

Figure 3.25: Growth of *Fusarium* sp. strain VM1 with 5 mM salicylate as the sole carbon source in MSM at 25°C and 100 rpm. Flasks were inoculated with 2 x 10^6 conidia per ml.

When the fungus, *Fusarium* sp. strain VM1, was grown in MSM and 5 mM salicylate as sole carbon source, an exponential growth phase without a lag phase was evident, until day 4 (Figure 3.25). Thereafter, a death phase was evident from day 4 to day 5. No growth was observed in the absence of the substrate and with heated inactivated conidia in the presence of 5 mM substrate. The doubling time (t_d) under the specified growth conditions was established as ~24 hours.

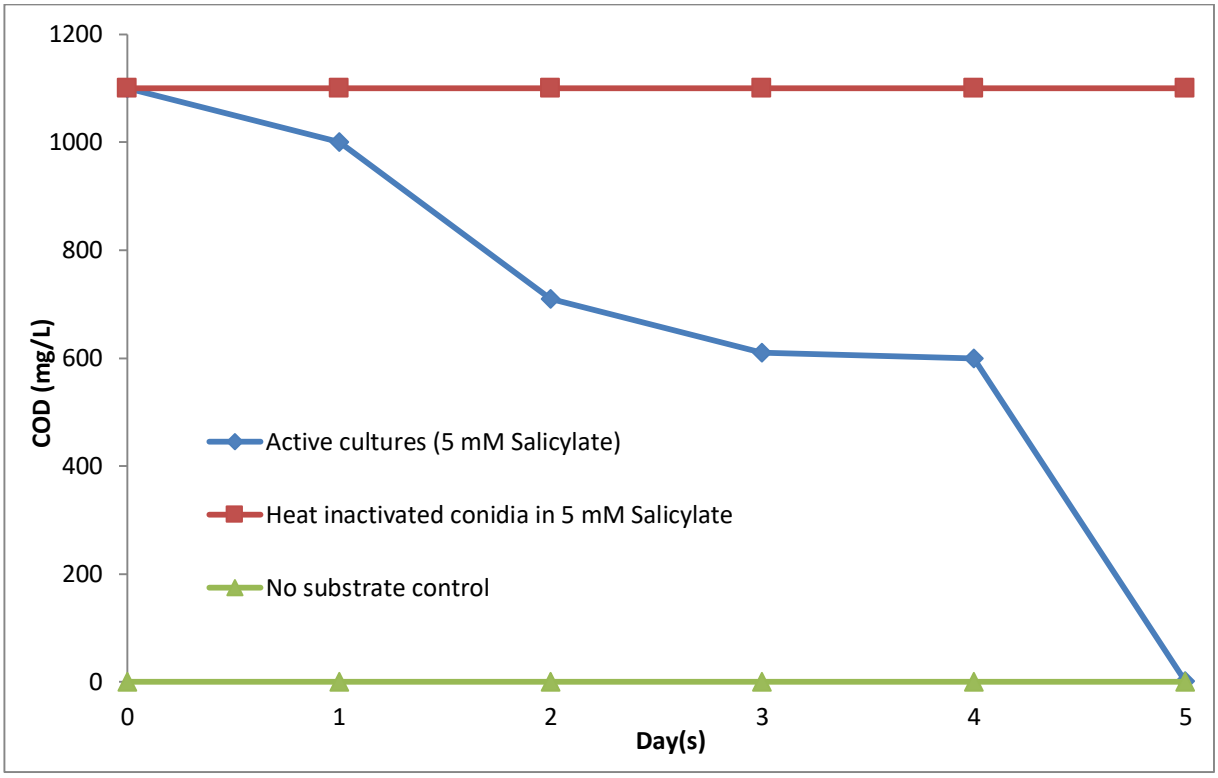

Figure 3.26: COD analysis of *Fusarium* sp. strain VM1 cultures grown with 5 mM salicylate as the sole carbon source in MSM at 25°C and 100 rpm. Flasks were inoculated with 2 x 10^6 conidia per ml.

The COD analysis of cultures of strain VM1 in the presence of 5 mM salicylate showed that the substrate concentration decreased quantitatively over 5 days (Figure 3.26). 5 mM salicylate was completely catabolized by *Fusarium* sp. strain VM1 by day 5. The controls with heat inactivated conidia indicated that the substrate concentration remained stable at ~1100 COD mg/L, close to the theoretical COD of 5 mM salicylate (1120 mg O_2) and the controls without added substrate showed that there was no measureable COD unless salicylate was present. The highest molar biomass yield under the specified growth conditions was established as ~42 g/M substrate.

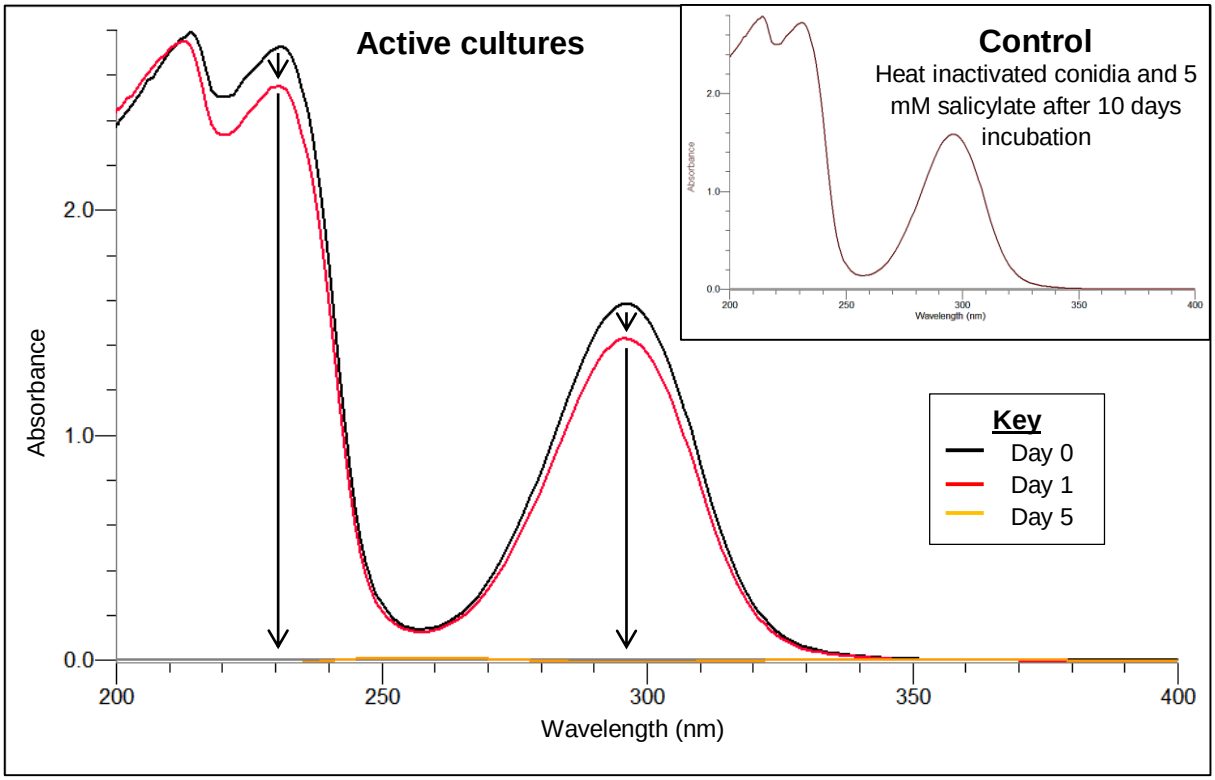

Figure 3.27: UV-Vis spectral analysis of the catabolism of 5 mM salicylate in MSM in the presence of *Fusarium* sp. strain VM1 in cultures incubated at 25°C and 100 rpm from day 0 to day 5. The insert graph shows the UV-Vis spectrum for the abiotic control after 5 days.

No observable change in the UV-Vis spectrum of salicylate was observed after 5 days in cultures with heat inactivated conidia, demonstrating that the aromatic body of salicylate remained intact throughout the incubation period. However, in the presence of active cultures, salicylate was catabolized over time (Figure 3.27). The decrease of the absorbance maxima at 230nm and ~300nm indicates that the aromatic body of salicylate was completely catabolized by *Fusarium* sp. strain VM1 by day 5, which is in accordance with Figure 3.26. The concentration of salicylate had decreased on day 5 to only 0.03 mM according to the molar extinction coefficient of salicylate at 295nm (ε = 3840 L x mol^{-1} x cm^{-1}) (Ungar *et al*., 1952), confirming the COD analysis. Therefore, only active cultures of *Fusarium* sp. strain VM1 eliminated salicylate in the medium.

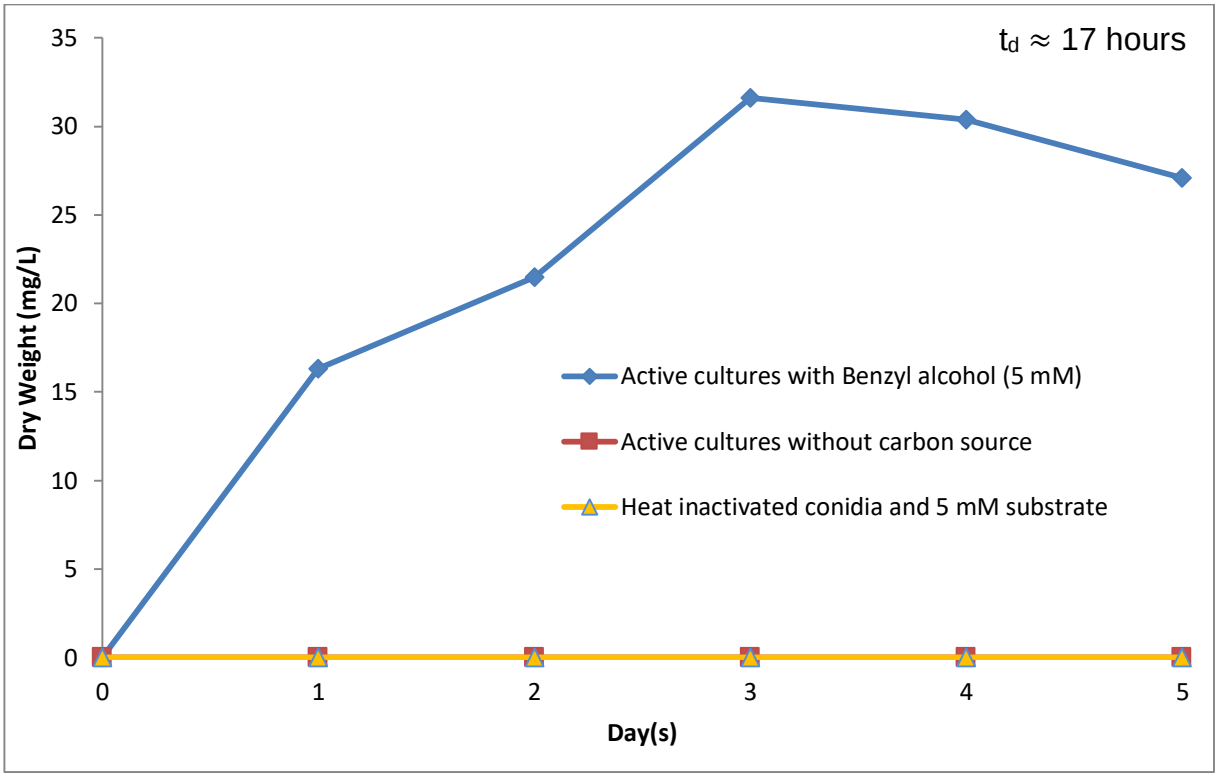

Figure 3.28: Growth of *Fusarium* sp. strain VM1 with 5 mM benzyl alcohol as the sole carbon source in MSM at 25°C and 100 rpm. Flasks were inoculated using 2 x 10^6 conidia per ml.

Figure 3.28 shows the growth of *Fusarium* sp. strain VM1 when incubated in MSM and 5 mM benzyl alcohol as sole source of carbon and energy. Initially, there was a rapid increase in biomass until day 3, indicating exponential growth. A decrease in biomass occurred from day 3 to day 5, possibly representing the stationary phase followed by the death phase. No growth was observed in the absence of the substrate or any other carbon source and when heat inactivated conidia were incubated in the presence of 5 mM substrate. The doubling time (t_d) under the specified growth conditions was established as ~17 hours.

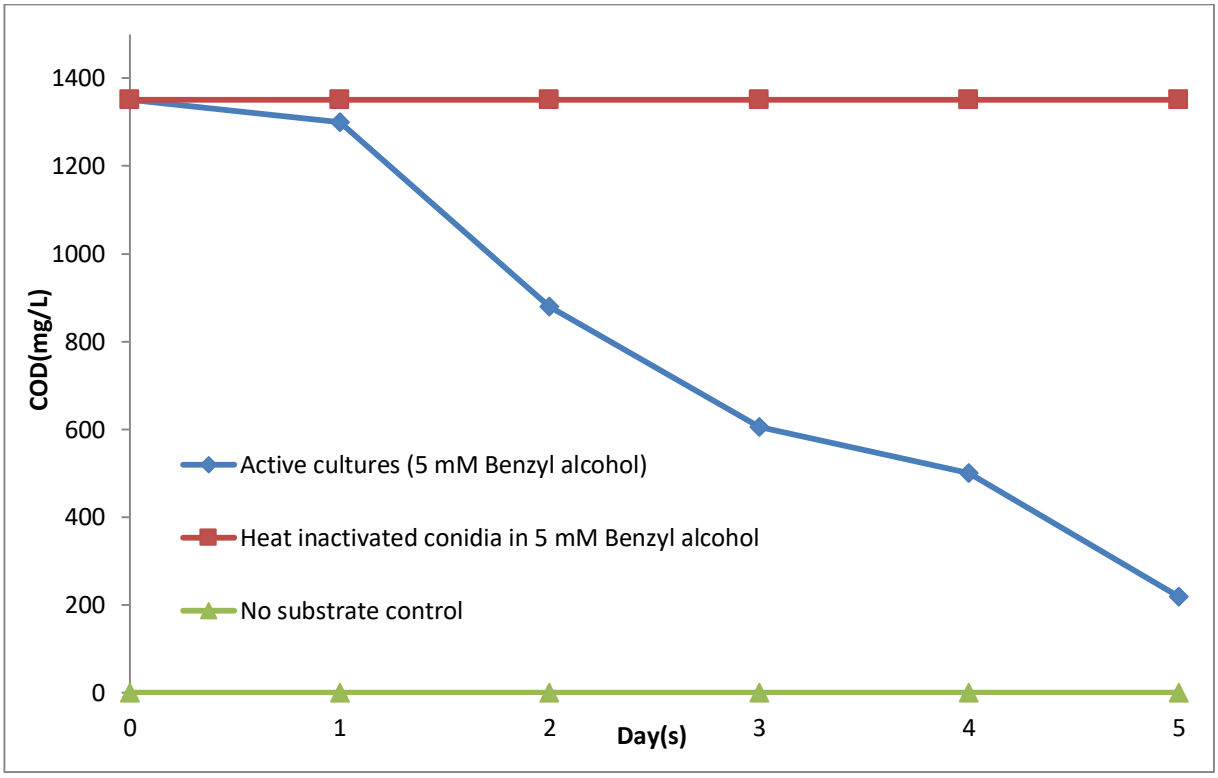

Figure 3.29: COD analysis of *Fusarium* sp. strain VM1 cultures grown with 5 mM benzyl alcohol as the sole carbon source in MSM at 25°C and 100 rpm. Flasks were inoculated using 2 x 10^6 conidia per ml.

The COD analysis of cultures of strain VM1 in the presence of 5 mM benzyl alcohol as sole carbon source showed that the substrate concentration decreased over time only in active cultures (Figure 3.29). The substrate concentration determined as the COD decreased rapidly over the 5 day period, which nicely matched the growth curve pattern (Figure 3.28). Judged by the COD, ~83% of 5 mM benzyl alcohol was catabolized by *Fusarium* sp. strain VM1 by day 5. The controls with heat inactivated conidia indicated that the substrate concentration remained stable at ~1350 COD mg/L, close to the theoretical COD of 5 mM benzyl alcohol (1360 mg O_2) and controls without added substrate showed that there was no measureable COD unless benzyl alcohol was present. The highest molar biomass yield under the specified growth conditions was established as ~55 g/M substrate.

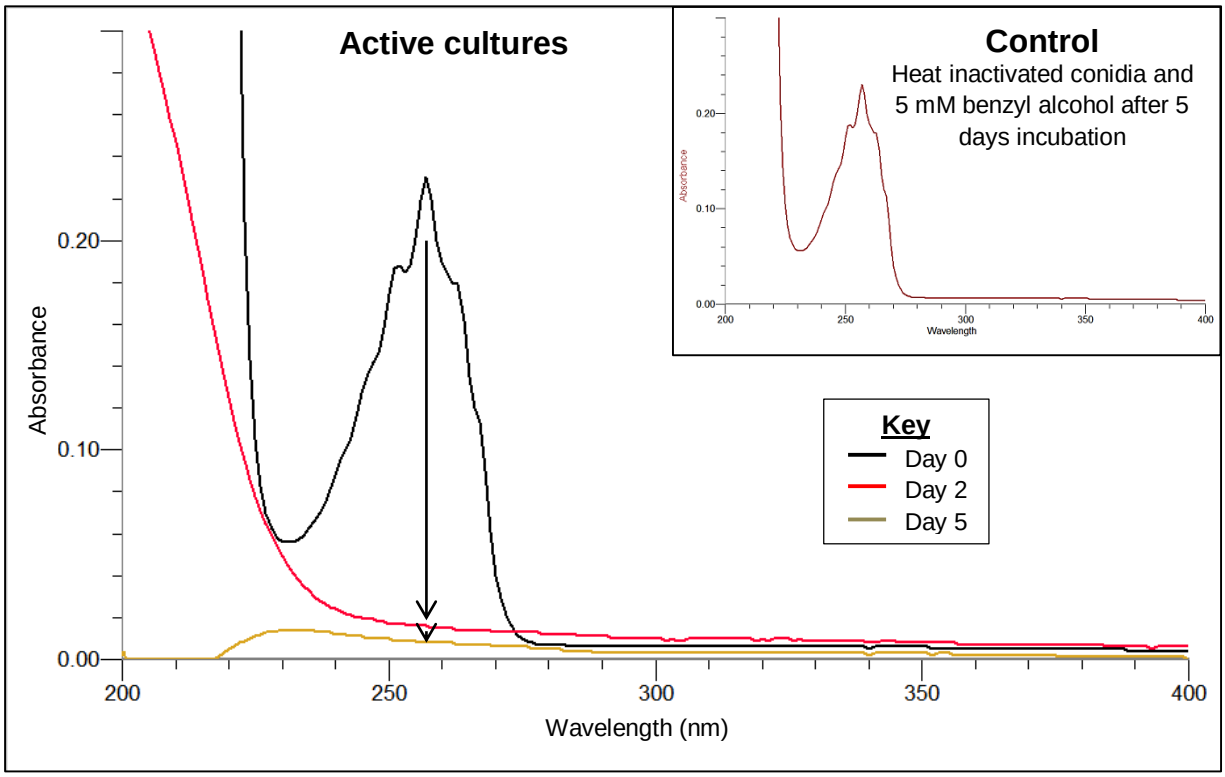

Figure 3.30: UV-Vis spectral analysis of the catabolism of 5 mM benzyl alcohol in MSM in the presence of *Fusarium* sp. strain VM1 cultures incubated at 25°C and 100 rpm from day 0 to day 5. The insert graph shows the UV-Vis spectrum for the abiotic control after 5 days.

The culture supernatants, when analysed via UV-Vis spectroscopy, demonstrated that only in the presence of active cultures, the aromatic body of benzyl alcohol (exhibiting a clear absorbance maximum at 256nm) was catabolized over time (Figure 3.30). The disappearance of the distinct absorbance maximum at 256nm indicated that the aromatic body of benzyl alcohol was catabolized by *Fusarium* sp. strain VM1. The abiotic control with heat inactivated conidia and substrate shows that the aromatic body of benzyl alcohol remained stable over the 5 day period. Therefore, active cultures are solely responsible for the disappearance of benzyl alcohol in the medium.

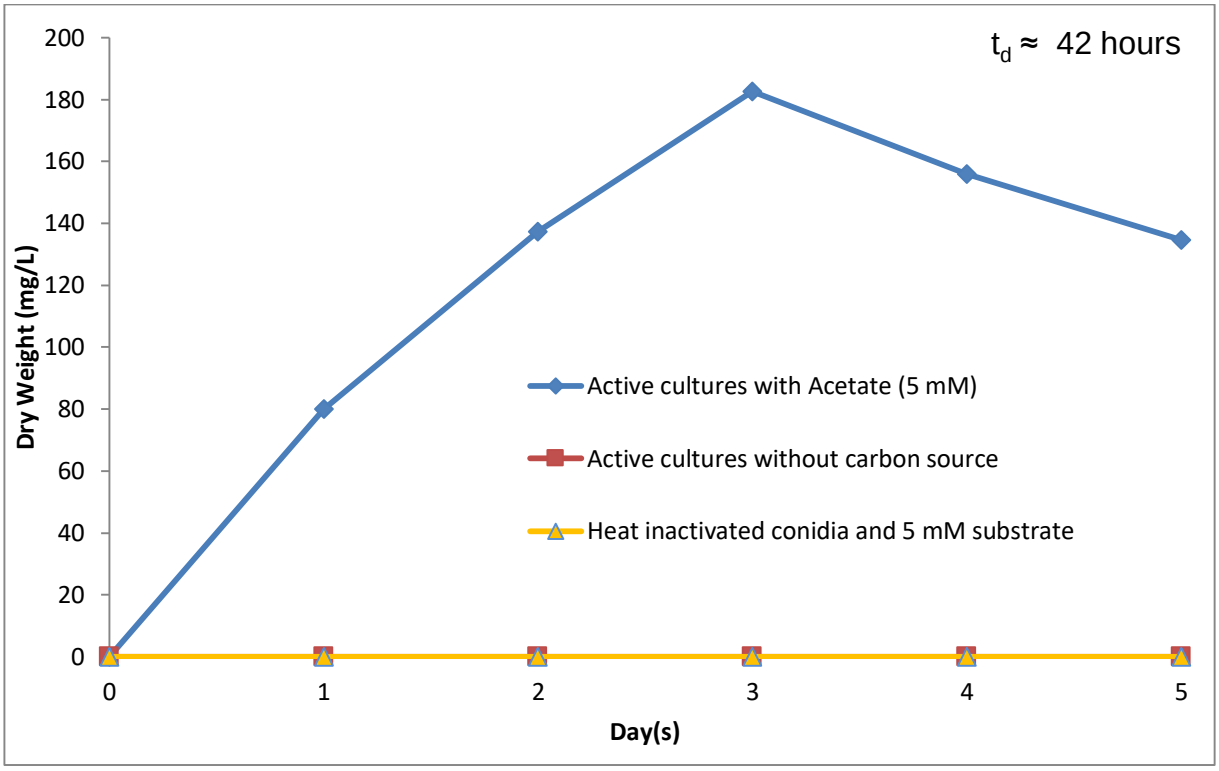

Figure 3.31: Growth of *Fusarium* sp. strain VM1 with 5 mM acetate as the sole carbon source in MSM at 25°C and 100 rpm. Flasks were inoculated using 2 x 10^6 conidia per ml.

Figure 3.31 shows the growth of strain VM1 in the presence of 5 mM acetate as sole carbon and energy. Initially, a rapid, exponential increase in biomass occurred until day 3, followed by the death phase. No growth was observed in the absence of the substrate and when heat inactivated conidia were incubated in the presence of 5 mM substrate. The doubling time (t_d) under the specified growth conditions was established as ~42 hours.

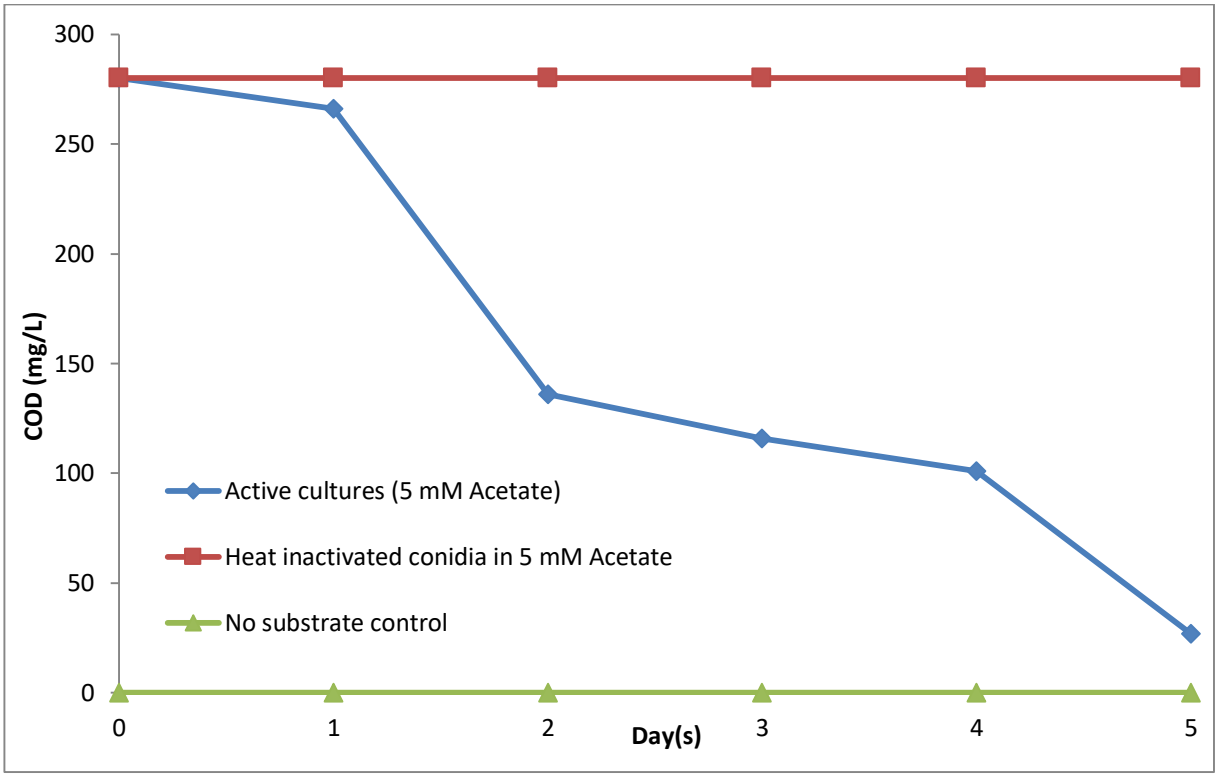

Figure 3.32: COD analysis of *Fusarium* sp. strain VM1 cultures grown with 5 mM acetate as the sole carbon source in MSM at 25°C and 100 rpm. Flasks were inoculated using 2 x 10^6 conidia per ml.

The COD analysis of cultures of strain VM1 in the presence of 5 mM acetate showed that the substrate concentration decreased over time (Figure 3.32). The substrate concentration determined as the COD decreased rapidly over the 5 day period until ~90% of 5 mM acetate was catabolized by the fungus. This is in accordance with the growth curve pattern (Figure 3.31). The controls with the heat inactivated conidia indicated that the substrate concentration remained stable at a COD of ~280 mg/L, which is close to the theoretical COD of 5 mM acetate (320 mg O_2). The controls without the substrate added show that there was no measureable COD, unless the substrate was present. The highest biomass yield under the specified growth conditions was established as ~38 g/M substrate.

3.3. Growth of *Fusarium* sp. strain VM1 with different concentrations of the target compounds

For the optimum growth of microorganisms, the concentration of the growth substrate needs to meet the threshold concentration that the microorganism will thrive at. A concentration of the growth substrate that is lower or higher than the threshold concentration can significantly reduce the growth of the microorganism. High concentrations may even exhibit toxic effects, thus hindering the growth of the microorganism.

Therefore, the effect of varying concentrations of the target compounds (salol, benzyl salicylate, phenylacetate, phenol, salicylate, benzyl alcohol and acetate) on the growth of strain VM1 was determined in Mineral Salts Medium at different concentrations of the target compounds as sole carbon and energy source.

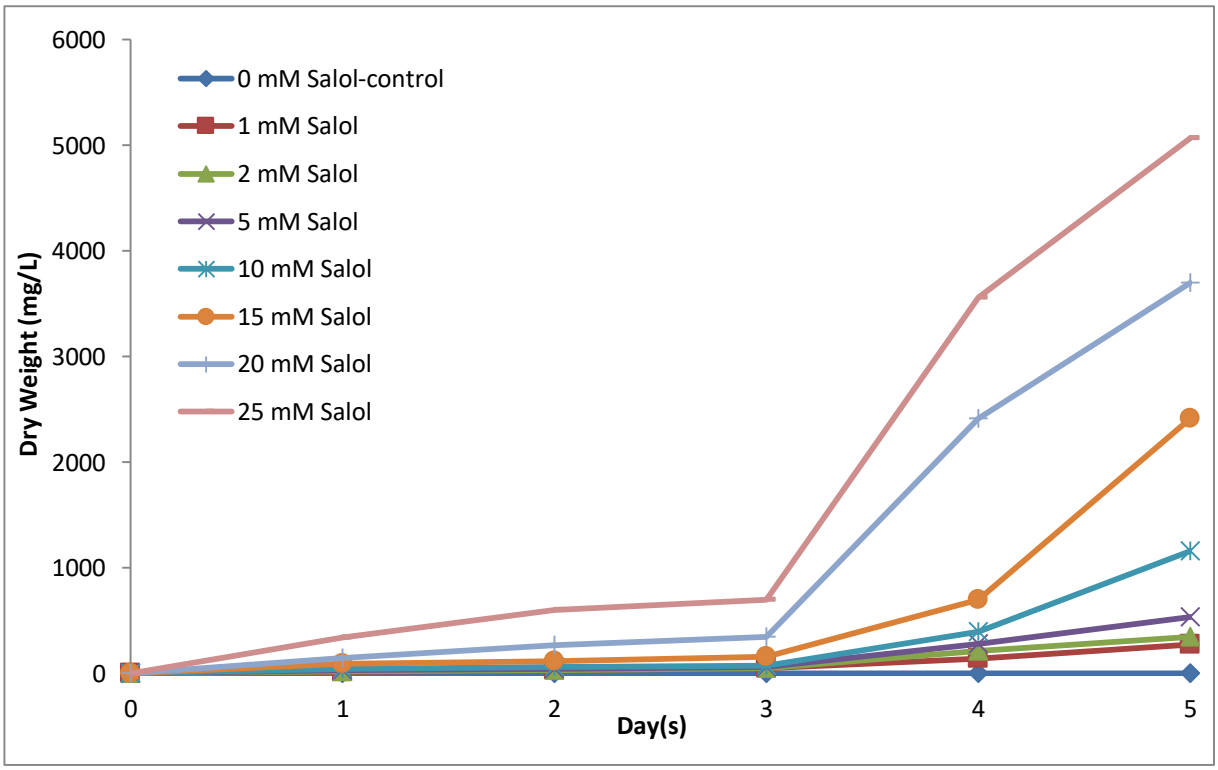

Figure 3.33: Growth of *Fusarium* sp. strain VM1 in the presence of varying concentrations of salol as the sole carbon source in MSM at 25°C and 100 rpm when inoculated with 2 x 10^6 conidia per ml.

The growth of *Fusarium* sp. strain VM1 increased in the presence of increased concentrations of salol (Figure 3.33). The highest quantity of biomass was produced at 25 mM phenyl salicylate, while no growth was observed when there was no carbon source present in the medium. Within the tested concentration range, growth inhibition was not evident.

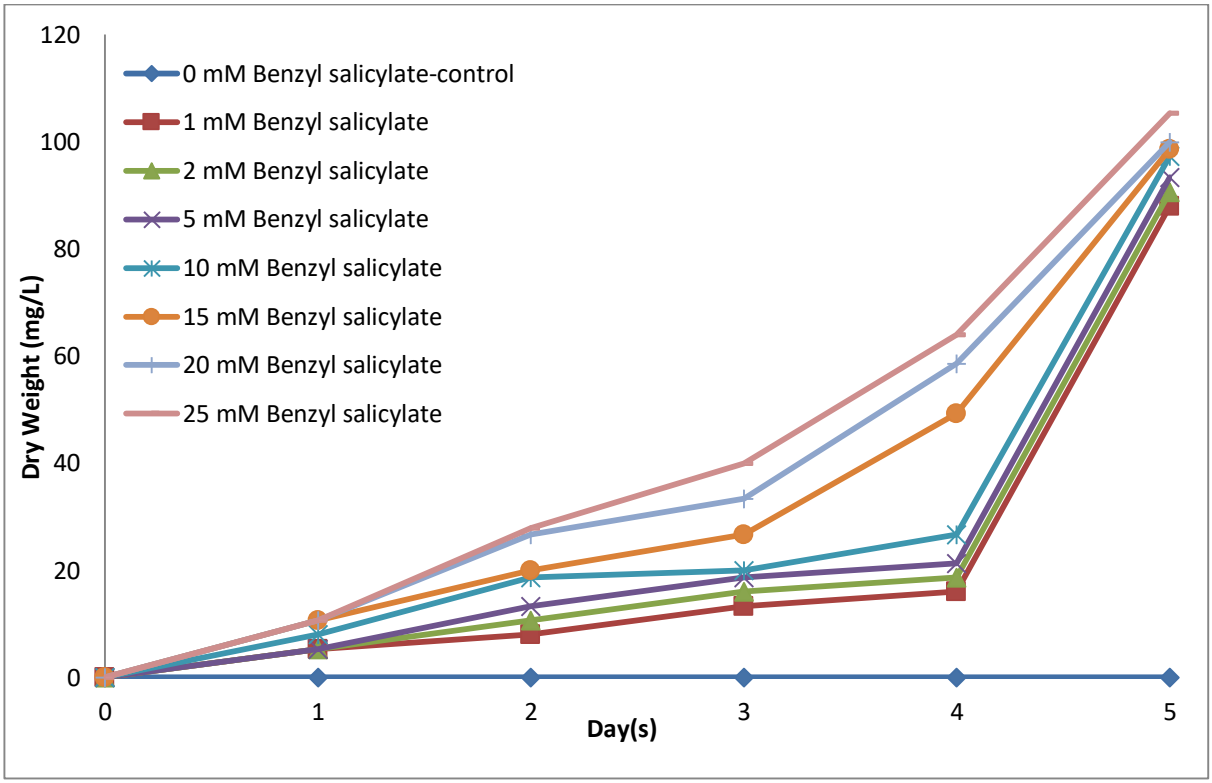

Figure 3.34: Growth of *Fusarium* sp. strain VM1 in the presence of varying concentrations of benzyl salicylate as the sole carbon source in MSM at 25°C and 100 rpm when inoculated with 2 x 10^6 conidia per ml.

Figure 3.34 shows the growth of strain VM1 in the presence of varying concentrations of benzyl salicylate. The highest biomass production of the fungus was at a concentration of 25 mM benzyl salicylate on day 5, whereas the lowest biomass produced was at a concentration of 1 mM benzyl salicylate on day 5. No growth was observed in the control (0mM benzyl salicylate). Similar to salol, benzyl salicylate showed no evident toxicity even at the highest concentration tested.

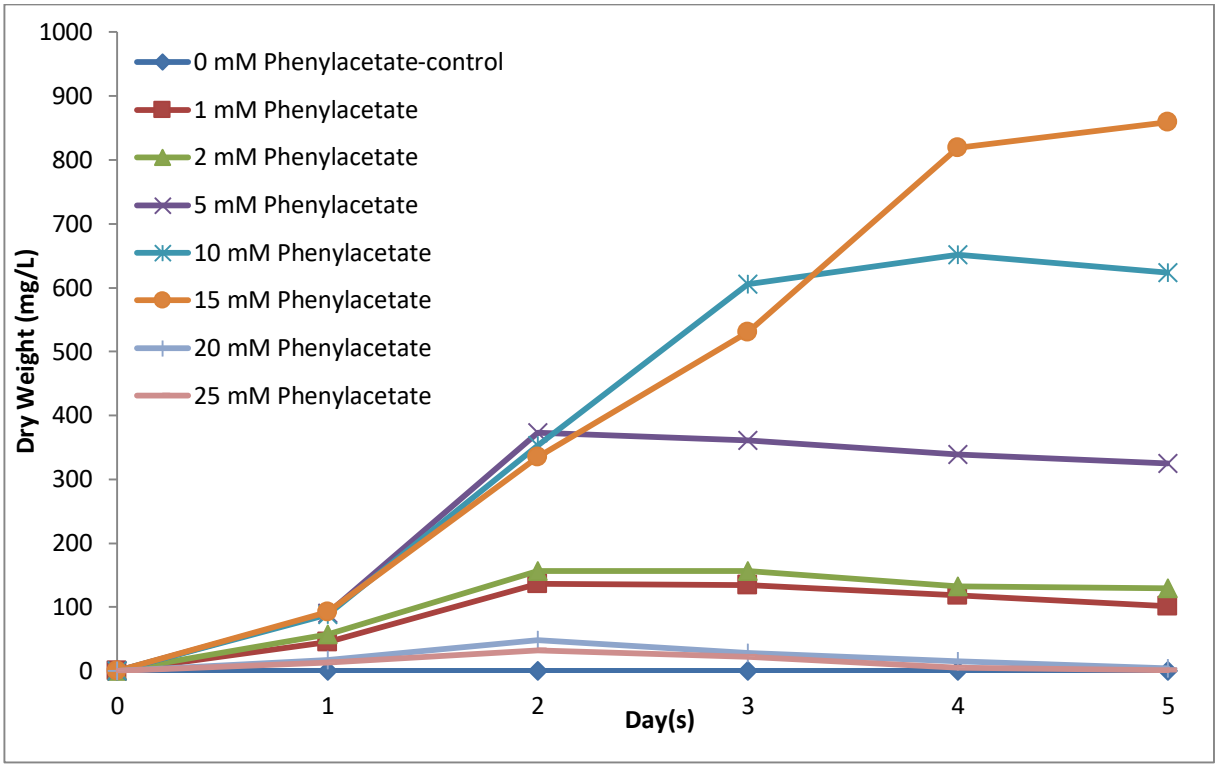

Figure 3.35: Growth of *Fusarium* sp. strain VM1 in the presence of varying concentrations of phenylacetate as the sole carbon source in MSM at 25°C and 100 rpm when inoculated with 2 x 10^6 conidia per ml.

Figure 3.35 shows that the growth of *Fusarium* sp. strain VM1 was almost completely inhibited at concentrations of phenylacetate ≥20 mM. However, the biomass production of strain VM1 increased with an increase in the concentrations of phenylacetate up to 15 mM, with the highest biomass detected after 5 days at 15 mM phenylacetate, again matching the growth experiments with 10 mM phenylacetate (Figure 3.19). There was no growth observed in the absence of the substrate.

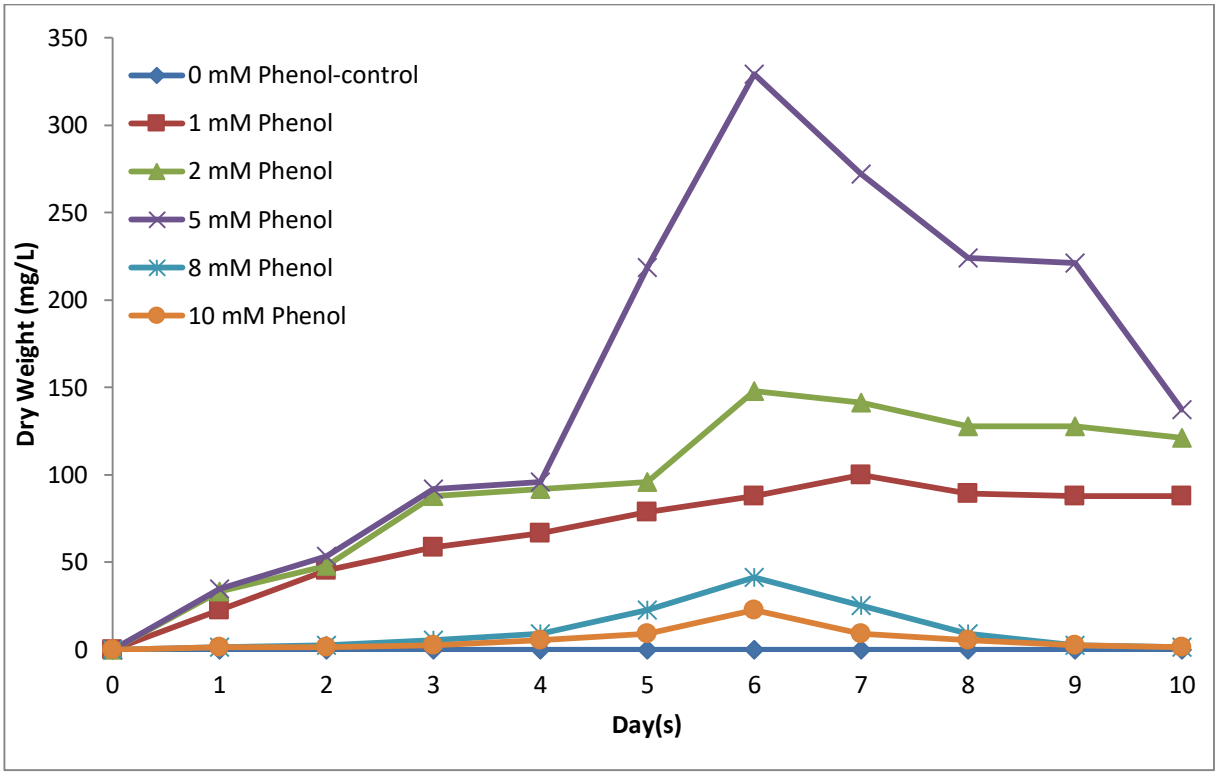

Figure 3.36: Growth of *Fusarium* sp. strain VM1 in the presence of varying concentrations of phenol as the sole carbon source in MSM at 25°C and 100 rpm when inoculated with 2 x 10^6 conidia per ml.

As demonstrated in Figure 3.36, no observable growth was exhibited in the absence of phenol. However, biomass formation increased with the increase in substrate concentration of up to 5 mM phenol. At phenol concentrations exceeding 5 mM, the biomass formation was severely reduced. The highest amount of biomass was produced at 5 mM phenol whereas the lowest amount of biomass was produced at 10 mM phenol, highlighting potentially toxic effects of the substrate at such elevated concentrations.

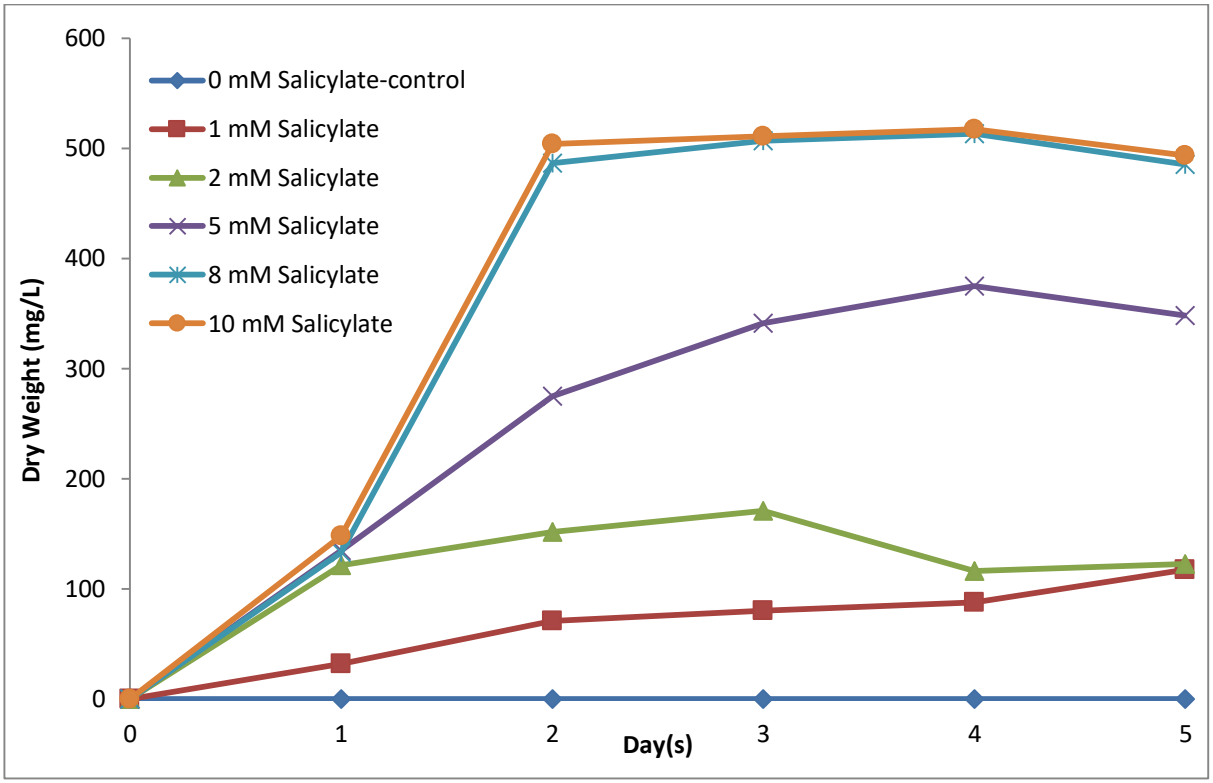

Figure 3.37: Growth of *Fusarium* sp. strain VM1 in the presence of varying concentrations of salicylate as the sole carbon source in MSM at 25°C and 100 rpm when inoculated with 2 x 10^6 conidia per ml.

The growth of *Fusarium* sp. strain VM1 increased with an increase in concentration of salicylate (Figure 3.37). Even though the highest amount of biomass was produced at 10 mM salicylate after 5 days incubation but only slightly exceeding that observed at 8 mM salicylate, the graph indicates that ≥8 mM salicylate becomes possibly toxic, matching the biocidal effect observed for phenol at 10 mM. However, as expected, no growth was observed in the absence of the carbon source.

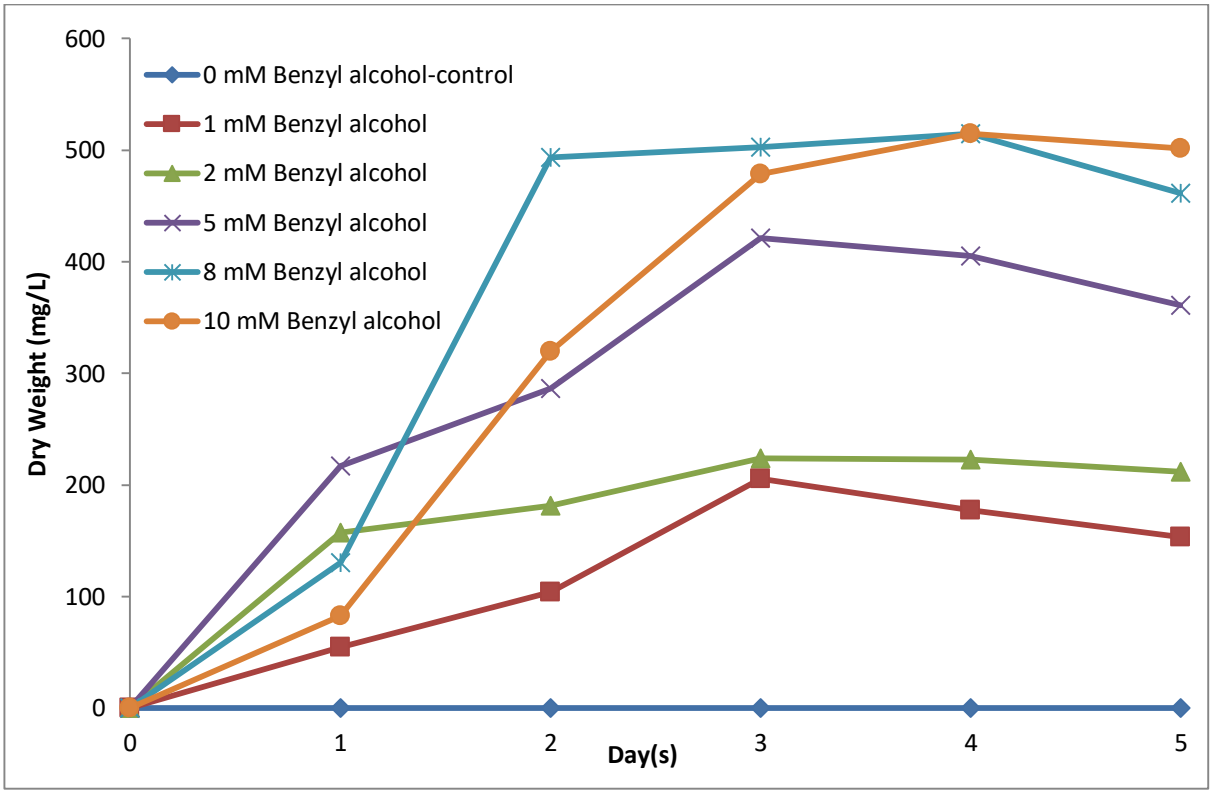

Figure 3.38: Growth of *Fusarium* sp. strain VM1 in the presence of varying concentrations of benzyl alcohol as the sole carbon source in MSM at 25°C and 100 rpm when inoculated with 2 x 10^6 conidia per ml.

The biomass production of strain VM1 increased in the presence of increased concentrations of benzyl alcohol (Figure 3.38). The highest amount of biomass was produced for both 8 mM and 10 mM benzyl alcohol on day 4. No growth was observed in the absence of benzyl alcohol.

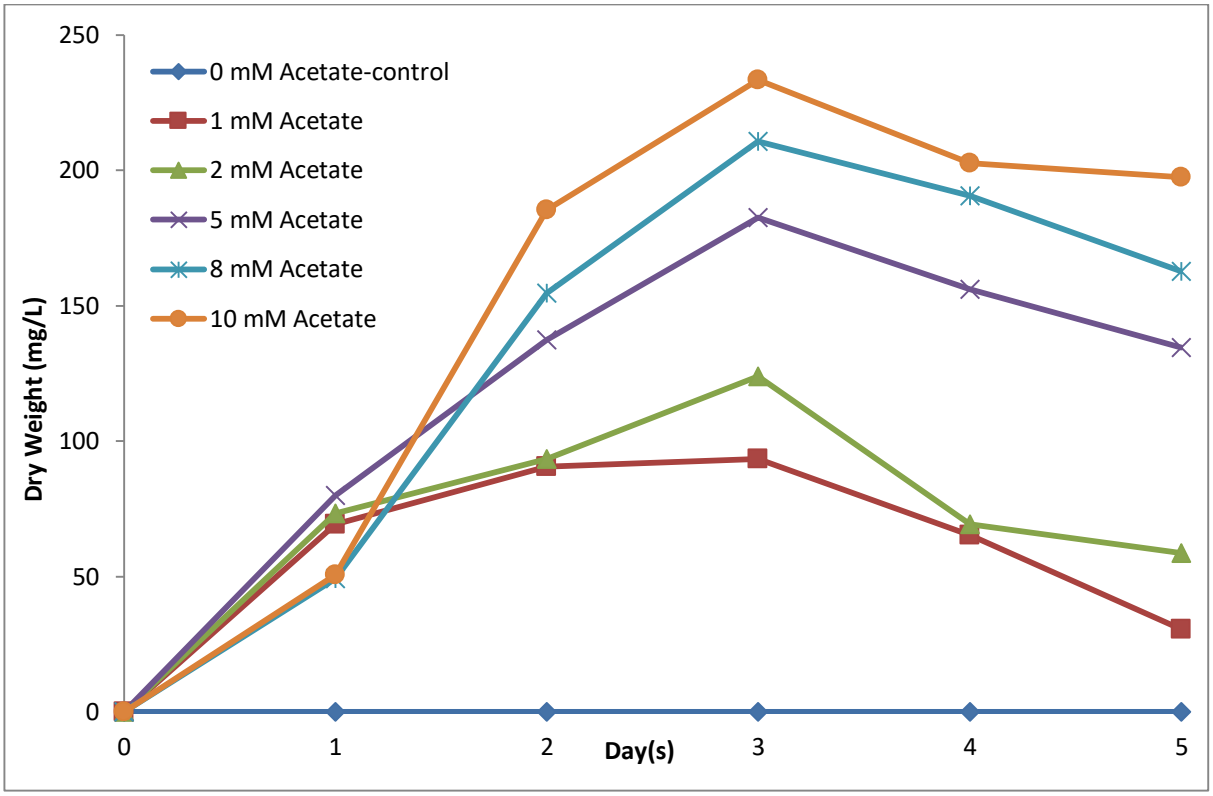

Figure 3.39: Growth of *Fusarium* sp. strain VM1 in the presence of varying concentrations of acetate as the sole carbon source in MSM at 25°C and 100 rpm when inoculated with 2 x 10^6 conidia per ml.

Figure 3.39 shows the growth of strain VM1 in the presence of varying concentrations of acetate. The growth of the fungus increased with increasing concentrations of acetate, with the highest amount of biomass produced at a concentration of 10 mM of acetate after 5 days incubation and the lowest amount of biomass produced at 1 mM acetate. There was no growth observed in the control.

3.4. Growth of *Trichosporon* sp. strain VM2 and utilization of target compounds

To determine whether salol, benzyl salicylate, phenylacetate, phenol, salicylate, benzyl alcohol or acetate can serve as a carbon and energy sources for the growth of the isolated yeast, strain VM2 was initially grown with 10 mM of the diaryl esters and 5 mM of the intermediates as the sole carbon source. The growth was analysed over time via OD_{600} measurements and microscopic cell counts. The substrate utilization was analysed by measuring the Chemical Oxygen Demand and verified by UV-Vis spectroscopy.

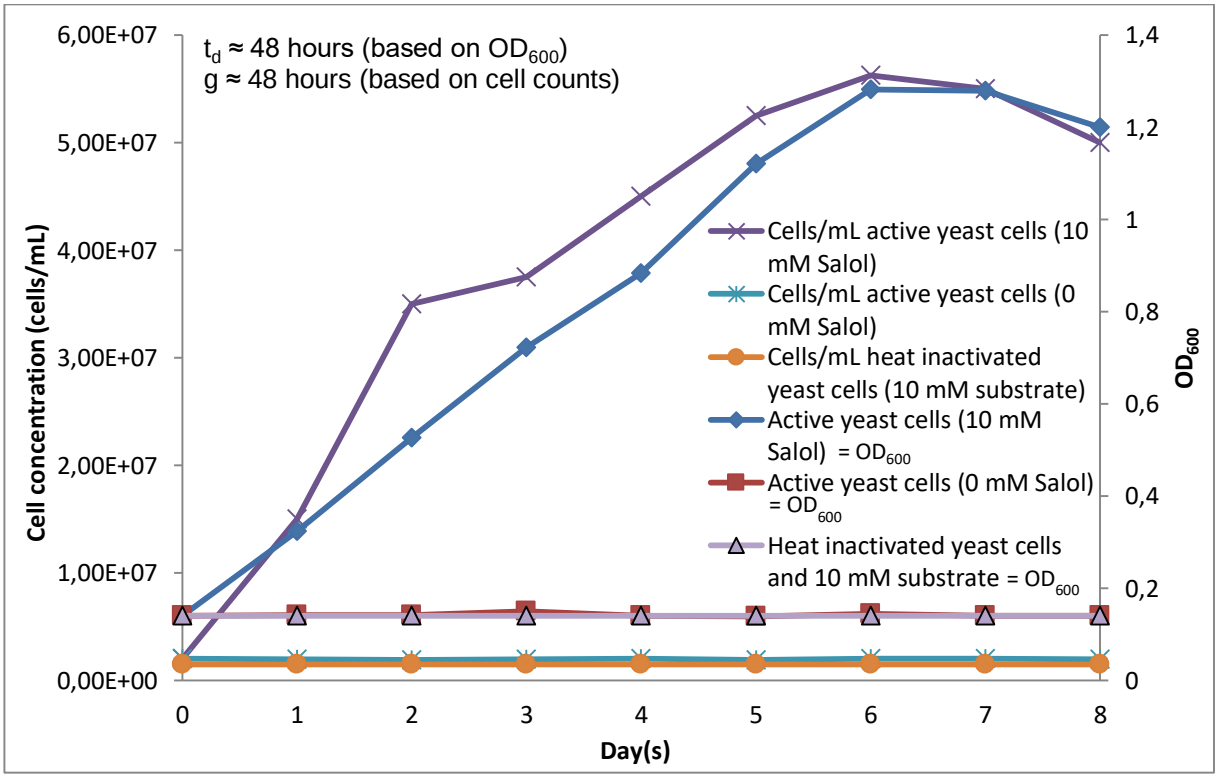

Figure 3.40: Growth of *Trichosporon* sp. strain VM2 with 10mM salol as the sole carbon source in MSM at 25°C and 100 rpm with inoculation of 2 x 10^6 yeast cells per ml.

Figure 3.40 shows the growth of *Trichosporon* sp. strain VM2 when grown over time with 10 mM salol as sole carbon and energy source. Both OD_{600} and microscopic cell counts were used to determine growth of cultures over time. Initially, a rapid increase in biomass occurred until day 6, which related to the exponential phase. Thereafter,

a stationary phase was evident. No increase in growth was observed in the absence of the substrate and with heat inactivated yeast cells in the presence of 10 mM salol. The doubling time (t_d) and generation time (g) under the specified growth conditions was established as ~48 hours and ~48 hours respectively.

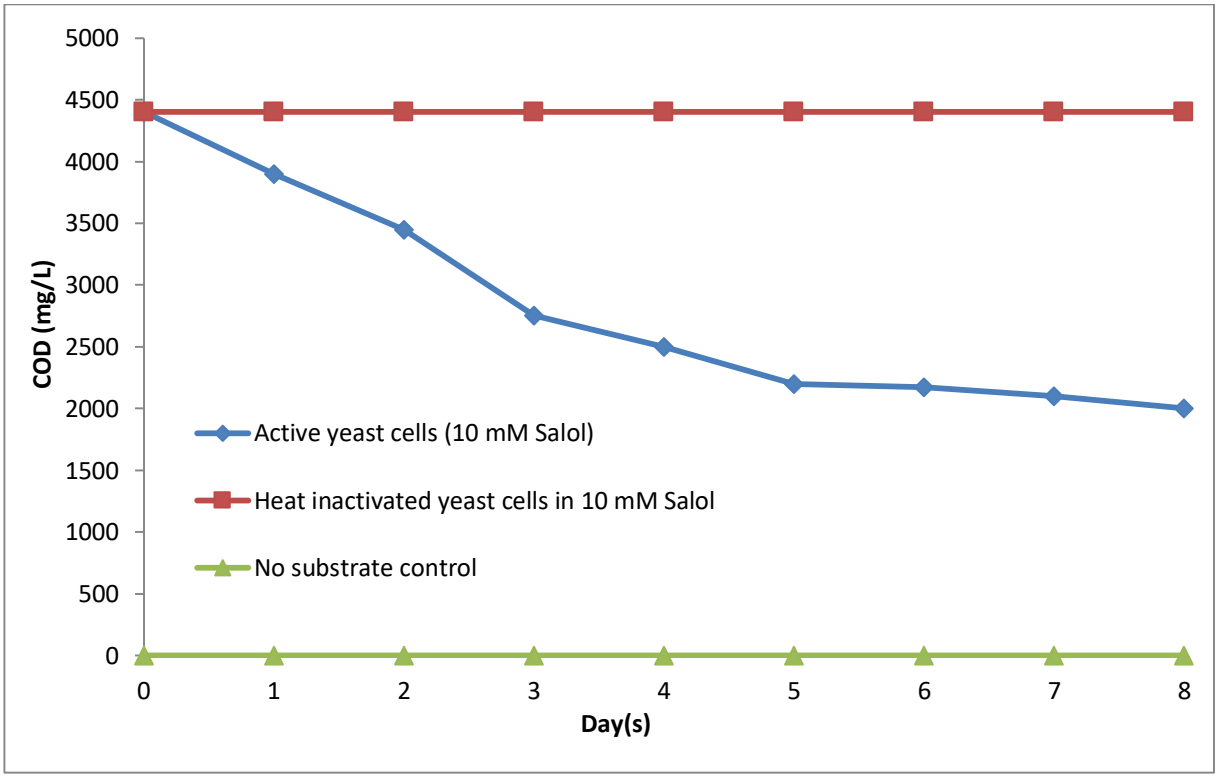

Figure 3.41: COD analysis of *Trichosporon* sp. strain VM2 cultures grown with 10 mM salol as the sole carbon source in MSM at 25°C and 100 rpm with inoculation of 2 x 10^6 yeast cells per ml.

The COD analysis of *Trichosporon* sp. strain VM2 cultures grown in the presence of 10 mM salol showed that the substrate concentration decreased over time (Figure 3.41). The substrate concentration determined as the COD decreased rapidly over the 8 day period until ~55% of 10 mM salol was catabolized by the yeast. This is in accordance with the growth curve pattern, which showed that growth did last until about day 6 (Figure 3.40). The controls with heat inactivated yeast cells indicated that the substrate concentration remained stable at ~4400 COD mg/l, close to the theoretical COD of 10 mM salol (4480 mg O_2) and the controls without substrate added show that there was no measureable COD unless salol was present.

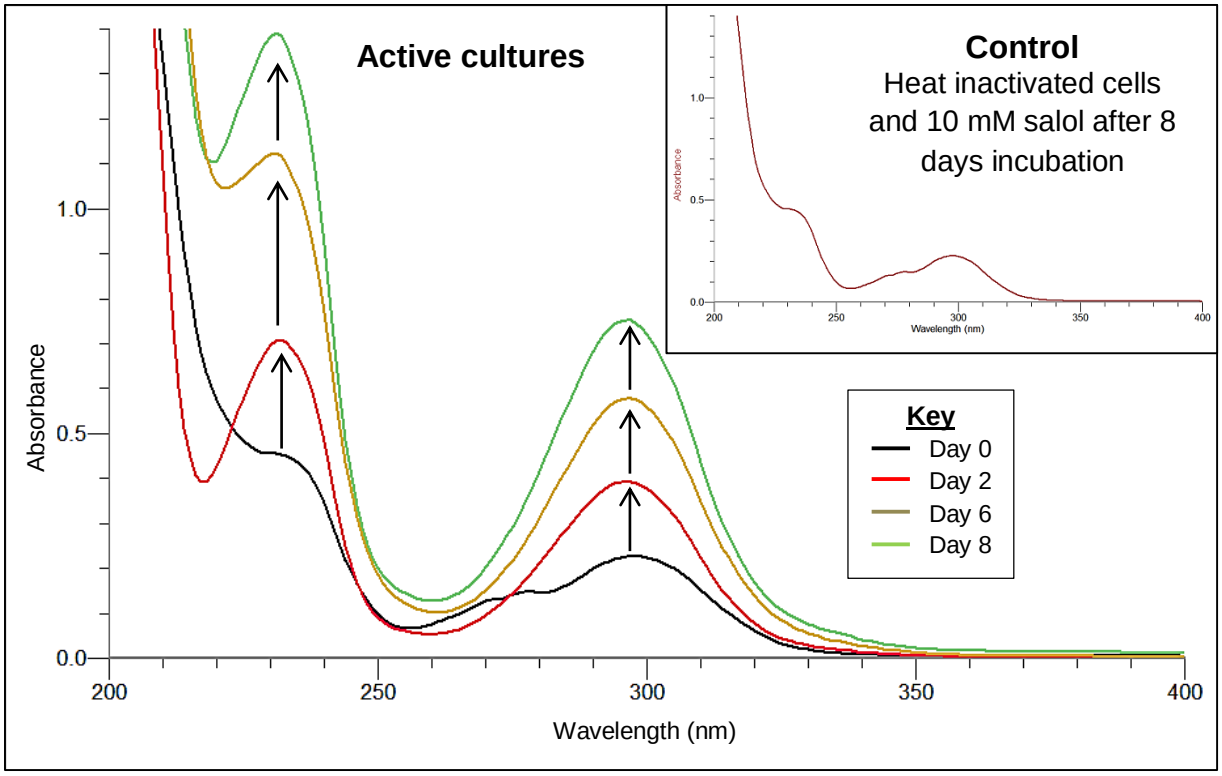

Figure 3.42: UV-Vis spectral analysis of the catabolism of 10 mM salol in MSM in the presence of *Trichosporon* sp. strain VM2 cultures incubated at 25°C and 100 rpm from day 0 to day 8. The insert graph shows the UV-Vis spectrum for the abiotic control after 8 days.

The UV-Vis spectral analysis of the culture supernatants demonstrated that in the presence of active cultures, the aromatic body of salol was partially catabolized over time (Figure 3.42) as an increase in absorbance at 230nm and 290nm indicated that the expected intermediate salicylate accumulated in the medium to ~4 mM on day 8 based on the molecular extinction coefficient of salicylate at 295nm (Ungar *et al*., 1952), thereby matching the COD analysis in Figure 3.41. However, while phenol absorbing at 270nm was obviously catabolized as no accumulation of this intermediate was evident in the spectrum. Therefore, *Trichosporon* sp. strain VM2 has the ability to catabolize the phenol moiety of the diary ester, phenyl salicylate after hydrolysis of the ester bond. The abiotic control with heat inactivated yeast cells and the substrate, shows that the aromatic body of phenyl salicylate remained stable over the 8 day period.

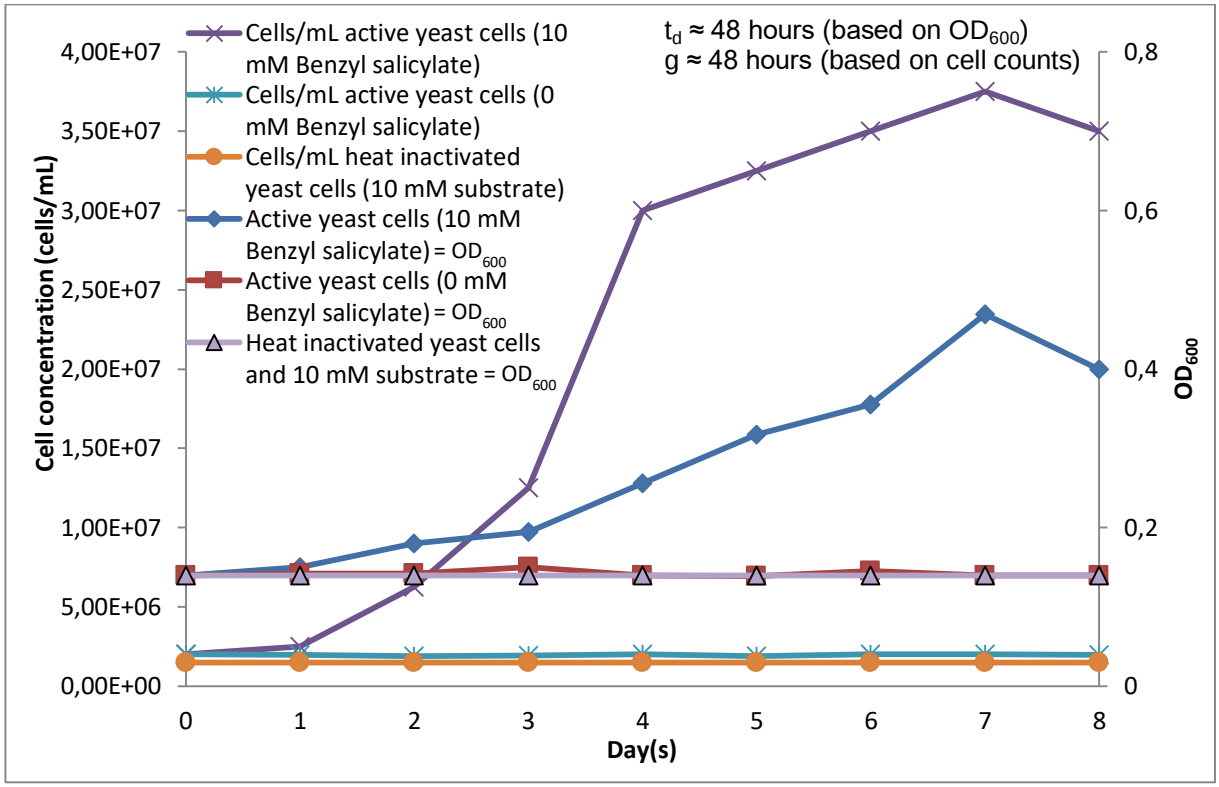

Figure 3.43: Growth of *Trichosporon* sp. strain VM2 with 10mM benzyl salicylate as the sole carbon source in MSM at 25°C and 100 rpm with inoculation of 2 x 10^6 yeast cells per ml.

The growth kinetics for *Trichosporon* sp. strain VM2 when grown in 10 mM benzyl salicylate over time (Figure 3.43) demonstrated that OD_{600} and microscopic cell counts both follow the same pattern. After an initial lag phase of about 1 day, an exponential phase followed until day 7. In the absence of the substrate and with heat inactivated yeast cells in the presence of 10 mM benzyl salicylate, there was no observable increase in growth. The doubling time (t_d) and generation time (g) under specified growth conditions was established as ~48 hours and ~48 hours.

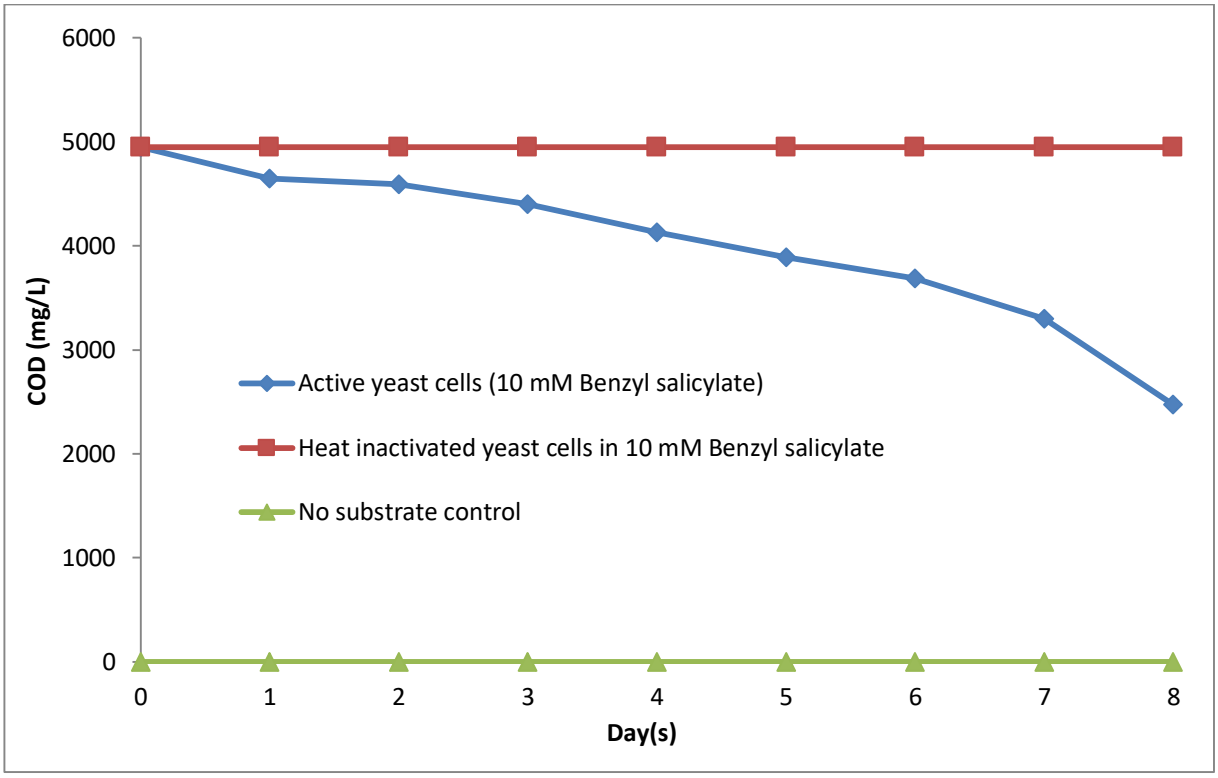

Figure 3.44: COD analysis of *Trichosporon* sp. strain VM2 cultures grown with 10 mM benzyl salicylate as the sole carbon source in MSM at 25°C and 100 rpm with inoculation of 2 x 10^6 yeast cells per ml.

The COD analysis of strain VM2 cultures when growing in the presence of 10 mM benzyl salicylate showed that the substrate concentration decreased over time (Figure 3.44). The substrate concentration determined as the COD gradually decreased over the 8 day period until ~50% of 10 mM benzyl salicylate was catabolized by strain VM2. The controls with heat inactivated yeast cells indicated that the substrate concentration remained stable at ~4950 COD mg/l, close to the theoretical COD of 10 mM benzyl salicylate (4960 mg O_2). The controls without substrate added shows that there was no measurable COD unless benzyl salicylate was present.

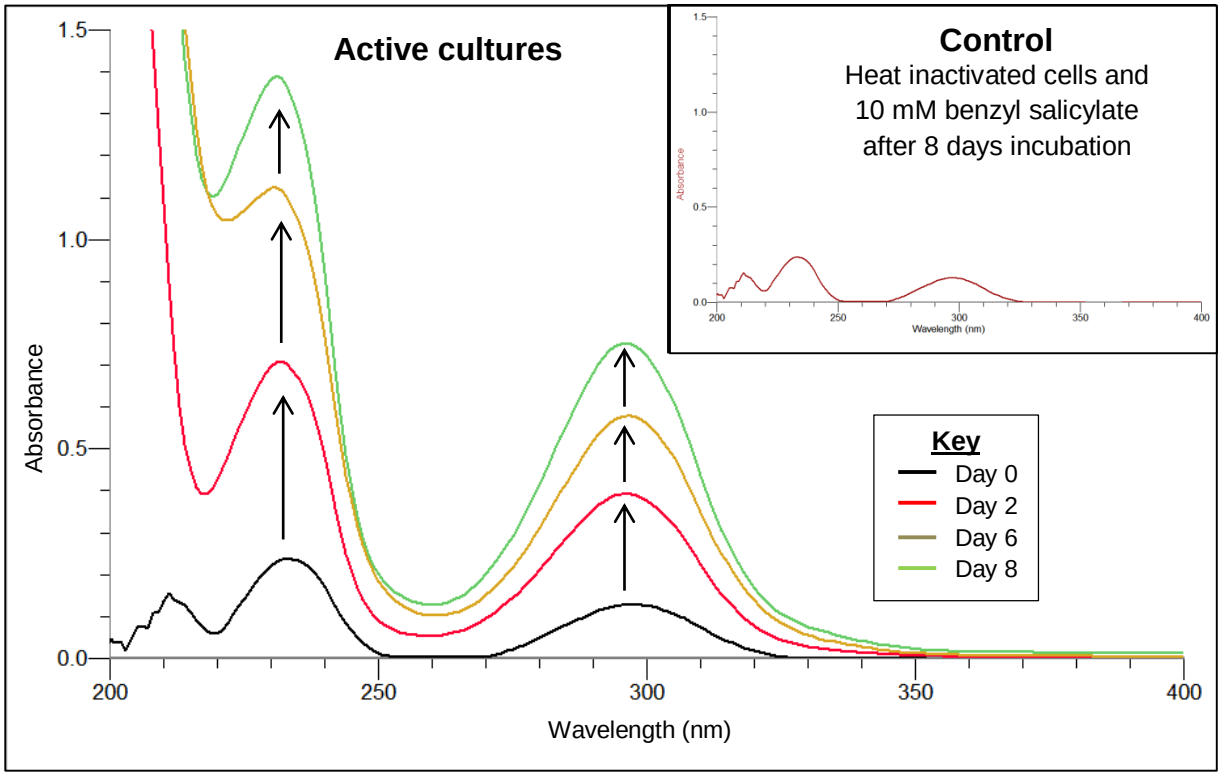

Figure 3.45: UV-Vis spectral analysis of the catabolism of 10 mM benzyl salicylate in MSM in the presence of *Trichosporon* sp. strain VM2 cultures incubated at 25°C and 100 rpm from day 0 to day 8. The insert graph shows the UV-Vis spectrum for the abiotic control after 8 days.

Figure 3.45 shows that culture supernatants, when analysed by UV-Vis spectroscopy, demonstrated that in the presence of active cultures, the aromatic body of benzyl salicylate was partially catabolized over time as an increase in absorbance at 290nm indicates that salicylate accumulated in the medium to ~4 mM on day 8 based on the molecular extinction coefficient of salicylate at 295nm (Ungar *et al*., 1952), while benzyl alcohol was potentially catabolized as no accumulation of this intermediate was evident in the spectrum. Therefore, strain VM2 has the ability to catabolize the benzyl alcohol moiety of the diary ester, benzyl salicylate. This is similar to the results obtained when the strain was grown using salol as sole source for carbon and energy (Figure 3.42). The abiotic control with heat inactivated yeast cells and the substrate shows that the aromatic body of benzyl salicylate remained stable over the 8 day period.

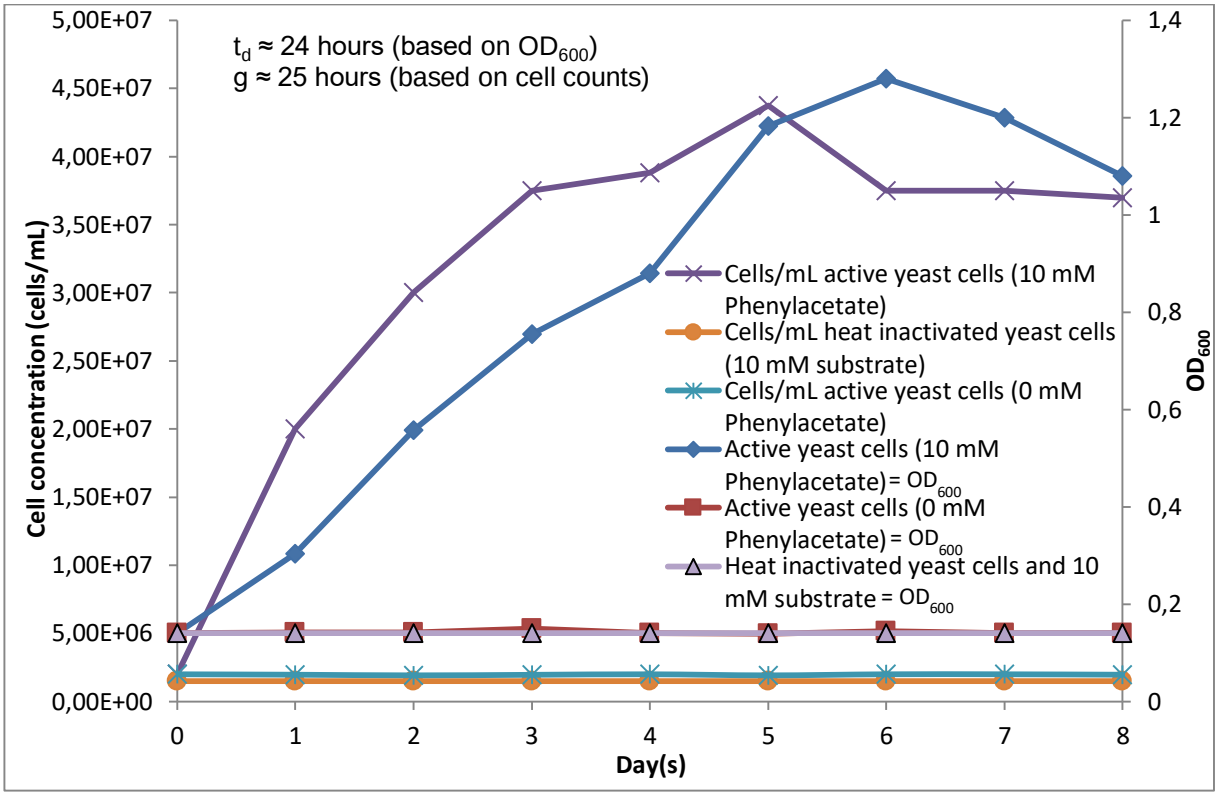

Figure 3.46: Growth of *Trichosporon* sp. strain VM2 with 10mM phenylacetate as the sole carbon source in MSM at 25°C and 100 rpm with inoculation of 2 x 10^6 yeast cells per ml.

The growth curves for strain VM2 represented as OD_{600} and microscopic cell counts both follow a similar pattern over time when 10 mM phenylacetate was employed as sole carbon and energy source (Figure 3.46). There was an initial rapid increase in biomass and cell numbers until day 5, relating to the exponential growth phase. The stationary and death phase followed with a decline in biomass. There was no observable growth with heat inactivated yeast cells in the presence of 10 mM substrate and in the absence of the substrate. The doubling time (t_d) and generation time (g) under specified growth conditions was established as ~24 hours and ~25 hours respectively.

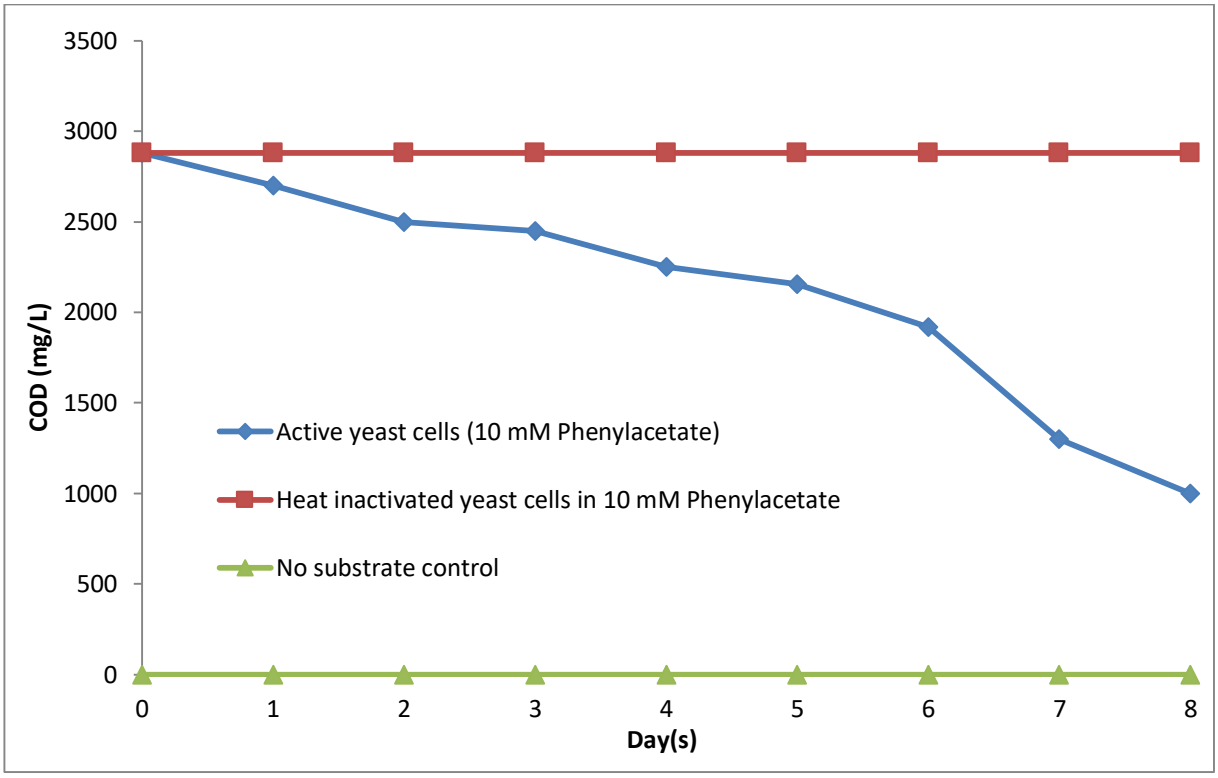

Figure 3.47: COD analysis of *Trichosporon* sp. strain VM2 cultures grown with 10 mM phenylacetate as the sole carbon source in MSM at 25°C and 100 rpm with inoculation of 2 x 10^6 yeast cells per ml.

The COD analysis of cultures of strain VM2 grown in the presence of 10 mM phenylacetate showed that the substrate concentration decreased over time (Figure 3.47). The substrate concentration, determined as the COD, decreased rapidly over the 8 day period until ~65% of 10 mM phenylacetate was catabolized by the yeast. This relates to the growth curve pattern observed in Figure 3.46. The controls with heat inactivated yeast cells indicated that the substrate concentration remained stable at ~2880 COD mg/l, exactly as the theoretical COD of 10 mM phenylacetate (2880 mg O_2) and the controls without added substrate show that there was no measureable COD unless phenylacetate was present.

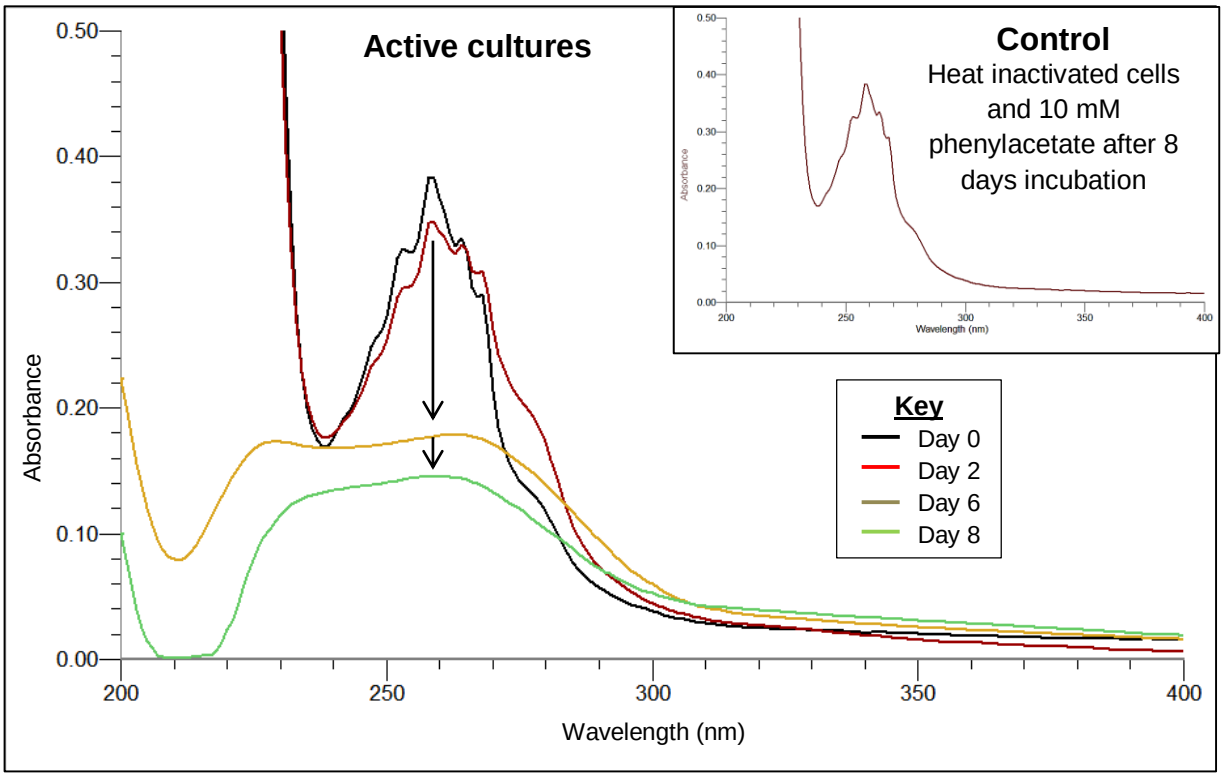

Figure 3.48: UV-Vis spectral analysis of the catabolism of 10 mM phenylacetate in MSM in the presence of *Trichosporon* sp. strain VM2 cultures incubated at 25°C and 100 rpm from day 0 to day 8. The insert graph shows the UV-Vis spectrum for the abiotic control after 8 days.

The UV-Vis analysis of the culture supernatants demonstrated that in the presence of active cultures phenylacetate with an absorbance maximum at ~260nm was catabolized by strain VM2 over time (Figure 3.48), as the absorbance at 260nm decreased to about 30% of the initial A_{260}. However, this was not done to completion. Nevertheless, only active cultures are responsible for the partial catabolism of phenylacetate, as an abiotic control (heat inactivated yeast cells and the substrate) showed that the aromatic body of phenylacetate remained stable over the 8 day period.

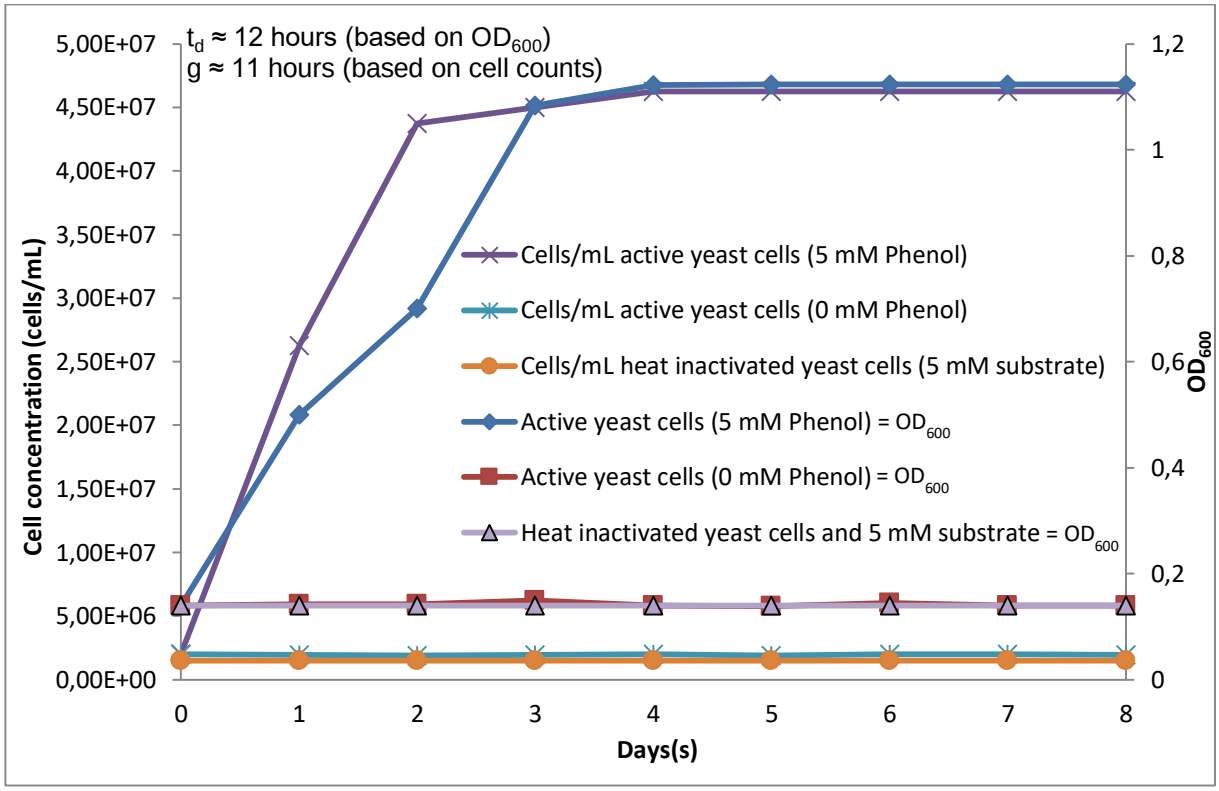

Figure 3.49: Growth of *Trichosporon* sp. strain VM2 with 5 mM phenol as the sole carbon source in MSM at 25°C and 100 rpm with inoculation of 2 x 10^6 yeast cells per ml.

Figure 3.49 shows the growth curve obtained for strain VM2 when grown in the presence of 5 mM phenol. It was demonstrated as OD_{600} and verified via microscopic cell counts. The respective growth curves both follow the same pattern when strain VM2 was grown in 5 mM phenol over time. Initially, a rapid increase in biomass and cell numbers occurred relating to the exponential growth phase. Thereafter, the growth when reaching the stationary phase. No growth was observed in the absence of the substrate and with heat inactivated yeast cells in the presence of the substrate. The doubling (t_d) and generation time (g) under specified growth conditions was established as ~12 hours and ~11 hours respectively.

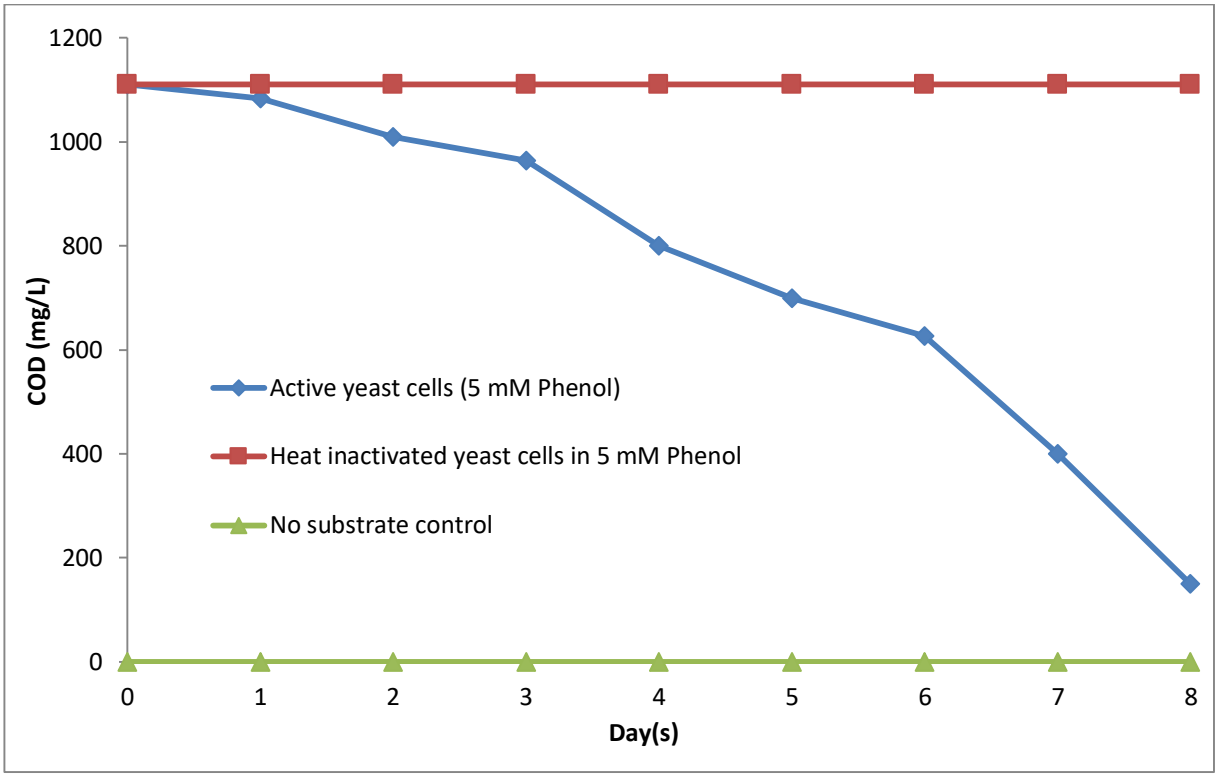

Figure 3.50: COD analysis of *Trichosporon* sp. strain VM2 cultures grown with 5 mM phenol as the sole carbon source in MSM at 25°C and 100 rpm with inoculation of 2 x 10^6 yeast cells per ml.

The COD analysis of strain VM2 cultures grown in the presence of 5 mM phenol showed that the substrate concentration decreased over time only in active cultures (Figure 3.50). The substrate concentration determined as the COD decreased rapidly over the 8 day period until ~86% of 5 mM phenol was catabolized by the yeast. This matches the growth curve in Figure 3.49, showing high biomass formation and cell growth. The substrate concentration remained stable at ~1110 COD mg/l for the controls with heat inactivated cells, close to the theoretical COD of 5 mM phenol (1120 mg O_2). In addition, the controls without added substrate show that there was no measureable COD unless phenol was present.

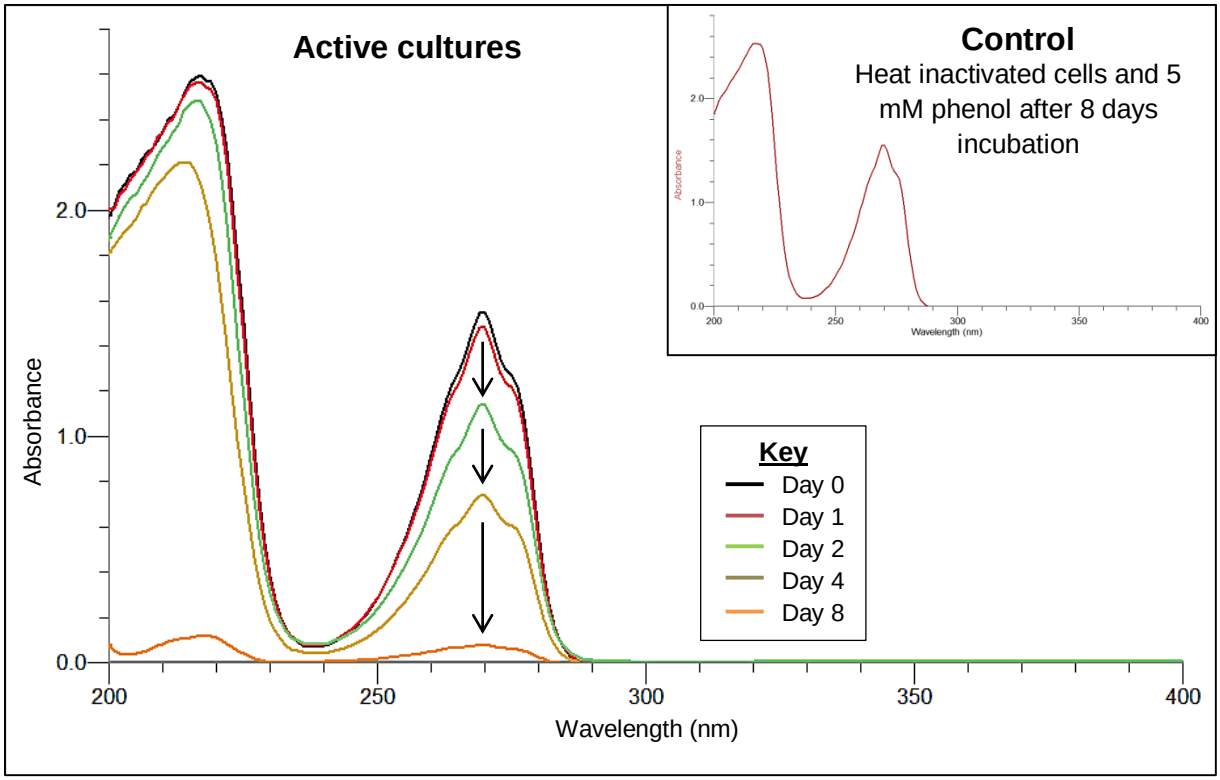

Figure 3.51: UV-Vis spectral analysis of the catabolism of 5 mM phenol in MSM in the presence of *Trichosporon* sp. strain VM2 cultures incubated at 25°C and 100 rpm from day 0 to day 8. The insert graph shows the UV-Vis spectrum for the abiotic control after 8 days.

The UV-Vis analysis of culture supernatants demonstrated that only in the presence of active cultures, phenol – showing a distinct absorbance maximum at 270nm – was catabolized over time (Figure 3.51). Based on the molar extinction coefficient of phenol at 270nm (ε = 1700 L x mol^{-1} x cm^{-1}) (Mach *et al*., 1992), ~4.3 mM substrate was utilized by the yeast by day 8, thereby matching the COD based on the percentage of 86% substrate eliminated. The abiotic controls, heat inactivated yeast cells and the substrate, show that the aromatic body of phenol remained stable over the 8 day period. Therefore, active cultures of *Trichosporon* sp. strain VM2 are solely responsible for the catabolism of phenol in the experiments.

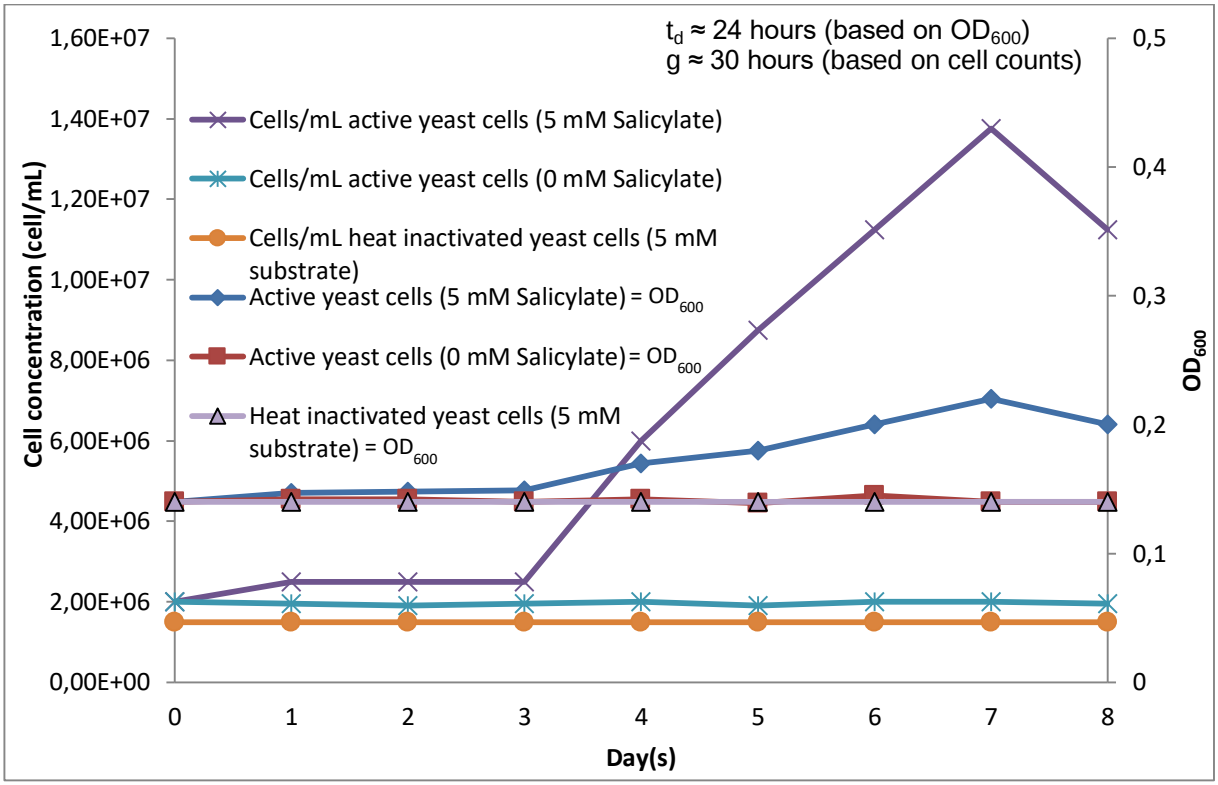

Figure 3.52: Growth of *Trichosporon* sp. strain VM2 with 5 mM salicylate as the sole carbon source in MSM at 25°C and 100 rpm with inoculation of 2 x 10^6 yeast cells per ml.

The growth of strain VM2 when monitored as OD_{600} and microscopic cell counts followed a similar pattern when grown in 5 mM salicylate over time (Figure 3.52). The lag phase lasted for 3 days, possibly indicating the biocidal inhibitory properties of the substrate. Thereafter, an exponential phase followed until day 7. This matches the growth experiments with salol and benzyl salicylate since the growth of the yeast caused an accumulation of salicylate in the medium. There was no observable growth in the absence of the substrate and with heat inactivated yeast cells in the presence of 5 mM salicylate. The doubling time (t_d) and generation time (g) under specified growth conditions was established as ~24 hours and ~30 hours respectively.

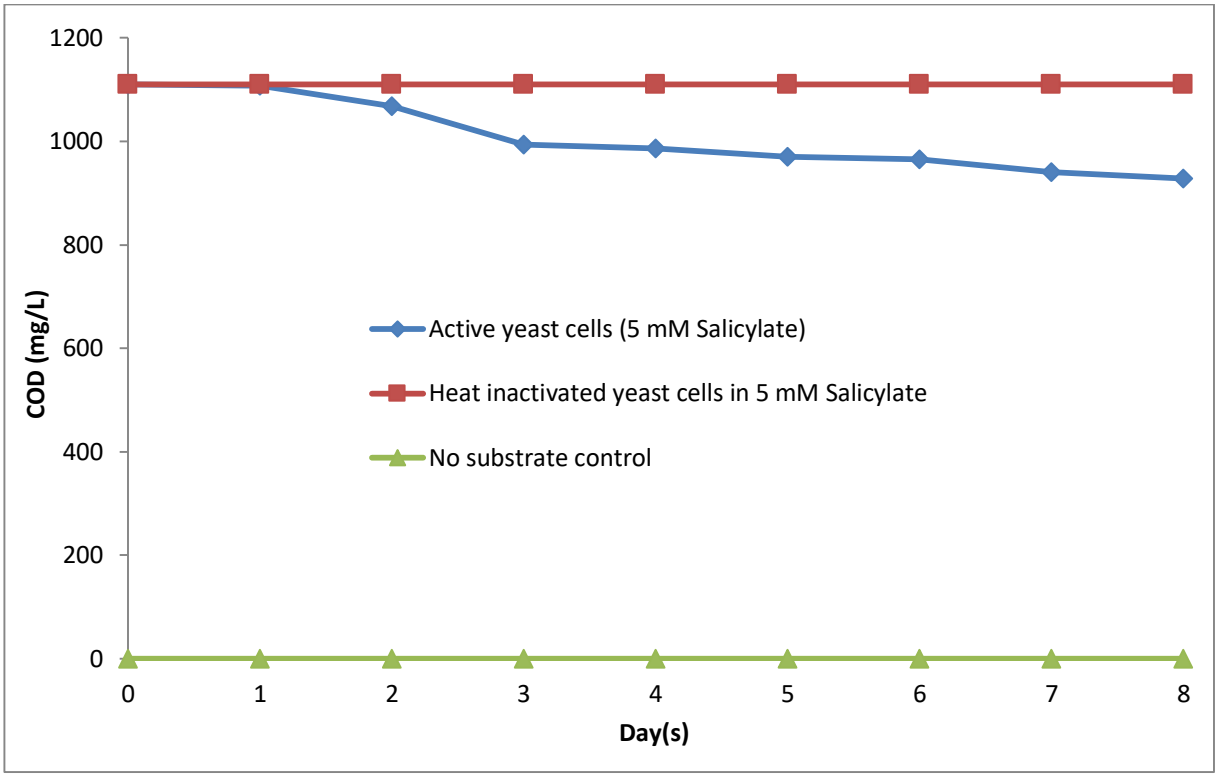

Figure 3.53: COD analysis of *Trichosporon* sp. strain VM2 cultures grown with 5 mM salicylate as the sole carbon source in MSM at 25°C and 100 rpm with inoculation of 2 x 10^6 yeast cells per ml.

The COD analysis of cultures of strain VM2 when grown in the presence of 5 mM salicylate showed that the substrate concentration decreased over time (Figure 3.53), albeit to a very limited extent. Over the 8 day period, only about 16% of 5 mM salicylate was catabolized by the yeast. This is in accordance with the growth curve pattern in Figure 3.52, showing limited biomass and cell increases. The controls with heat inactivated yeast cells indicated that the substrate concentration remained stable at ~1110 COD mg/l, close to the theoretical COD of 5 mM salicylate (1120 mg O_2) and the controls without substrate added show that there was no measureable COD, unless salicylate was present as the carbon source.

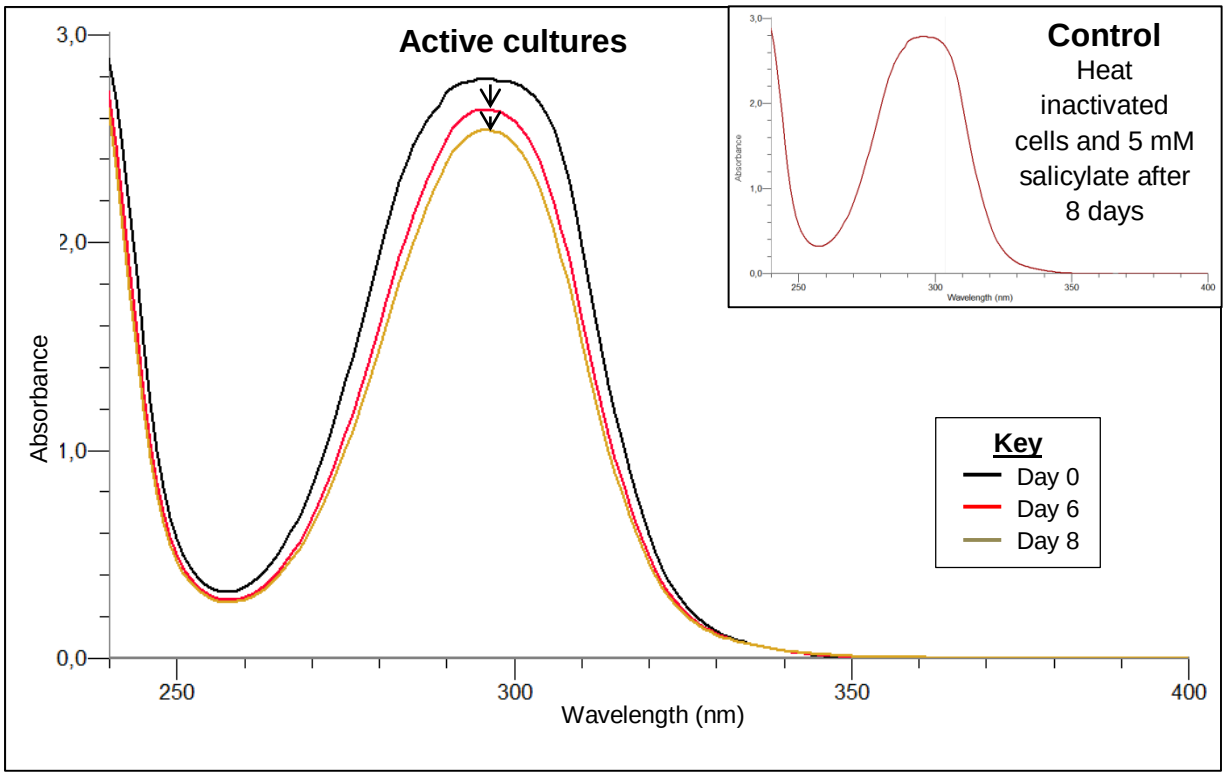

Figure 3.54: UV-Vis spectral analysis of the catabolism of 5 mM salicylate in MSM in the presence of *Trichosporon* sp. strain VM2 cultures incubated at 25°C and 100 rpm from day 0 to day 8. The insert graph shows the UV-Vis spectrum for the abiotic control after 8 days.

The UV-Vis spectral analysis of the culture supernatants showed that in the presence of active cultures, only a small fraction of the aromatic substrate (salicylate) was catabolized over time (Figure 3.54), as indicated by a minute decrease in absorbance at 295nm. According to the molar extinction coefficient of salicylate at 295nm (ε = 3840 L x mol^{-1} x cm^{-1}) (Ungar *et al*., 1952), ~0.3 mM substrate was utilized by the yeast by day 8. This confirms the limited substrate utilization detected via COD analysis. Therefore, *Trichosporon* sp. strain VM2 can only poorly catabolize salicylate, explaining why this compound accumulated upon hydrolysis of salol and benzyl salicylate in cultures of VM2. The abiotic control (heat inactivated yeast cells and the substrate) nevertheless shows that the aromatic body of salicylate remained stable over the 8 day period.

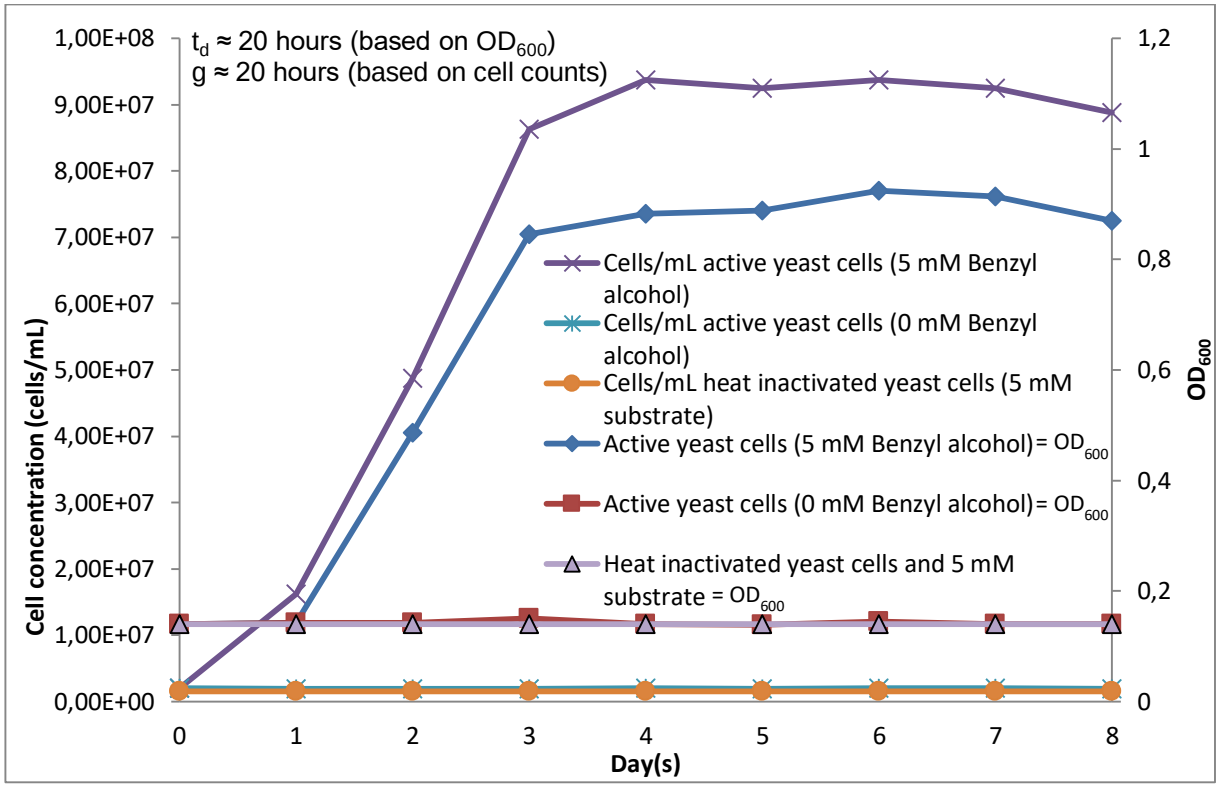

Figure 3.55: Growth of *Trichosporon* sp. strain VM2 with 5 mM benzyl alcohol as the sole carbon source in MSM at 25°C and 100 rpm with inoculation of 2 x 10^6 yeast cells per ml.

The growth curves for *Trichosporon* sp. strain VM2 established by recording OD_{600} and microscopic cell counts over time follow the same pattern when grown in 5 mM benzyl alcohol (Figure 3.55). The exponential growth phase occurs until day 3, followed by a stationary phase until day 8. No observable growth was detected in the absence of the substrate and with heat inactivated yeast cells in the presence of 5 mM benzyl alcohol. The doubling time (t_d) and generation time (g) under specified growth conditions was established as ~20 hours and ~20 hours respectively.

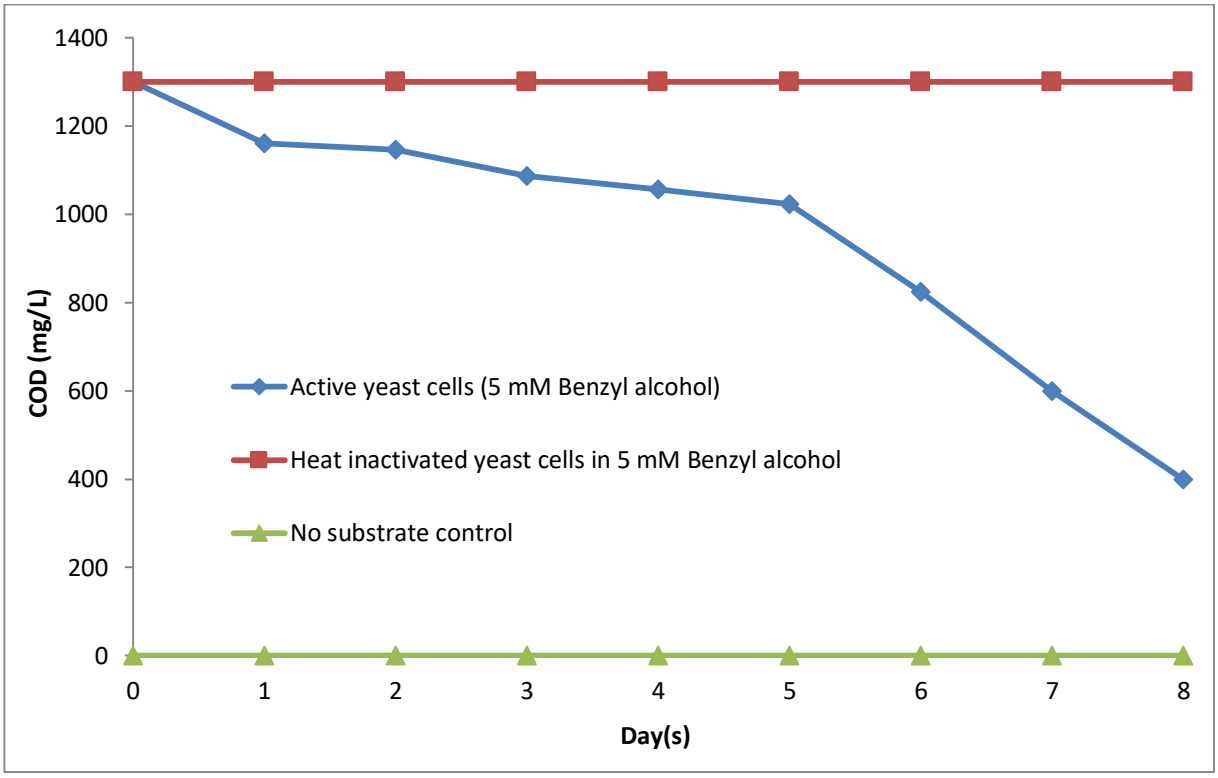

Figure 3.56: COD analysis of *Trichosporon* sp. strain VM2 cultures grown with 5 mM benzyl alcohol as the sole carbon source in MSM at 25°C and 100 rpm with inoculation of 2 x 10^6 yeast cells per ml.

The COD analysis of *Trichosporon* sp. strain VM2 cultures in the presence of 5 mM benzyl alcohol showed that the substrate concentration determined as COD decreased over time (Figure 3.56), until ~70% of 5 mM substrate had been catabolized by the yeast by day 8. Again, controls with heat inactivated yeast cells indicated that the substrate concentration remained stable at ~1300 COD mg/l, close to the theoretical COD of 5 mM benzyl alcohol (1360 mg O_2) and the controls without substrate added showed that there was no measureable COD, unless benzyl alcohol was present.

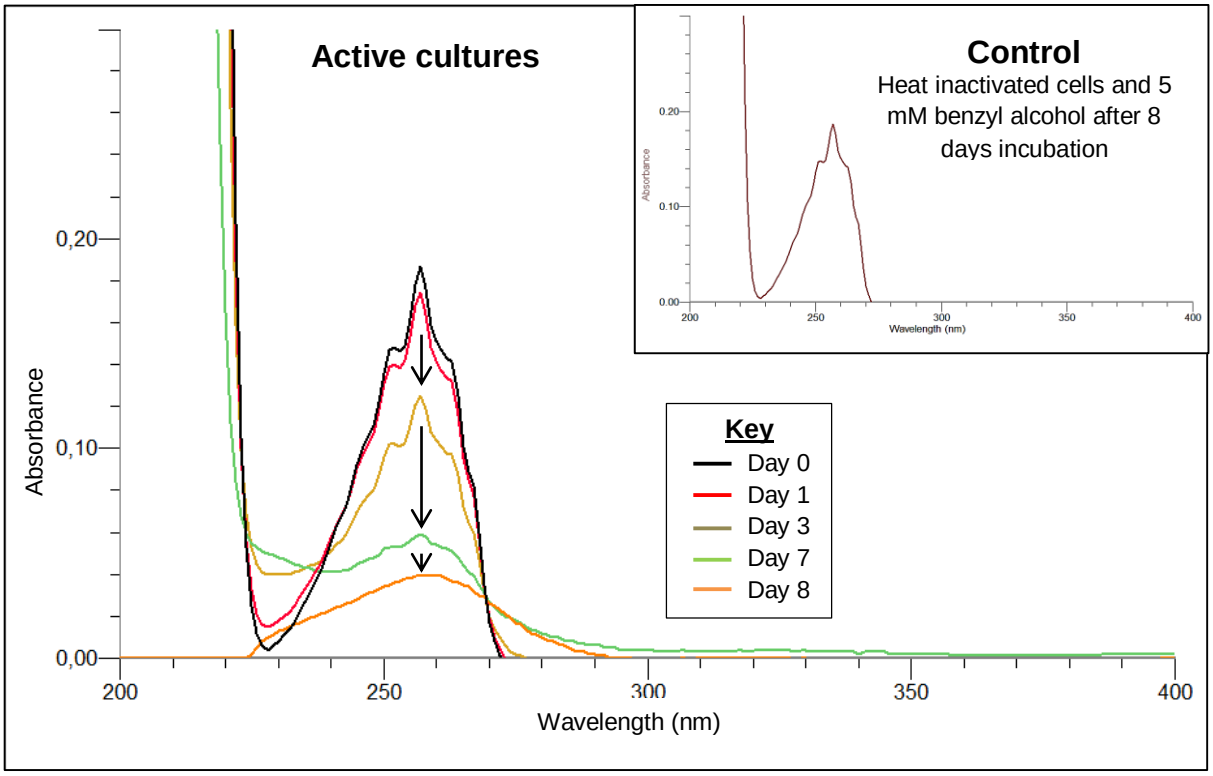

Figure 3.57: UV-Vis spectral analysis of the catabolism of 5 mM benzyl alcohol in MSM in the presence of *Trichosporon* sp. strain VM2 cultures incubated at 25°C and 100 rpm from day 0 to day 8. The insert graph shows the UV-Vis spectrum for the abiotic control after 8 days.

Culture supernatants, when analysed using UV-Vis spectroscopy, demonstrated that only in the presence of active cultures benzyl alcohol was catabolized over time (Figure 3.57). The decrease in absorbance at ~260nm indicates that the aromatic body of benzyl alcohol was catabolized; however not completely over the 8 day period, thereby matching the results of the COD analysis. The abiotic control with heat inactivated yeast cells and the substrate shows that the aromatic body of benzyl alcohol remained stable over the 8 day period, thus no abiotic loss was evident. Therefore, *Trichosporon* sp. strain VM2 is solely responsible for the catabolism of benzyl alcohol in these experiments.

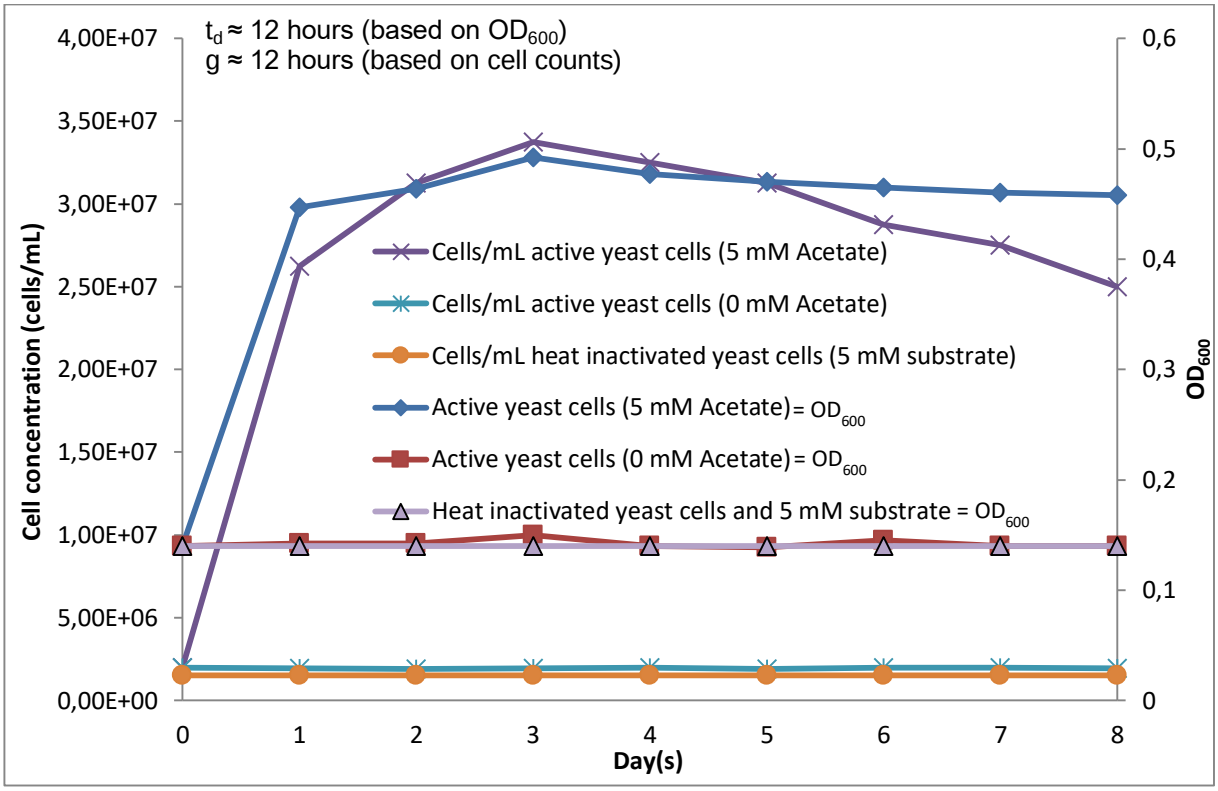

Figure 3.58: Growth of *Trichosporon* sp. strain VM2 with 5 mM acetate as the sole carbon source in MSM at 25°C and 100 rpm with inoculation of 2 x 10^6 yeast cells per ml.

When strain VM2 was grown with 5 mM acetate as sole carbon and energy source over time (Figure 3.58), an initial exponential growth phase occurred until day 1. Thereafter, the stationary phase followed. No increase in growth was observed in the absence of the substrate and with heat inactivated yeast cells in the presence of 5 mM acetate. The doubling time (t_d) and generation time (g) under specified growth conditions was established as ~12 hours and ~12 hours respectively.

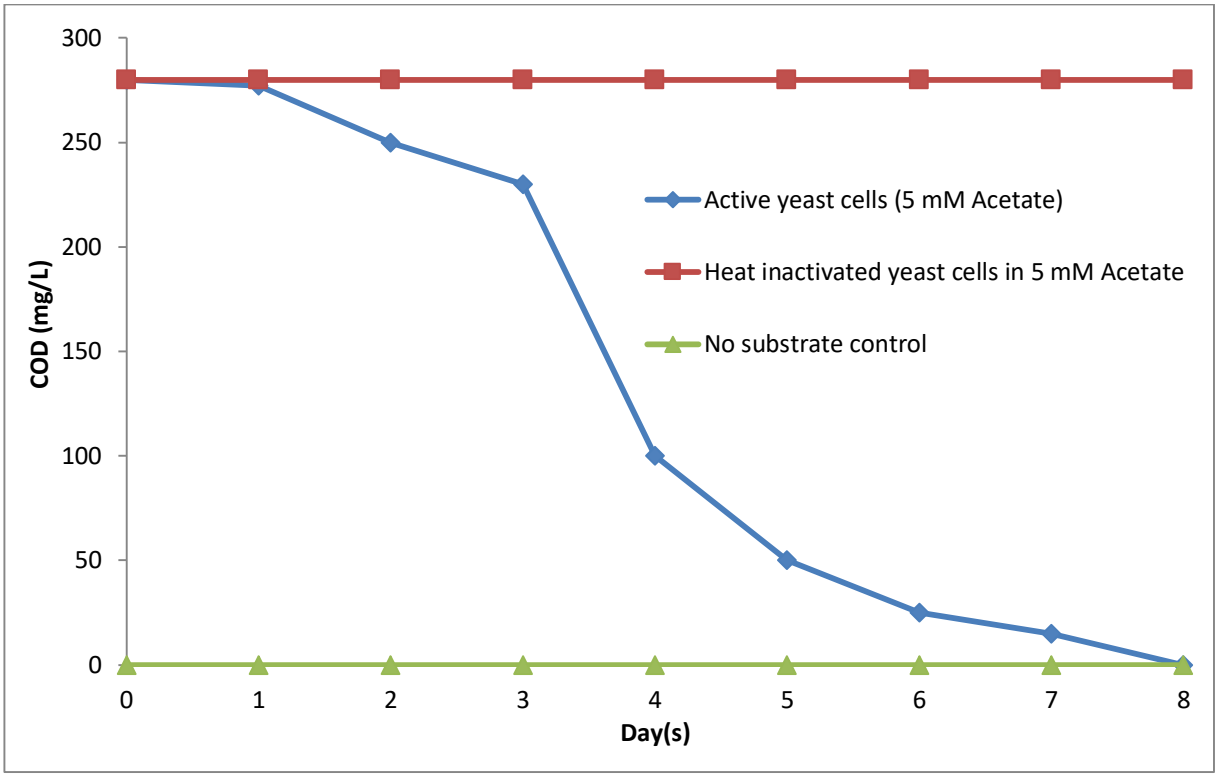

Figure 3.59: COD analysis of *Trichosporon* sp. strain VM2 cultures grown with 5 mM acetate as the sole carbon source in MSM at 25°C and 100 rpm with inoculation of 2 x 10^6 yeast cells per ml.

The COD analysis of cultures of strain VM2 grown in the presence of 5 mM acetate showed that the substrate concentration decreased over time (Figure 3.59), as the COD decreased rapidly over the 8 day period until 5 mM acetate was quantitatively catabolized by the yeast. The controls with heat inactivated yeast cells indicated that the substrate concentration remained stable at a COD of ~280 mg/l, closely matching the theoretical COD of 5mM acetate (320 mg O_2) and the controls without substrate added show that there was no measureable COD, unless acetate was present.

3.5. Growth of *Trichosporon* sp. strain VM2 in the presence of different concentrations of the target compounds

As previously stated, to enable optimum growth the concentration of the growth substrate must fall within an acceptable concentration range. Too high concentrations of the growth substrate may exhibit toxic effects, thus inhibiting the growth of the microorganism, while too low concentrations may not be sufficient for the microorganism to produce biomass.

Therefore, the effect of varying concentrations of the target compounds salol, benzyl salicylate, phenylacetate, phenol, salicylate, benzyl alcohol and acetate on the growth of strain VM2 was determined in MSM.

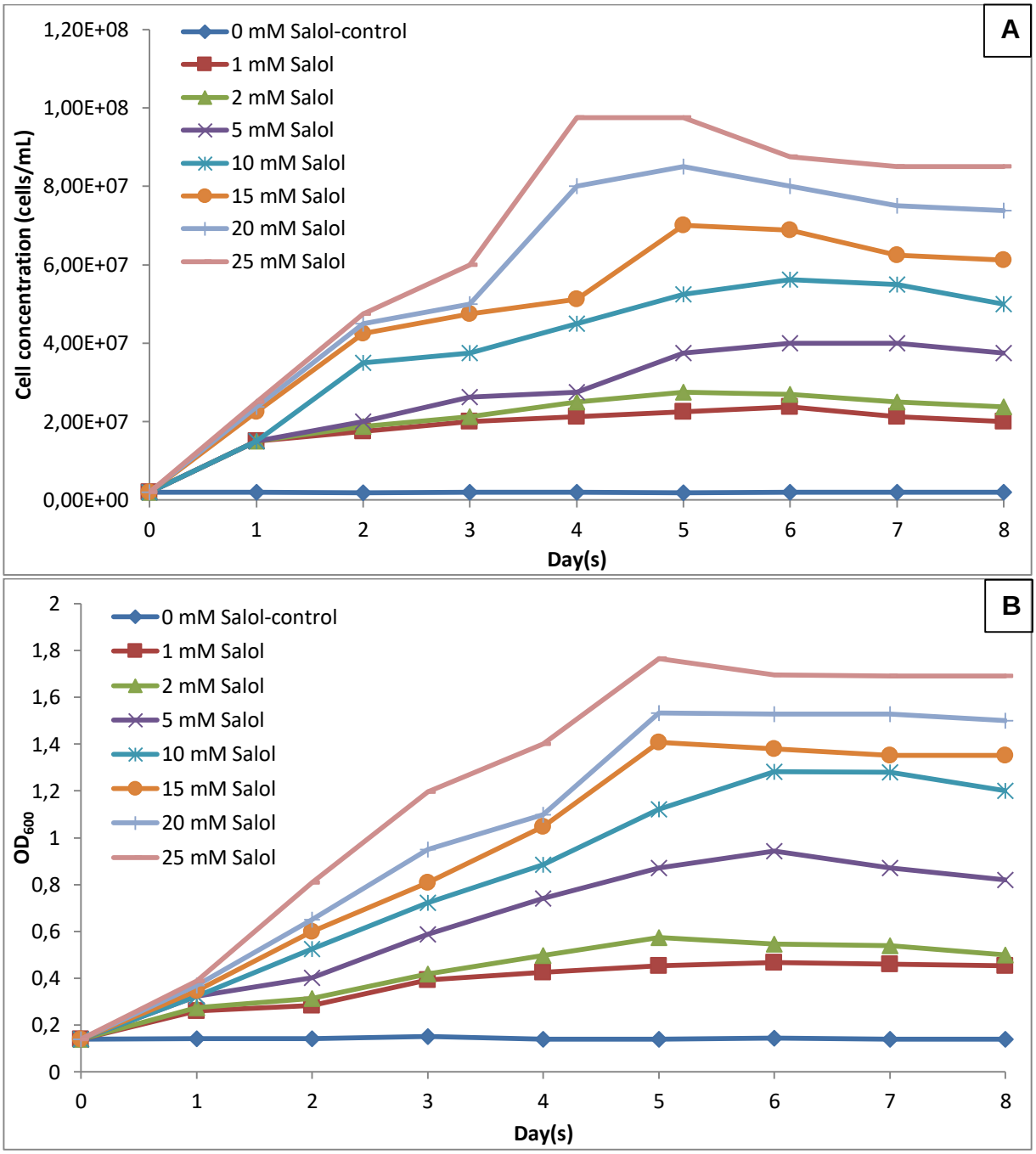

Figure 3.60: Growth (A) and Biomass formation (B) of *Trichosporon* sp. strain VM2 when grown in the presence of varying concentrations of salol as the sole carbon source in MSM at 25°C and 100 rpm when inoculated with 2 x 10^6 conidia per ml.

As demonstrated in Figure 3.60, concentrations of salol up to 25 mM did not inhibit the growth of strain VM2, as both biomass formation (B) and microscopic cell counts (A) increased. There was no detectable growth in the absence of the substrate.

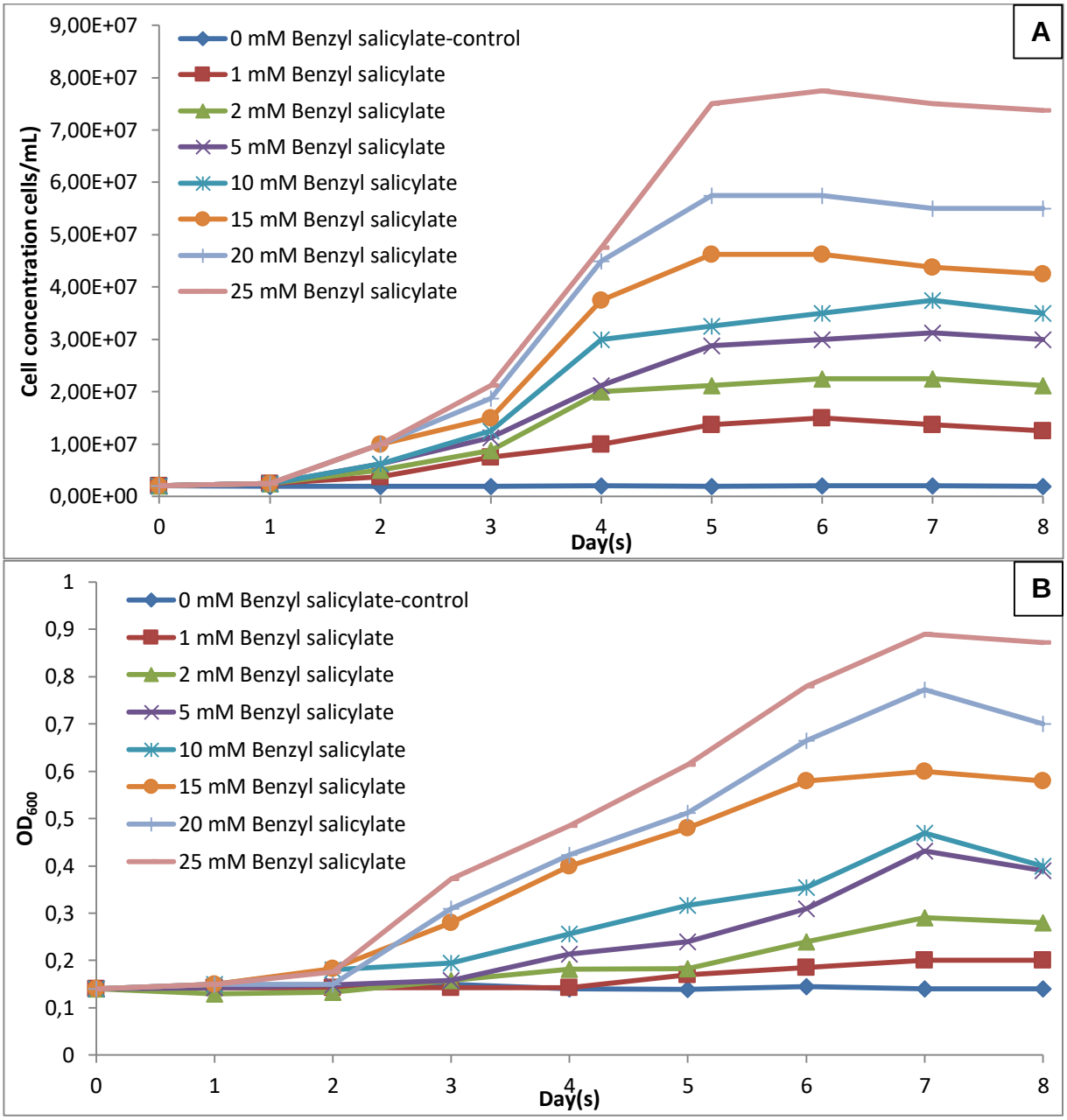

Figure 3.61: Growth (A) and Biomass formation (B) of *Trichosporon* sp. strain VM2 when grown in the presence of varying concentrations of benzyl salicylate as the sole carbon source in MSM at 25°C and 100 rpm when inoculated with 2 x 10^6 conidia per ml.

Figure 3.61 shows that the growth of the yeast strain VM2 increased with increased substrate concentrations up to a concentration of 25 mM. No growth observed in the controls without the carbon source.

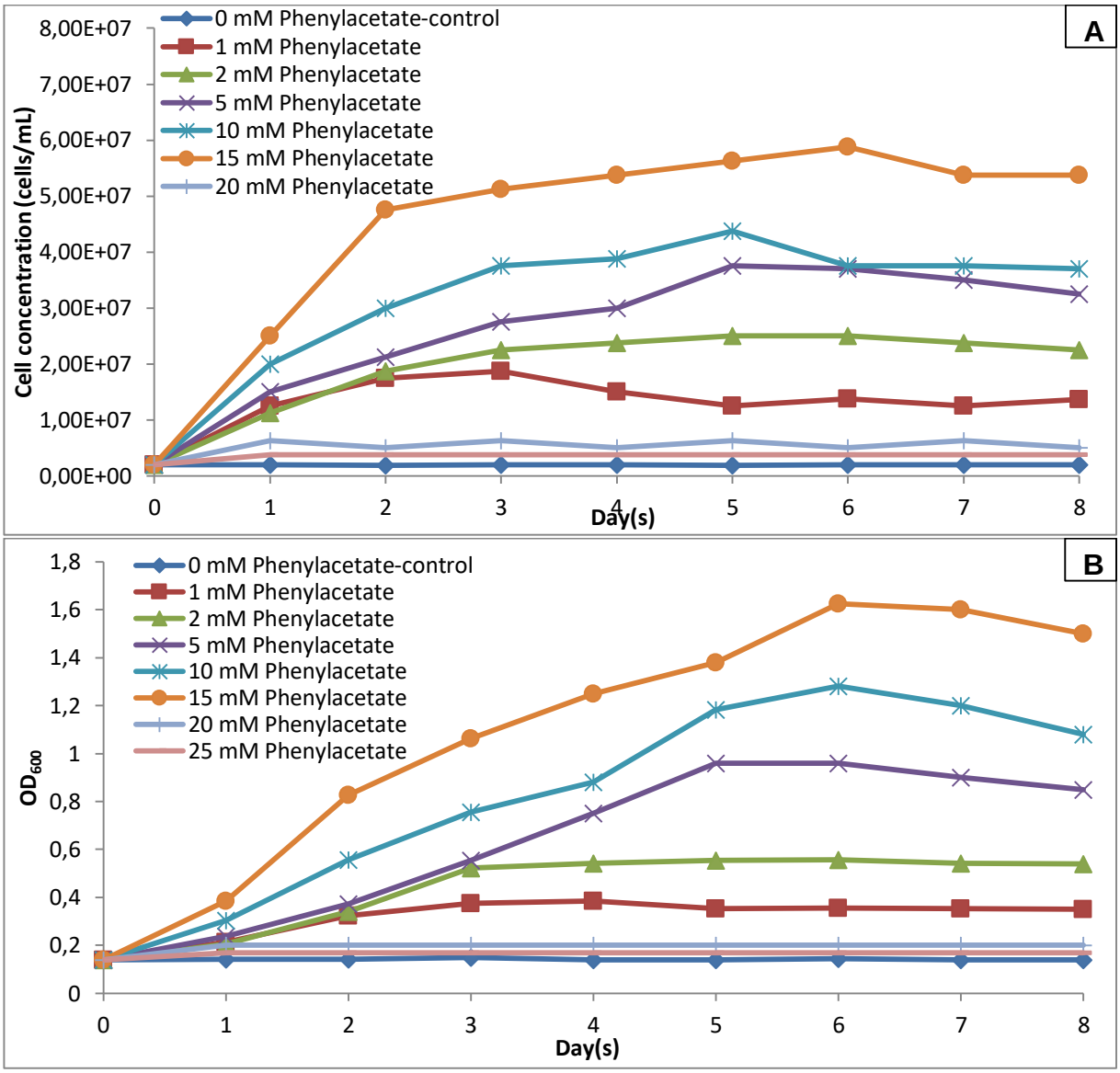

Figure 3.62: Growth (A) and Biomass formation (B) of Trichosporon sp. strain VM2 when grown in the presence of varying concentrations of phenylacetate as the sole carbon source in MSM at 25°C and 100 rpm when inoculated with 2 x 10^6 conidia per ml.

The growth of strain VM2 measured as OD_{600} (B) and verified via microscopic cell counts (A) shows that the biomass formation increased at phenylacetate concentrations up to 15 mM (Figure 3.62), while concentrations of ≥20 mM phenylacetate clearly inhibited the growth of *Trichosporon* sp. strain VM2, with only minute amounts of biomass formed. There was no detectable growth in the absence of the substrate.

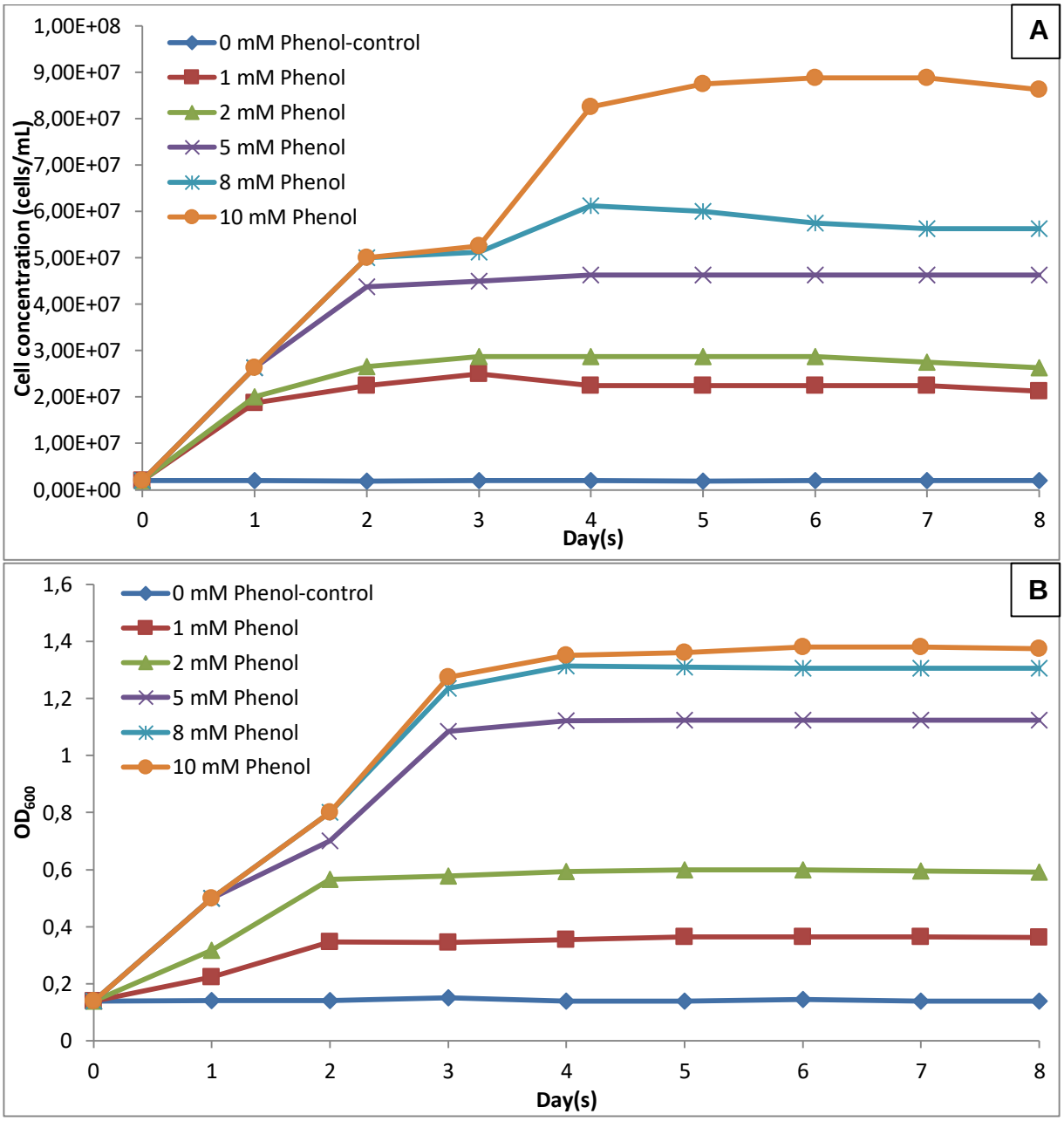

Figure 3.63: Growth (A) and Biomass formation (B) of *Trichosporon* sp. strain VM2 when grown in the presence of varying concentrations of phenol as the sole carbon source in MSM at 25°C and 100 rpm when inoculated with 2 x 10^6 conidia per ml.

The tested concentrations from 1 mM to 10 mM phenol supported the growth of strain VM2. The biomass formation and cell numbers increased with increasing phenol concentrations (Figure 3.63), even though this is more evident for cell numbers than for OD_{600}. Again, no growth was observed for the control without carbon source present.

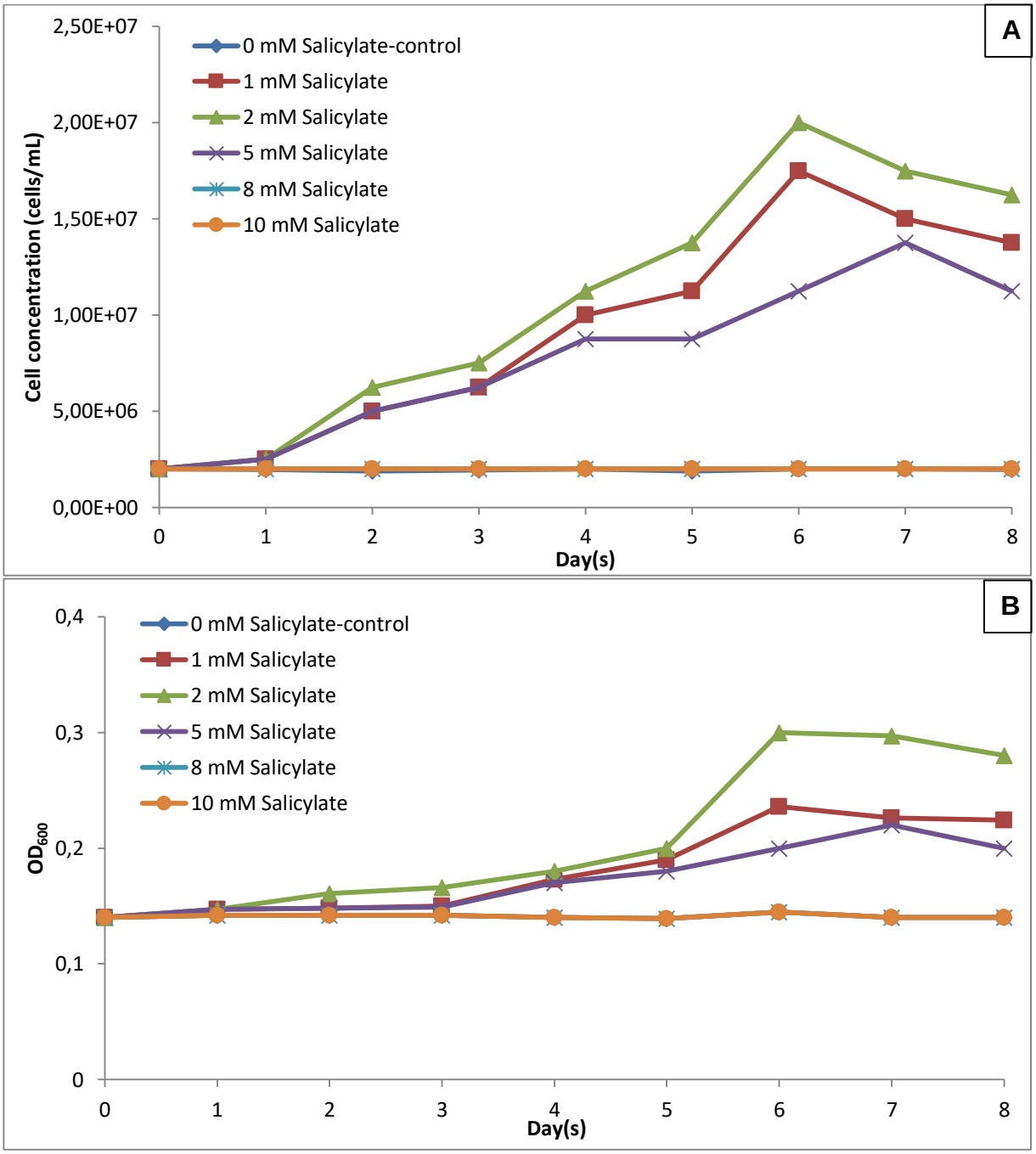

Figure 3.64: Growth (A) and Biomass formation (B) of *Trichosporon* sp. strain VM2 when grown in the presence of varying concentrations of salicylate as the sole carbon source in MSM at 25°C and 100 rpm when inoculated with 2 x 10^6 conidia per ml.

Strain VM2 was able to grow at salicylate concentrations up to 5 mM, even though the highest biomass yields were lower at this concentration after 6 days than at 2

mM substrate (Figure 3.64). However, concentrations of 8 mM and above became inhibitory and were similar to the no substrate control, since no growth was observed either via OD_{600} (B) or microscopic cell counts (A).

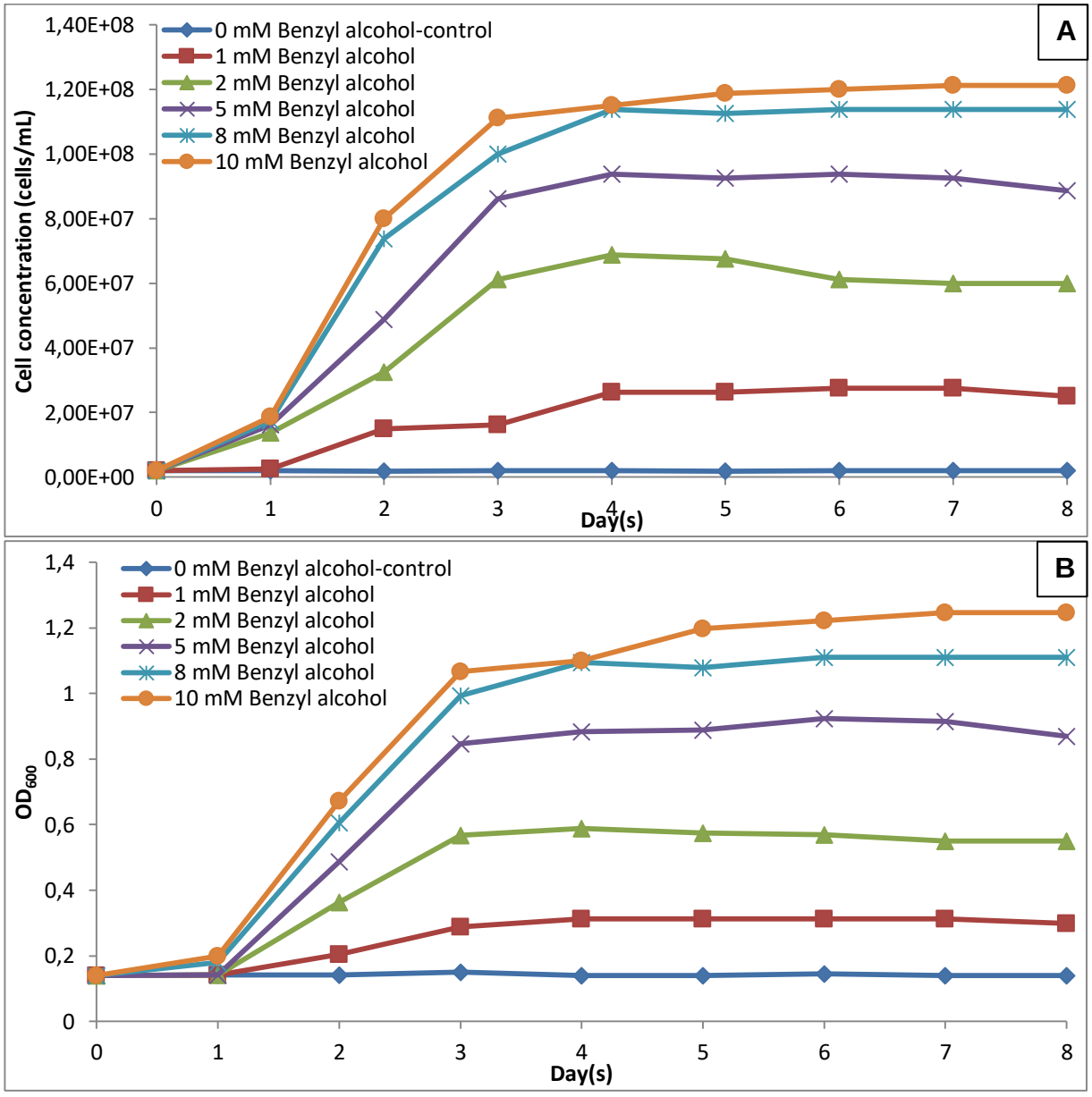

Figure 3.65: Growth (A) and Biomass formation (B) of *Trichosporon* sp. strain VM2 when grown in the presence of varying concentrations of benzyl alcohol as the sole carbon source in MSM at 25°C and 100 rpm when inoculated with 2 x 10^6 conidia per ml.

When benzyl alcohol was tested in a concentration range of 1 to 10 mM, both biomass and cell numbers of isolate VM2 increased with increasing benzyl alcohol

concentrations. The highest biomass and cell numbers were produced at 10 mM (Figure 3.65). However, no growth was observed in the absence of the substrate.

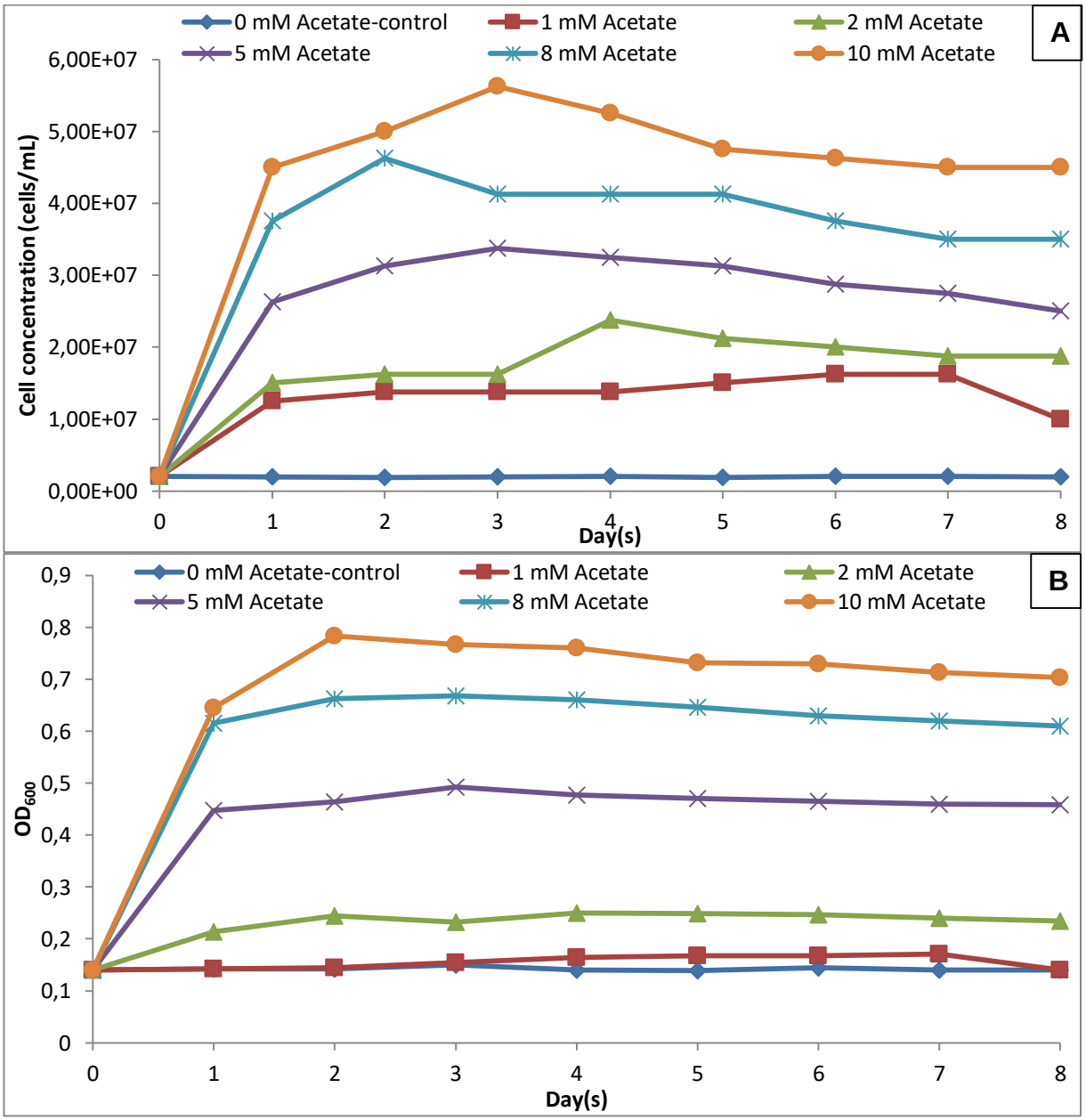

Figure 3.66: Growth (A) and Biomass formation (B) of *Trichosporon* sp. strain VM2 when grown in the presence of varying concentrations of acetate as the sole carbon source in MSM at 25°C and 100 rpm when inoculated with 2 x 10^6 conidia per ml.

The growth of strain VM2 detected via OD_{600} and microscopic cell counts increased in the presence of acetate concentrations up to 10 mM (Figure 3.66). The highest

quantity of biomass was produced at 10 mM substrate, while only minute growth was observed at 1 mM (OD_{600} (B)). No growth was observed for the control without carbon source present, which was verified by microscopic cell counts (A).

3.6. Utilization of other compounds

The two fungal and yeast isolates were further tested for their ability to use a number of additional aromatic and non-aromatic compounds.

Table 3.3: Growth of strain VM1 and strain VM2 in MSM with various carbon sources at 2.5 mM after a week of incubation at 25°C and 100 rpm.

Compound tested	*Fusarium* sp. strain VM1	*Trichosporon* sp. strain VM2
No carbon source (control)	-	-
Aromatic compounds		
Benzoic acid	+	+
4-Methylbenzoate	+	+
Non-aromatic compounds		
Glucose	+	+
Citric acid	+	+
Succinic acid	+	+

Key: (+) visible growth and (-) no visible growth

No visible growth was observed in the absence of substrate as was expected for these heterotrophic fungi. *Fusarium* sp. strain VM1 and *Trichosporon* sp. strain VM2 had the ability to utilize both aromatic and non-aromatic compounds to produce biomass (Table 3.3). More specifically, the isolates utilized benzoic acid, a possible intermediate upon the cleavage of benzyl salicylate and oxidation of benzyl alcohol to benzoic acid.

3.7. Analysis of specific enzyme activities for *Fusarium* sp. strain VM1 and *Trichosporon* sp. strain VM2

The type of enzyme activities induced by microorganisms is usually dependent upon the growth substrate. In addition, the efficiency of the catabolic pathway used for a given growth substrate is determined by the catabolic properties of the enzymes involved.

Hence, assays were performed for selected key enzymes potentially required for the catabolism of the growth substrates and potential metabolites to determine whether these activities were induced at which level and therefore involved in the metabolism of the substrates.

Table 3.4: Specific activities of catabolic enzymes in crude extracts of *Fusarium* sp. strain VM1 and *Trichosporon* sp. strain VM2 after growth with different target compounds.

Enzyme/ substrate	Specific activity after growth with:						
	Salol	Benzyl salicylate	Phenylacetate	Phenol	Salicylate	Benzyl alcohol	Acetate
***Fusarium* sp. strain VM1**							
Esterase							
p-Nitrophenylacetate	1712	1323	1068	495	470	464	401
Catechol-1,2-dioxygenase							
Catechol	121	171	30	1990	533	64	8
3-Methylcatechol	15	19	8	278	67	17	<5
4-Methylcatechol	65	88	17	751	158	28	<5
Catechol-2,3-dioxygenase							
Catechol	-	-	-	-	-	-	-
3-Methylcatechol	-	-	-	-	-	-	-
4-Methylcatechol	-	-	-	-	-	-	-
***Trichosporon* sp. strain VM2**							
Esterase							
p-Nitrophenylacetate	1545	1213	1009	483	318	370	401
Catechol-1,2-dioxygenase							
Catechol	365	60	68	1290	230	138	8
3-Methylcatechol	52	7	21	33	19	6	<5
4-Methylcatechol	94	17	29	225	82	29	<5
Catechol-2,3-dioxygenase							
Catechol	-	-	-	-	-	-	-
3-Methylcatechol	-	-	-	-	-	-	-
4-Methylcatechol	-	-	-	-	-	-	-

All data shown are the average of at least three independently performed experiments and the specific activities were expressed as nmol x min^{-1} x mg^{-1} protein. (-) = no activity detected.

Crude extracts from acetate grown cultures for both strain VM1 and VM2 exhibited specific esterase activity similar to that observed in crude extracts obtained from biomass grown with non-ester aromatic substrates. However, specific esterase activity was clearly increased in crude extracts from cultures of strain VM1 and VM2 grown with the aromatic esters salol, benzyl salicylate and phenylacetate. This is expected as salol and benzyl salicylate are salicylate esters and phenylacetate is an acetate ester, all of which require ester bond hydrolysis to initiate catabolism. Specific esterase activity for strain VM2 was somewhat lower than that of strain VM1 for *p*-nitrophenylacetate. The crude extracts from *Fusarium* sp. strain VM1 and *Trichosporon* sp. strain VM2 when grown with the selected aromatic target compounds showed inducible activity of catechol-1,2-dioxygenase (Table 3.4). The specific catechol-1,2-dioxgenase activity of *Trichosporon* sp. strain VM2 and *Fusarium* sp. strain VM1 was always lower for 3- and 4-methylcatechol than for catechol. However, no activity was detected for catechol-2,3-dioxygenase.

3.8. Spectral analysis of enzyme activity for *Fusarium* sp. strain VM1 and *Trichosporon* sp. strain VM2

-Isolate VM1

The crude extract acquired from *Fusarium* sp. strain VM1 after growth with phenol was used to analyse the transformation of *p*-nitrophenylacetate, catechol, 3-methylcatechol and 4-methylcatechol in enzyme assays.

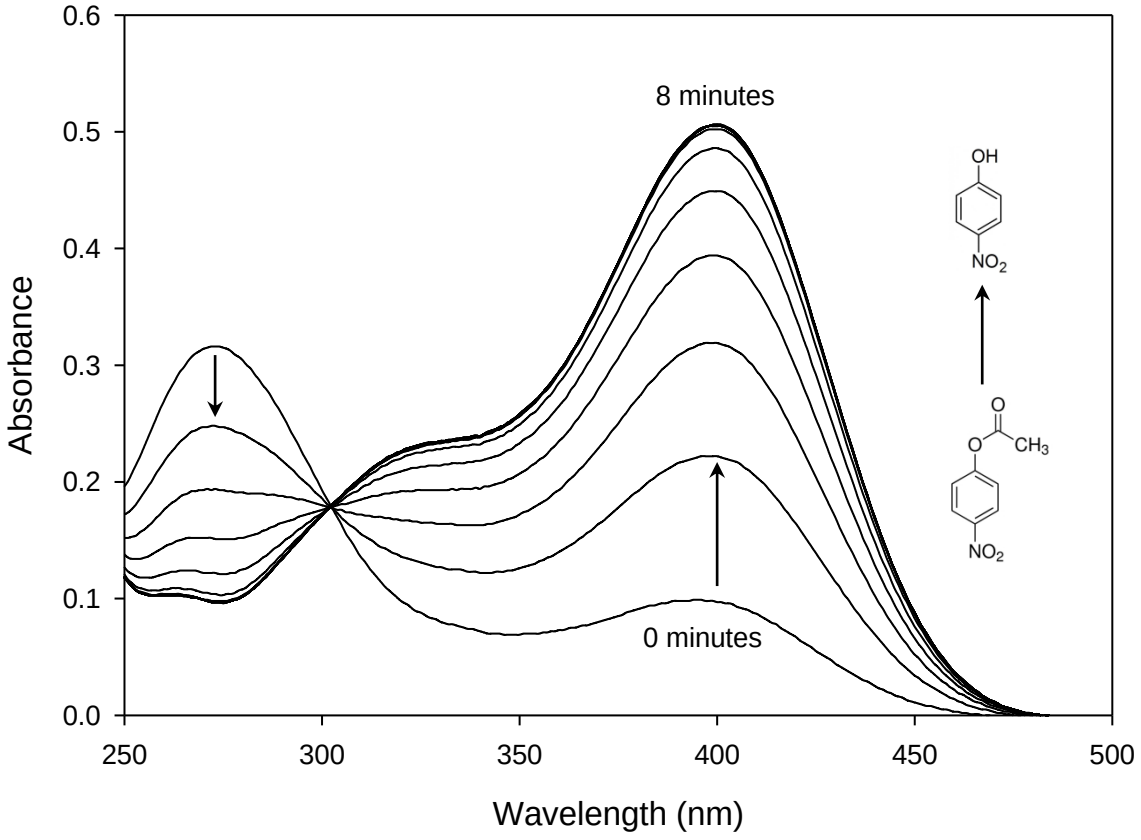

Figure 3.67: Enzymatic hydrolysis of *p*-nitrophenylacetate to *p*-nitrophenol by crude extract of *Fusarium* sp. strain VM1 (4.34µg protein) after growth with phenol. The assay was run at 25°C. The arrows indicate the decrease in *p*-nitrophenylacetate and the formation of *p*-nitrophenol.

The ester *p*-nitrophenylacetate displayed an absorption maximum at 270nm (Figure 3.67). After the addition of crude extract from *Fusarium* strain VM1 cultures grown with phenol, this absorption maximum at 270nm typical for *p*-nitrophenylacetate

decreased whilst a new maximum appeared at 405nm, indicating the accumulation of *p*-nitrophenol. This maximum for *p*-Nitrophenol increased in intensity over time until ~28 µM had been formed, at a specific enzyme activity of 495 nmol x mg^{-1} x min^{-1}. A characteristic isobestic point forming at ~300nm was detected. These results confirmed that *p*-nitrophenol was formed upon hydrolysis from *p*-nitrophenylacetate. Heat inactivated crude extract did not generate *p*-nitrophenol from *p*-nitrophenylacetate.

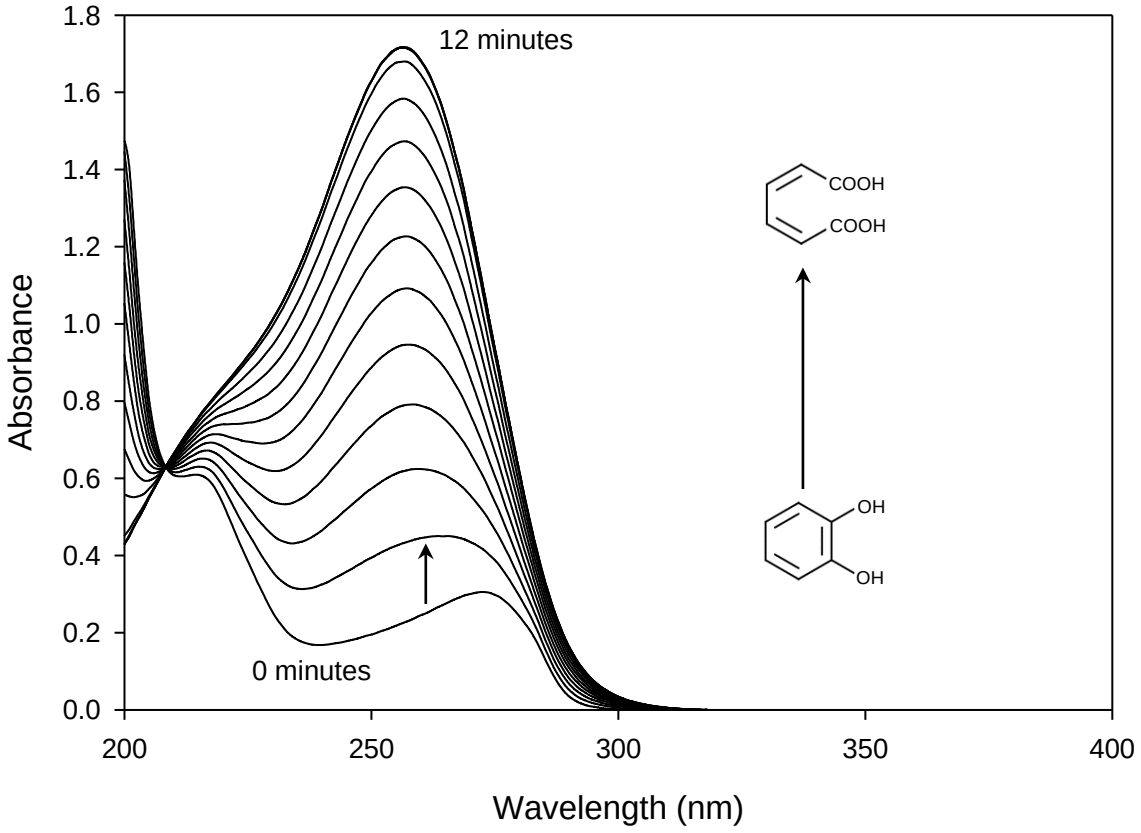

Figure 3.68: Enzymatic intradiolic cleavage of catechol to *cis*,*cis*-muconic acid by crude extract of *Fusarium* sp. strain VM1 (4.34µg protein) after growth with phenol. The assay was run at 25°C. The arrow indicates the formation of *cis*,*cis*-muconic acid.

Spectral analysis confirmed the formation of *cis,cis*-muconate from catechol for crude extract of strain VM1 cultures grown with phenol, since an absorbance maximum at 260nm characteristic for *cis,cis*-muconate formed until ~101 µM was

formed at a specific enzyme activity of 1990 nmol x mg^{-1} x min^{-1} (Figure 3.68). Heat inactivated crude extract did not generate *cis,cis*-muconic acid.

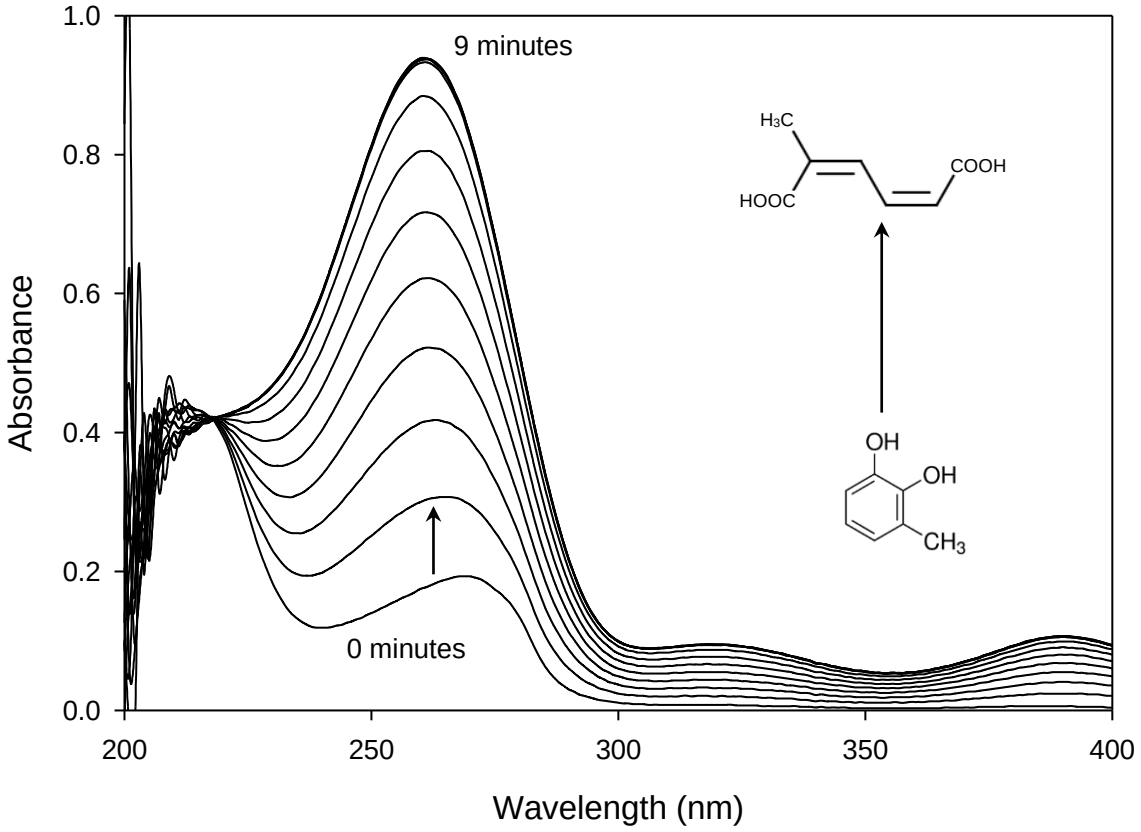

Figure 3.69: Enzymatic intradiolic cleavage of 3-methylcatechol to 2-methyl-*cis,cis*-muconate by crude extract of *Fusarium* sp. strain VM1 (21.7µg protein) after growth with phenol. The assay was run at 25°C.The arrow indicates the formation of 2-methyl-*cis,cis*-muconate.

The spectral analysis demonstrated the accumulation of 2-methyl-*cis,cis*-muconate from 3-methylcatechol when using crude extract from strain VM1 cultures grown with phenol, since the absorbance increased at 260nm until ~68 µM 2-methyl-*cis,cis*-muconate had been formed, at a specific enzyme activity of 278 nmol x mg^{-1} x min^{-1} (Figure 3.69). Again, heat inactivated crude extract did not generate 2-methyl-*cis,cis*-muconate.

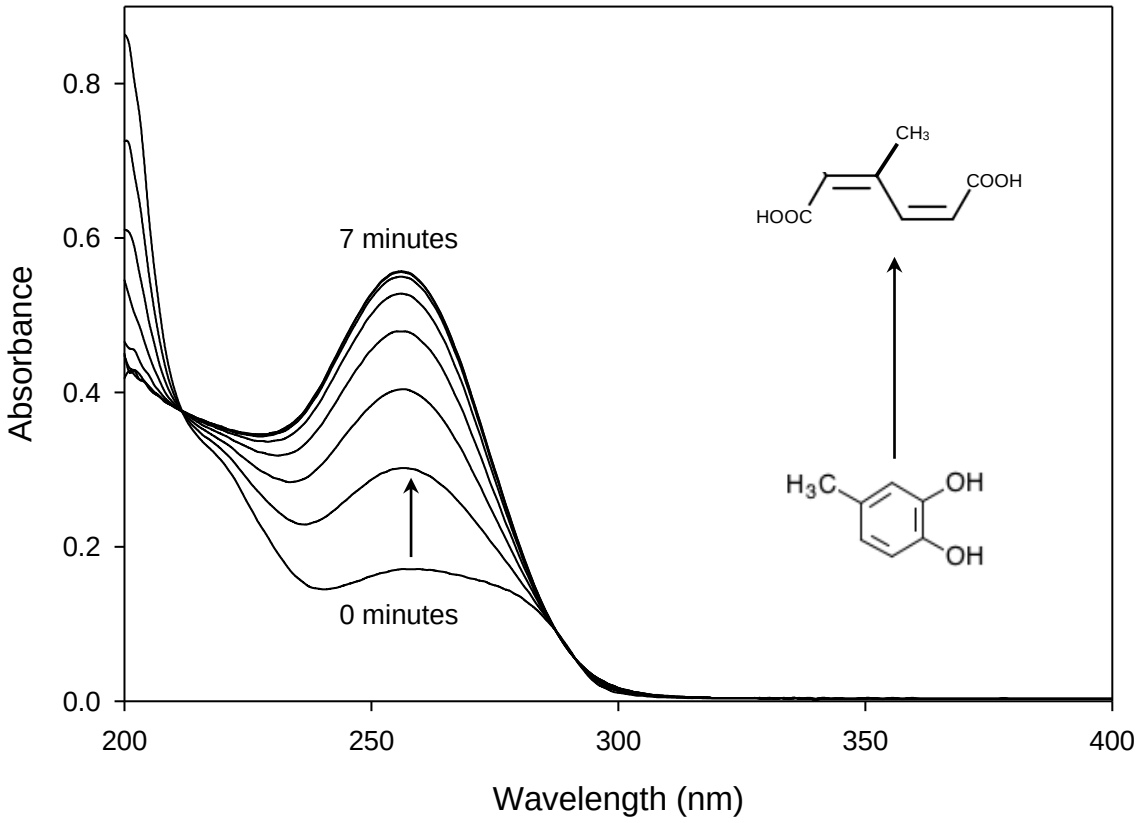

Figure 3.70: Enzymatic intradiolic cleavage of 4-methylcatechol to 3-methyl-*cis,cis*-muconate by crude extract of *Fusarium* sp. strain VM1 (8.68µg protein) after growth with phenol. The assay was run at 25°C. The arrow indicates the formation of 3-methyl-*cis,cis*-muconate.

As for catechol and 3-methylcatechol, the spectral analysis confirmed the formation of the matching muconic acid from the catechol substrate by crude extracts from *Fusarium* sp. strain VM1 after growth with phenol, yielding ~43 µM 3-methyl-*cis,cis*-muconate after 7 minutes at a specific enzyme activity of 751 nmol x mg^{-1} x min^{-1} (Figure 3.70). Heat inactivated crude extract did not generate 3-methyl-*cis,cis*-muconate.

-Isolate VM2

As for *Fusarium* sp. strain VM1, the enzymatic transformation of catechol, 3-methylcatechol, 4-methylcatechol and *p*-nitrophenylacetate by crude extract of *Trichosporon* sp. strain VM2 after growth with phenol was verified by UV-Vis spectroscopy.

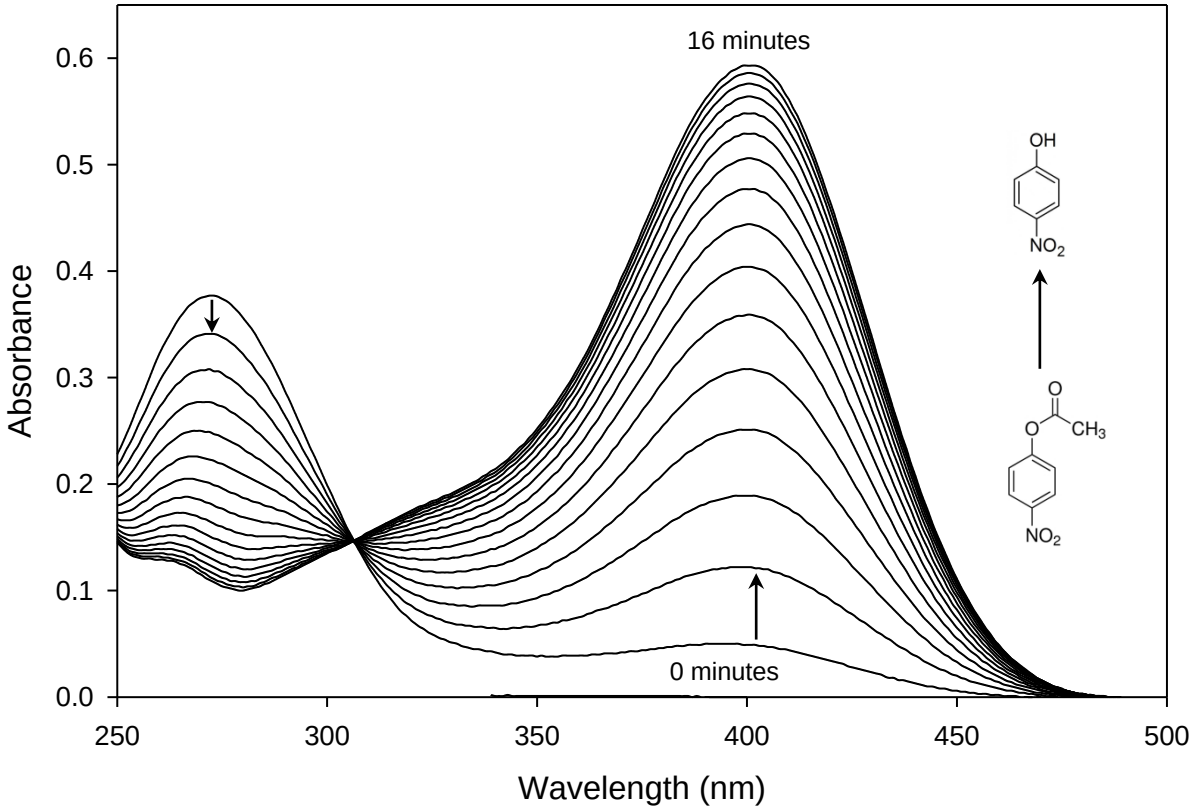

Figure 3.71: Enzymatic hydrolysis of *p*-nitrophenylacetate to *p*-nitrophenol by crude extract of *Trichosporon* sp. strain VM2 (4.5µg protein) after growth with phenol. The assay was run at 25°C. The arrows indicate the decrease in *p*-nitrophenylacetate and the formation of *p*-nitrophenol.

As for the strain *Fusarium* sp. VM1, spectral analysis confirmed the formation of *p*-nitrophenol from p-nitrophenylacetate when using crude extract obtained from strain VM2 after growth with phenol. As expected, the absorbance increased in intensity at 405nm while it decreased in intensity at 270nm. In addition, an isobestic point formed at ~300nm (Figure 3.71). In total, ~32 µM *p*-nitrophenol was formed after 16

minutes at a specific enzyme activity of 483 nmol x mg^{-1} x min^{-1}. Heat inactivated crude extract did not generate *p*-nitrophenol.

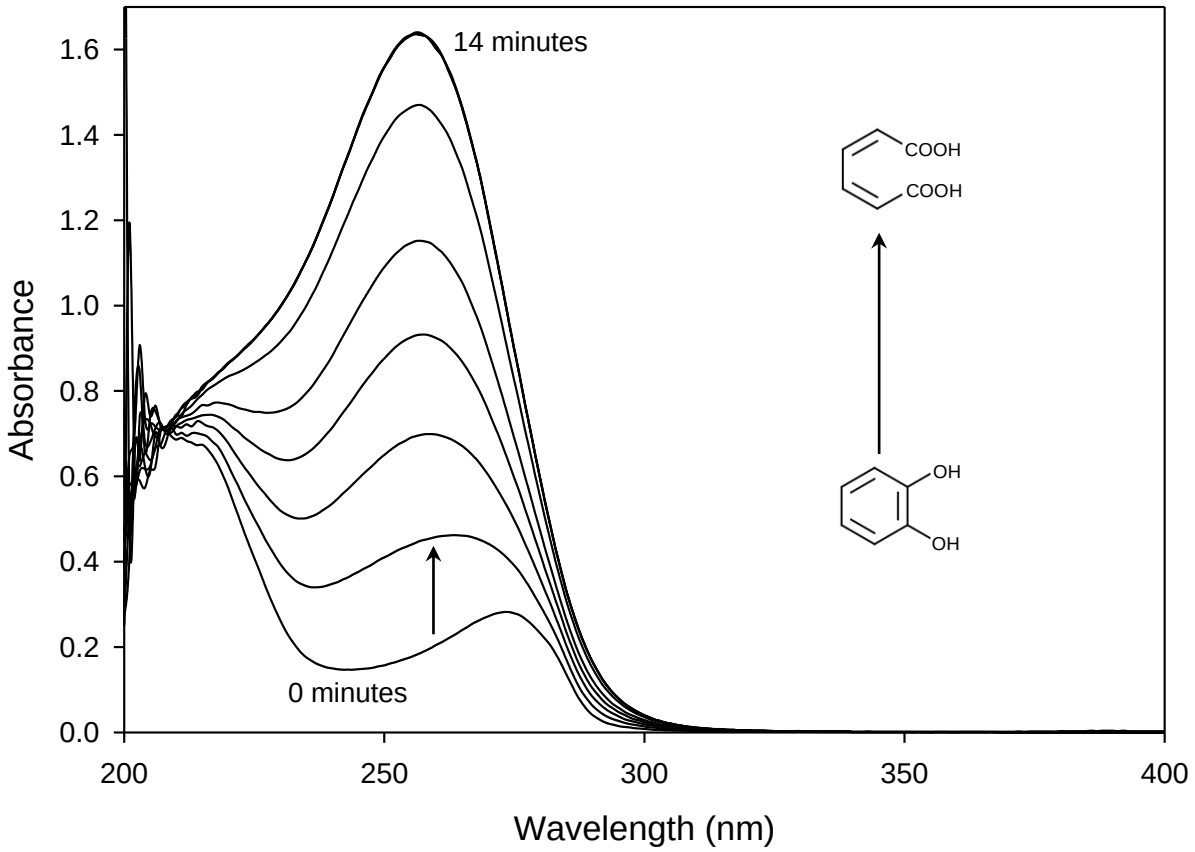

Figure 3.72: Enzymatic intradiolic cleavage of catechol to *cis,cis*-muconic acid by crude extract of *Trichosporon* sp. strain VM2 (4.5µg protein) after growth with phenol. The assay was run at 25°C.The arrow indicates the formation of *cis,cis*-muconic acid.

When performing the catechol-1,2-dioxygenase assay using *Trichosporon* sp. strain VM2 cultures grown with phenol, spectral analysis confirmed the formation of *cis,cis*-muconic acid from catechol until ~95 µM *cis,cis*-muconic acid was formed at a specific activity of 1290 nmol x mg^{-1} x min^{-1} (Figure 3.72). Heat inactivated crude extract did not generate *cis,cis*-muconic acid.

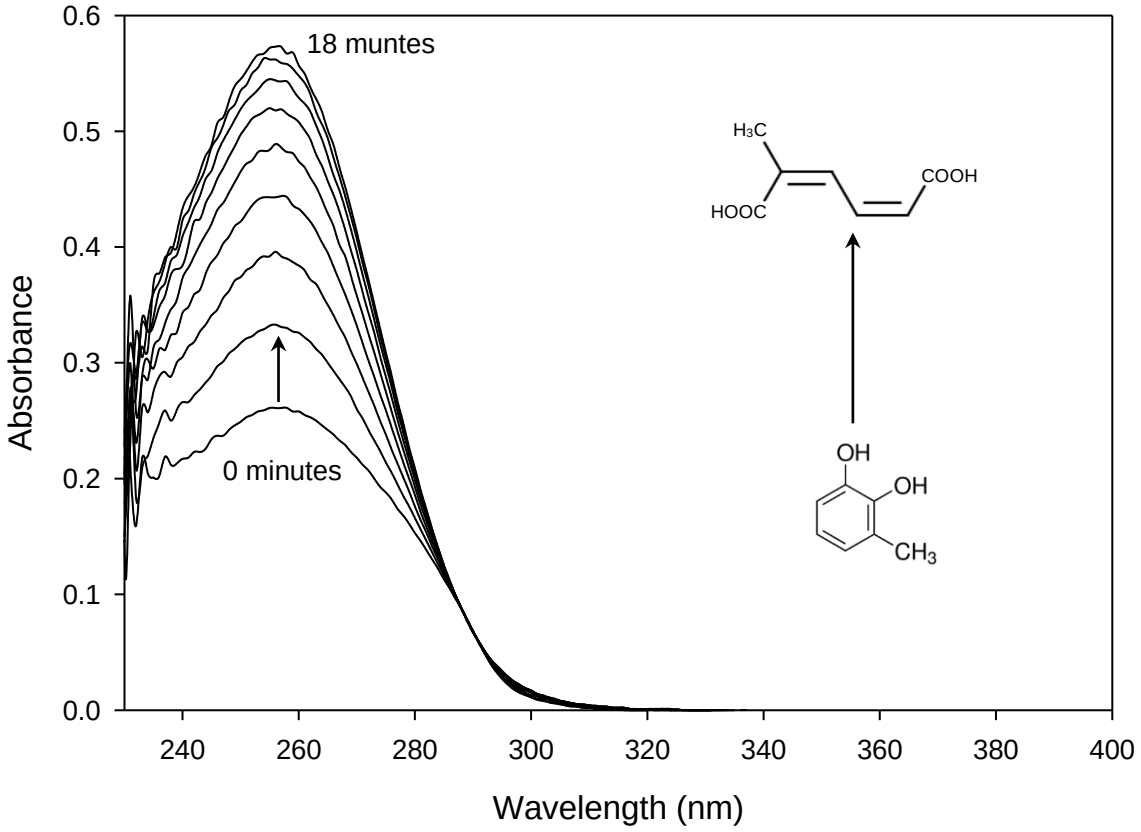

Figure 3.73: Enzymatic intradiolic cleavage of 3-methylcatechol to 2-methyl-*cis,cis*-muconate by crude extract of *Trichosporon* sp. strain VM2 (22.5µg protein) after growth with phenol. The assay was run at 25°C. The arrow indicates the formation of 2-methyl-*cis,cis*-muconate.

Spectral analysis demonstrated the formation of 2-methyl-*cis,cis*-muconate from 3-methylcatechol until ~40 µM was formed at a specific enzyme activity was 33 nmol x mg^{-1} x min^{-1} (Figure 3.73). Heat inactivated crude extract did not generate 2-methyl-*cis,cis*-muconate.

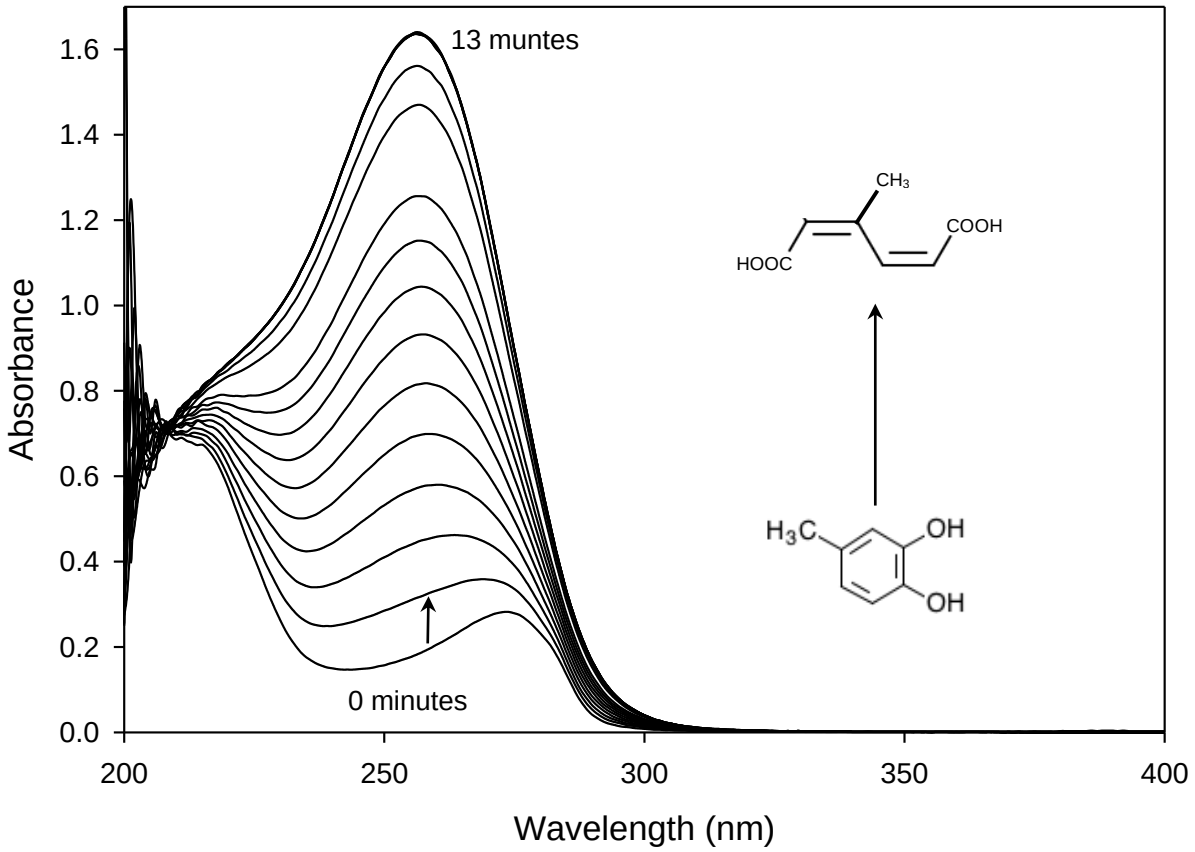

Figure 3.74: Enzymatic intradiolic cleavage of 4-methylcatechol to 3-methyl-*cis,cis*-muconate by crude extract of *Trichosporon* sp. strain VM2 (4.5µg protein) after growth with phenol. The assay was run at 25°C. The arrow indicates the formation of 3-methyl-*cis,cis*-muconate.

When using 4-methylcatechol and crude extract from *Trichosporon* sp. strain VM2 grown with phenol, spectral analysis confirmed the production of 3-methyl-*cis,cis*-muconate as the absorbance maximum formed at 260nm (Figure 3.74). About 107 µM 3-methyl-*cis,cis*-muconate formed within 13 minutes at a specific enzyme activity of 225 nmol x mg^{-1} x min^{-1}. Heat inactivated crude extract did not generate 3-methyl-*cis,cis*-muconate.

CHAPTER 4: DISCUSSION

Isolation and characterization

Fungi with the ability to biodegrade selected man-made organic pollutants have been previously isolated from soil environments (Clauβen and Schmidt, 1998; Mineki *et al.,* 2015; Schmidt, 2002; Henderson, 1961a). However, increasing amounts of chemicals that enter the environment through waste disposal and industrial activities far outnumber the microbial specialists available (Schmidt, 2002). Therefore, importance lies in the screening of microorganisms with the potential to detoxify or eliminate specific organic contaminants. Soil environments such as nature reserves are rich in lignocellulosic material, a complex polymer of aromatic hydrocarbons (Song, 2009). The transformation of this macromolecule would produce moieties similar to those of diaryl esters since it possesses aryl ester moieties (Henderson, 1961a). A study by Clauβen and Schmidt (1999) demonstrated how a diaryl ester, phenyl benzoate, was utilized by *Scedosporium apiospermum,* a hyphomycete isolated from agricultural soil. Diaryl esters such as salol and benzyl salicylate are found in many personal care products. However, these salicylate esters are biocides that exhibit endocrine-disrupting properties and have the potential to bioaccumulate and biomagnify in the environment (Caliman and Gavrilescu, 2009; Ying and Kookana, 2003). This may cause detrimental biological effects to living organisms. Therefore, diaryl esters such as salol and benzyl salicylate were chosen as target compounds as a means to assess if and how these compounds can be catabolized by soil fungi.

A well-established mineral salts medium (Göttsching and Schmidt, 2007) was chosen for enrichment purposes. The selective enrichment performed in this study led to the isolation of several fungal cultures. However, one fungal isolate and one yeast isolate were selected and characterized based on their cellular properties, growth characteristics and the sequence of their ITS1-5.8S rRNA-ITS2 region.

Fusarium species can have septate hyphae and produce conidiophores in aerial mycelia and members of this genus typically produce macro- and microconidia (Nelson *et al.,* 1994). *Fusarium* sp. strain VM1 isolated in the present study was

found to form septate hyphae (Figure 3.2 and 3.3) and the fungus also produced conidiophores (Figure 3.2 and 3.3) and ovoid microconidia that ranged from 5 to 9 µm in length (Figure 3.4), thereby matching the morphological characteristics of the *Fusarium* strain isolated by Teixeria *et al*. (2017). *F. subglutinans* was reported to produce cottony aerial mycelium with a pink pigmentation when grown on PDA (Nelson *et al.,* 1994), matching strain VM1, since this isolate formed cottony aerial mycelium with a pink pigmentation when grown on PDA (Figure 3.1). Ultrastructural analysis of strain VM1 showed fungal hyphae containing mitochondria with cristae and a septum (Figure 3.5).

Macroscopic features of *Trichosporon* species include yeast-like colonies usually with radial furrows that are dull, cream or white coloured and have a heap at the center of the colony (Larone, 1995; Sutton *et al.,* 1998). This relates to the colony morphology of the second isolate of this study – strain VM2, as it produces circular colonies (on nutrient agar) with radial furrows that are cream in colour, have a dull appearance and an umbonate elevation (Figure 3.6). Microscopically, this genus produces pseudohyphae and hyphae as well as blastoconidia that are unicellular and variable in shape (Larone, 1995). The septate hyphae fragment into elongated arthroconidia (Sutton *et al.,* 1998). Isolate VM2 showed cell structures typical for *Trichosporon* species, as elongated arthroconidia formed within the pseudohyphal buds (Figure 3.7). Strain VM2 also produces blastoconidia that are ~3 µm in diameter (Figure 3.8), again matching the features of other *Trichosporon* isolates (Sutton *et al.,* 1998). The genus *Trichosporon* has had many name changes over the years. An example of this is *Cutaneotrichosporon oleaginosus* ATTC 20509, a new potential cell factory for custom tailored microbial oils that was previously known as *Trichosporon oleaginosus*, *Crytococcus curvatus*, *Apiotrichum curvatum* or *Candida curvata* D (Bracharz *et al.,* 2017). Therefore, due to the numerous changes to the name of this genus, reports on this genus are scattered and poorly cited.

Fungal pathogens can be identified at the species level via the 18S, 5.8S and 28S sequence analysis of rRNA genes (O'Donnell, 1992). The rRNA encoding genes possess variable ITS regions that permit accurate distinction between closely related species of a fungal genus (Hennequin *et al.,* 1999). The identification at genus level can typically be assumed if sequence similarity scores are greater than 97%, while

scores of 99% or greater are considered to allow for species level assignment (Janda and Abbott, 2007). Strain VM1, when compared to sequences deposited in GenBank for strains of *Fusarium* spp. had sequence similarity scores of ≥99%, which allowed for genus level assignment (Table 3.1). Therefore, strain VM1, showing a similarity score of 100% to the ITS1-5.8S rRNA-ITS2 region sequence of a cultured isolate of *F. oxysporum*, was assigned to the genus *Fusarium* (Table 3.1). However, strain VM2 was assigned to the genus *Trichosporon*, with high sequence similarity to *Trichosporon terricola* (now known as *Cutaneotrichosporon terricola*) with an identity score of 99% (Table 3.2).

The phylogenetic analysis illustrates the relationship between the isolated strains and selected type strains or environmental isolates of the same genus based on their ITS region sequences (Figure 3.9 – 3.12). The phylogenetic analysis (Figure 3.9) showed that strain VM1 closely clustered with members of the genus *Fusarium* and *Gibberella*, grouping with *Fusarium oxysporum, Fusarium nygamai* and *Gibberella thapsina,* the teleomorph of *Fusarium thapsinum* (Klittich *et al.,* 1997). The maximum likelihood method confirmed that strain VM1 clustered within the genus *Fusarium* (Figure 3.10). The phylogenetic assessment revealed that strain VM2 clustered with members of the genus *Trichosporon,* closely grouping with *Cutaneotrichosporon terricola* (formerly known as *Trichosporon terricola*) (Figure 3.11). Again, the maximum likelihood model confirmed the placement of strain VM2 within the genus *Trichosporon* (Figure 3.12). Species of the genus *Fusarium* and the genus *Trichosporon* are frequently detected in soil environments (Dix and Webster, 1995; Saremi and Saremi, 2013; Sugita *et al.,* 2002). Therefore, the presence of the aerobic, metabolically versatile ascomycete fungus in soil samples from Bisley Nature Reserve and the basidiomycetous anamorphic yeast from a local farm confirms the presence of such species with the ability to catabolize aromatic compounds in South African soil environments.

Utilization of the target compounds

A typical growth curve was established when strain VM1 was grown with 10mM phenyl salicylate and no growth was observed in the controls (Figure 3.13). The growth curve correlated to the substrate utilization pattern when COD analysis was

employed since the lag phase observed in growth experiments corresponded to the stable COD concentration in salol utilization studies (Figure 3.14). The exponential phase of the biomass formation also relates to the rapid decline in COD concentration. Similarly, the increase in optical density, verified by microscopic cell counts, for strain VM2 correlates with the decrease in salol concentration observed in the COD analysis (Figure 3.40 and 3.41). However, while the fungus catabolized 10 mM salol completely during the incubation period, the yeast catabolized only about 55% of 10 mM salol (Figure 3.14 and 3.41). Controls showed that the substrate was not removed unless active conidia or yeast cells were present. The doubling times for strain VM1 and strain VM2 were ~24 hours and ~48 hours respectively (Figure 3.13 and 3.40). The highest molar biomass yield for strain VM1 was established as ~138 g dry weight /M salol consumed respectively (Figure 3.14), which matches data for other diaryl esters and structurally related compounds (Clauβen and Schmidt, 1998; Göttsching and Schmidt, 2007).

Strain VM1 when grown in 10 mM benzyl salicylate shows a maximum biomass yield of ~97 mg/L (Figure 3.16). This compound is therefore not an ideal growth substrate when compared to salol since the maximum biomass yield is significantly lower when grown in benzyl salicylate than when grown in salol (Figure 3.13). The same is evident for strain VM2 since yeast cells grown in salol showed a higher biomass yield than yeast cells grown in benzyl salicylate (Figure 3.40 and 3.43). The COD analysis confirmed the slow utilization of benzyl salicylate with only about 30% of 10 mM substrate being catabolized by the fungus and about 50% of 10 mM benzyl being catabolized by the yeast (Figure 3.17 and 3.43). This is possibly due to the low water solubility of benzyl salicylate at ~0.15 mg/L (Belsito *et al.*, 2007). Poorly water soluble compounds exist in water as a non-aqueous phase. Therefore, the mass transfer of these compounds is limited and the rate of mineralization is slow (Law and Aitken, 2003; Tang *et al.,* 2005).

Phenylacetate was a suitable compound for both the fungus and the yeast since the doubling time was ~24 hours (Figure 3.19 and Figure 3.46). The COD analysis confirmed the utilization of phenylacetate with over 80% of 10 mM phenylacetate being catabolized by strain VM1 and over 60% of 10 mM phenylacetate being utilized by strain VM2 within 10 and 8 days respectively (Figure 3.20 and 3.47). The

highest molar biomass yield under the specified growth conditions was ~96 g dry weight/M phenylacetate consumed for strain VM1, which is in agreement with results obtained for structurally related compounds (Clauβen and Schmidt, 1998). Phenylacetate occurs naturally in the soil environment since it is a known metabolite of phenylalanine. Therefore, microorganisms in this environment would possess catabolic enzymes to utilize this ester compound (Piscitelli *et al.,* 1995).

Strain VM1 was able to utilize phenol, salicylate and benzyl alcohol, the possible intermediates of the tested salicylate esters upon the cleavage of the ester-linkage. Although the fungus had a long lag phase of 4 days when grown in 5 mM phenol, the COD analysis showed that the strain could catabolize over 80% of the substrate by day 10 with a molar biomass yield of ~49 g dry weight/M phenol consumed (Figure 3.22 and Figure 3.23). COD analysis showed that *Fusarium* sp. strain VM1 utilized 5 mM salicylate to completion within 5 days, with a molar biomass yield of ~42 g dry weight/M substrate consumed (Figure 3.25 and 3.26). Similarly, the COD analysis showed that over 80% of 5 mM benzyl alcohol was utilized by this fungus within 5 days and the molar biomass yield was established as ~55 g/M substrate (Figure 3.29). Although these simple aromatic compounds are known antimicrobials, a study by Santos and Linardi (2004) demonstrated that *Fusarium* sp. strain FE11 catabolized about 70% of 10 mM phenol in 168 hours while Rabe *et al.,* (2013) reported the biodegradation of salicylate by the fungus *Ustilago maydis.* Benzyl alcohol and phenol were also reported to be utilized by *Penicillium* strain Bi 7/2 (Hofrichter and Scheibner, 1993).

Similarly, to strain VM1, phenol and benzyl alcohol supported the growth of strain VM2. However, salicylate was not an ideal growth substrate for strain VM2 since the doubling time under the specified growth conditions was established as ~24 hours and the COD analysis showed only a slight decrease in substrate concentration (Figure 3.52 and 3.53). The biocide, salicylic acid, is in fact toxic to species within the genus *Trichosporon* (Taj-Aldeen *et al.,* 2009). The yeast when grown with 5 mM phenol had a doubling time of ~12 hours and the exponential phase lasted for 2 days followed by the stationary phase (Figure 3.49). This coincides with the COD analysis where the phenol concentration rapidly decreased over the 8 day period until over 80% of phenol was catabolized by the yeast (Figure 3.50). This relates to a study by

Aleksieva *et al.* (2002) who demonstrated that *Trichosporon cutaneum* R57 was able to degrade phenol and derivatives such as 3-nitrophenol, 2,6-dinitrophenol and 4-nitrophenol. The yeast strain *Trichosporon* sp. VM2 when grown with 5 mM benzyl alcohol for 8 days showed a similar growth curve pattern to that of phenol grown cultures; however, the exponential phase lasted for 3 days followed by the stationary phase (Figure 3.55). This relates to the COD analysis with ~70% of 5 mM benzyl alcohol utilized by strain VM2 by day 8 (Figure 3.56). Similarly, Hasegawa *et al.* 1990 reported that *Trichosporon cutaneum* KUY-6A was able to utilize benzyl alcohol and its derivative, benzoate, as sole carbon and energy source.

Microorganisms require physical contact with and access to organic compounds for substrate utilization. Therefore, the molecules must be in aqueous solution so that they are available to the microbial cell and can diffuse directly into the cell (Ortega-Calvo *et al.,* 1995). Many aromatic compounds are insoluble or have low solubility in water owing to their hydrophobic nature (Boopathy, 2000). As a result, the rate of mass transfer of these compounds into the microbial cell is restricted and mineralization is slow (Law and Aitken, 2003; Tang *et al.,* 2005). Both phenyl salicylate and benzyl salicylate are hydrophobic compounds that have low solubility of ~0.15 g/L and ~0.15 mg/L at 20°C in aqueous solution respectively (Belsito *et al.*, 2007). Therefore, the mass transfer of these compounds to microbial cells is slow, thus a longer lag phase is typically observed as was the case during the growth of strain VM1 when grown in salol and benzyl salicylate respectively (Figure 3.13 and Figure 3.16). However, there was no lag phase observed when strain VM2 was grown with salol and only a slight lag phase was observed for growth with benzyl salicylate (Figure 3.40 and 3.43). This is possibly due to yeasts forming extracellular enzymes as well as biofilms, which aid in successful utilization of the compounds. Yeast cells also have the ability to attach to hydrophobic substances, which allows for the decrease in substrate concentration as was observed for strain VM2. This strain attached to the surface of the benzyl salicylate droplets, aiding in the utilization of the compound. However, fungi when in aqueous solutions, lose their ability to adhere to surfaces owing to the longer lag phases when compared to yeasts (Pinedo-Rivilla *et al.,* 2009). In addition, the morphology of microorganisms also affects the rate of mass transfer of compounds into the microbial cell. Mycelial fungi have limited surface area when compared to its volume therefore nutrients are

unable to diffuse sufficiently to interior parts of the hyphae. This is seen for strain VM1 since there is longer lag phases when grown with salol and benzyl salicylate.

UV-Vis spectroscopy was employed to additionally demonstrate that the utilization of the target compounds was due to microbial activity. Aromatic compounds possess delocalized pi (π) electrons that absorb light in the UV region since the π electrons of unsaturated bonds are excited between wavelengths of 200 to 700 nm (Watson *et al.,* 2001). Phenyl salicylate and benzyl salicylate exhibit a maximum absorbance between 290 to 330nm, phenylacetate and benzyl alcohol exhibit maximum absorbances between 240 to 270nm, phenol exhibits absorbance maxima between 250 to 280nm and salicylate exhibits absorbance maxima between 270 to 320nm (Nielsen *et al.,* 2001), matching the spectra obtained in this study.

The UV-Vis analysis showed that incubation with active cultures resulted in the decrease of the absorbance maxima of phenyl salicylate over time (Figure 3.15). This indicated that the aromatic body of phenyl salicylate had been catabolized as no such decrease was observed in controls. Therefore, strain VM1 can utilize salol as sole carbon and energy source. However, the culture supernatants of strain VM1 grown in benzyl salicylate when analysed by UV-Vis spectroscopy demonstrated that even when active cultures were present, benzyl salicylate was not completely eliminated within the incubation period (Figure 3.18). Benzyl salicylate is an antimicrobial and its mode of action is via its hydrolysis products, salicylate and benzyl alcohol, which are more bioavailable and more toxic than the parent compound (Radulović *et al.,* 2011; Sulaiman *et al.,* 2008). However, the fungus was able to utilize these compounds up to 10 mM. The UV-Vis analysis of the aerobic utilization of hydrolysis products of the salicylate esters, phenol, salicylate and benzyl alcohol showed that these were catabolized by strain VM1, with phenol and salicylate being quantitatively catabolized (Figure 3.24, 3.27 and 3.30). Based on the molar extinction coefficient of phenol and salicylate at 270nm and 295nm respectively, about 85% of phenol and about 83% of salicylate was utilized by the fungus over the incubation period (Figure 3.24 and 3.27). This is not unexpected as *Fusarium* species are known to catabolize simple aromatic compounds such as phenol and salicylate as sole carbon and energy source (Pinedo-Rivilla *et al.,* 2009).

The UV-Vis spectral analysis of culture supernatants of strain VM2 after growth with salol and benzyl salicylate showed that the phenol and benzyl alcohol moieties were utilized respectively. However, salicylate accumulated in the medium to ~4 mM based on the molar extinction coefficient of salicylate at 295nm (Figure 3.42 and 3.45). Therefore, strain VM2 was only able to partially catabolize these salicylate esters, since upon the cleavage of the esters, the yeast utilized only the most favourable compound formed. This matches Figure 3.54 as UV-Vis spectroscopy and COD analysis demonstrated that salicylate was only marginally catabolized by strain VM2. Based on the molar extinction coefficient of salicylate, about 6% of the substrate was utilized by the yeast. Salicylate is more bioavailable and therefore potentially more toxic than its parent compound (Radulović *et al.,* 2011). However, based on the UV-Vis analysis, about 85% phenol was used by the yeast by day 8, while benzyl alcohol was utilized by strain VM2 almost to completion over the 8 day period (Figure 3.51 and 3.47), which relates to the results shown in Figure 3.42 and 3.45. *Trichosporon* species, like *Fusarium* species, are known to catabolize simple aromatic compounds (Pinedo-Rivilla *et al.,* 2009).

Both strains as was already evident from the COD analysis utilized phenylacetate, causing an absorbance maxima decrease over time when analysed by UV-Vis spectroscopy (Figure 3.21 and 3.48). However, strain VM1 utilized phenylacetate with UV-Vis analysis indicating the transient formation of phenol (Figure 3.21), which was not evident for strain VM2 (Figure 3.48). The UV-Vis spectral analysis nicely matched the COD analysis for phenylacetate. The absorbance spectrum for heat inactivated cultures did not change over the incubation period, indicating that the aromatic body of the target compound remained intact.

Effect of substrate concentrations

The initial substrate concentration is responsible for the susceptibility of the substrate to microbial attack. If the concentration of the substrate is below the maintenance threshold required by the microorganism, biodegradation may not occur since the energy from the oxidation of the chemical is limited and cannot meet energy demands required by the microorganism. Thus, mineralization of the compound would be restricted (Boethling and Alexander, 1976). At the same time, increased

substrate concentrations may be toxic; hence, inhibiting the growth of the microorganism. The normal functioning of the cells is affected but this depends on the effective concentration of the toxic compound in a given environment (Sikkema *et al.,* 1995; El-Naas *et al.,* 2009).

Both strains were able to tolerate concentrations of up to 25 mM salol with the highest quantity of biomass produced at 25 mM salol (Figure 3.33 and 3.60). Like salol, strain VM1 and VM2 could tolerate benzyl salicylate concentrations of up to 25 mM (Figure 3.34 and 3.61). However, there was less growth evident when compared to that of salol. These two hydrophobic compounds have a low aqueous solubility. Therefore, the mass transfer of the molecule to the cell is limited and the interaction between the molecule and the cell is also limited (Boopathy, 2000). The compound must dissolve sufficiently in the aqueous solution for the microorganism to be susceptible to the impact of substrate toxicity. This was evident for phenylacetate, since this compound can dissolve in aqueous solution to a higher degree than the two tested salicylate esters. Therefore, concentrations ≥20 mM phenylacetate became limiting for the growth of both strains, possibly due to its toxicity (Figure 3.35 and 3.62).

Concentrations of up to 10 mM were employed for the known hydrolysis products of the salicylate esters: phenol, salicylate and benzyl alcohol. Strain VM1 could tolerate up to 5 mM phenol; however, above 8 mM growth inhibition was observed (Figure 3.36). A study by Park *et al.* (2009) reported that *Fusarium oxysporum* GJ4 was only able to utilize up to 2 mM phenol. This is possibly due to phenol being more bioavailable than its parent compound, phenyl salicylate. However, strain VM2 could grow with phenol up to 10 mM (Figure 3.63). Members of the genus *Trichosporon* were reported to utilize high concentrations of phenol (Pinedo-Rivilla *et al.,* 2009). However, strain VM2 was unable to utilize similarly high concentrations of salicylate, with 2 mM being the most favourable concentration for growth (Figure 3.64). Salicylate is a well-known biocide that interferes with enzymatic processes such as DNA replication, thus preventing cell replication and consequently limiting the growth of microorganisms (Block, 2001). However, strain VM1 could tolerate concentrations of up to 10 mM salicylate with the biomass increasing with an increase in substrate concentration (Figure 3.37). Mycelial fungi such as *Phanerochaete chrysosporium*

and *Piptoporus betulinus* are known to excrete extracellular enzymes such as oxidases and peroxidases that can aid in the catabolism or neutralization of toxic compounds (Pinedo-Rivilla *et al.,* 2009). Both strains are capable of utilizing up to 10 mM benzyl alcohol with biomass increasing with increase in substrate concentration (Figure 3.38 and 3.65). This indicates that benzyl alcohol is less toxic than salicylate for strain VM1 and VM2.

Utilization of organic pollutants

Both *Fusarium* sp. strain VM1 and *Trichosporon* sp. strain VM2 utilized aromatic and non-aromatic compounds. Utilization of individual hydrocarbons is highly specific since it depends on the enzymes produced by the microorganism required for the catabolism of a given hydrocarbon (Kirk et al., 1987; Have and Teunissen, 2001). Members of the genus *Fusarium* and *Trichosporon* have been reported to utilize various organic compounds (Prenafeta-Boldú *et al.,* 2006; Holland *et al.,* 1987; Pinedo-Rivilla *et al.,* 2009). However, the aerobic productive catabolism of diaryl esters by *Fusarium* and *Trichosporon* species has not been reported before. In addition to the tested esters and hydrolysis products, the two isolated strains utilized benzoic acid and 4-methylbenzoate (Table 3.3). Benzoic acid is the expected intermediate formed from the hydrolysis of benzyl salicylate when benzyl alcohol formed upon hydrolysis is further oxidized (Schmidt, 2002). The ability of microscopic fungi and yeasts to catabolize diverse benzoates is well established and therefore not surprising (Cain *et al.,* 1968). A study by Kawabe and Morita (1994) demonstrated how yeasts and fungi are capable of reducing benzoic acid and L-phenylalanine to benzaldehyde and benzyl alcohol. In addition to aromatic compounds, *Fusarium oxysporum* was previously reported to utilize glucose and acetate (Panagiotou *et al.,* 2008), as well as succinic acid and citric acid (Hassan *et al.,* 2015). Similarly, *Trichosporon* species can utilize various non-aromatic compounds including succinic acid, acetate and glucose (Piscitelli *et al.,* 1995; Pinedo-Rivilla *et al.,* 2009). Thus, it was not surprising that the isolates VM1 and VM2 utilized the above mentioned non-aromatic compounds.

Catabolic pathway for utilization of target compounds

To better understand the metabolism of aromatic compounds by microorganisms, the identification of key enzymes is required (Gibson, 1968). Determining the specific activity of key enzymes can elucidate and verify how these transform specific substrates and potential intermediates (Karegoudar and Kim, 2000; Dìaz, 2004).

Growth substrates influence the type of enzymes involved in metabolism via induction and the enzymes involved in the catabolism of aromatic compounds are usually inducible (Ornston and Stanier, 1966; Meagher and Ornston, 1973; Kurane *et al.,* 1980; Pèrez-Pantoja *et al.,* 2008). Catabolic enzymes involved in the utilization of the tested target compounds were induced in both strains after growth with these substrates (Table 3.4).

Salol and benzyl salicylate metabolism is initiated by esterase activity, which hydrolytically cleaves the substrates at the ester-linkage to transiently yield two monoaromatic metabolites: phenol and salicylate in the case of salol and benzyl alcohol and salicylate in the case of benzyl salicylate (Figure 4.1). This was confirmed as crude extracts from strains VM1 and VM2 after growth with the salicylate esters showed clearly induced elevated specific esterase activity for *p*-nitrophenylacetate, while growth on the non-esters showed base esterase activity; however, specific esterase activity for *p*-nitrophenylacetate was not induced or elevated. Phenol can further be metabolized to catechol via phenol hydroxylase while salicylate can be metabolized further by salicylate-1-hydroxylase. However, benzyl alcohol is further catabolized via benzaldehyde to yield benzoate, which is channelled via catechol into the ortho-pathway (Göttsching and Schmidt, 2007). Catechol, the key intermediate of the aforementioned growth substrates (phenol, salicylate and benzyl alcohol), was evidently cleaved via ortho-cleavage by catechol-1,2-dioxygenase to produce *cis,cis*-muconate (Figure 3.68 and 3.72). Phenylacetate is also channelled via catechol into the ortho-pathway since it induced specific activity for the tested catechols that was clearly higher than that detected in crude extracts from acetate grown cultures (Table 3.4). Spectral analysis confirmed esterase activity for strain VM1 and strain VM2 respectively, with a *p*-nitrophenol maximum increasing in intensity at 405nm (Su *et al.,* 2011). The crude extracts of

both strains VM1 and VM2 showed high specific catechol-1,2-dioxygenase activity for catechol, moderate activity for 4-methylcatechol and low activity for 3-methylcatechol with strain VM1 usually expressing higher activity than strain VM2 (Table 3.4). This is typical for type 1 catechol-1,2-dioxygenase activity, which catalyzes the oxygenolytic cleavage of catechol and has low or no activity for substituted catechols (Dorn and Knackmuss, 1978b). Again, spectral analysis confirmed catechol-1,2-dioxygenase activity for strain VM1 for crude extracts for phenol grown cultures since an absorbance maximum formed at 260nm. Similarly, catechol-1,2-dioxygenase activity was confirmed for strain VM2 since the formation of muconic acids from catechols was demonstrated (Figure 3.72 – 3.74).

The meta-cleavage activity by catechol-2,3-dioxgenase was not detected (Table 3.4). Ortho-cleavage is typically reported as the preferred pathway by fungi to channel catechol formed by microbial activity into central metabolism (Pèrez-Pantoja *et al.,* 2008). Therefore, hypothetic catabolic pathways for the aerobic utilization of the target compounds by the soil isolates *Fusarium* sp. strain VM1 and *Trichosporon* sp. strain VM2 are proposed based on enzymatic analysis and existing studies for similar compounds.

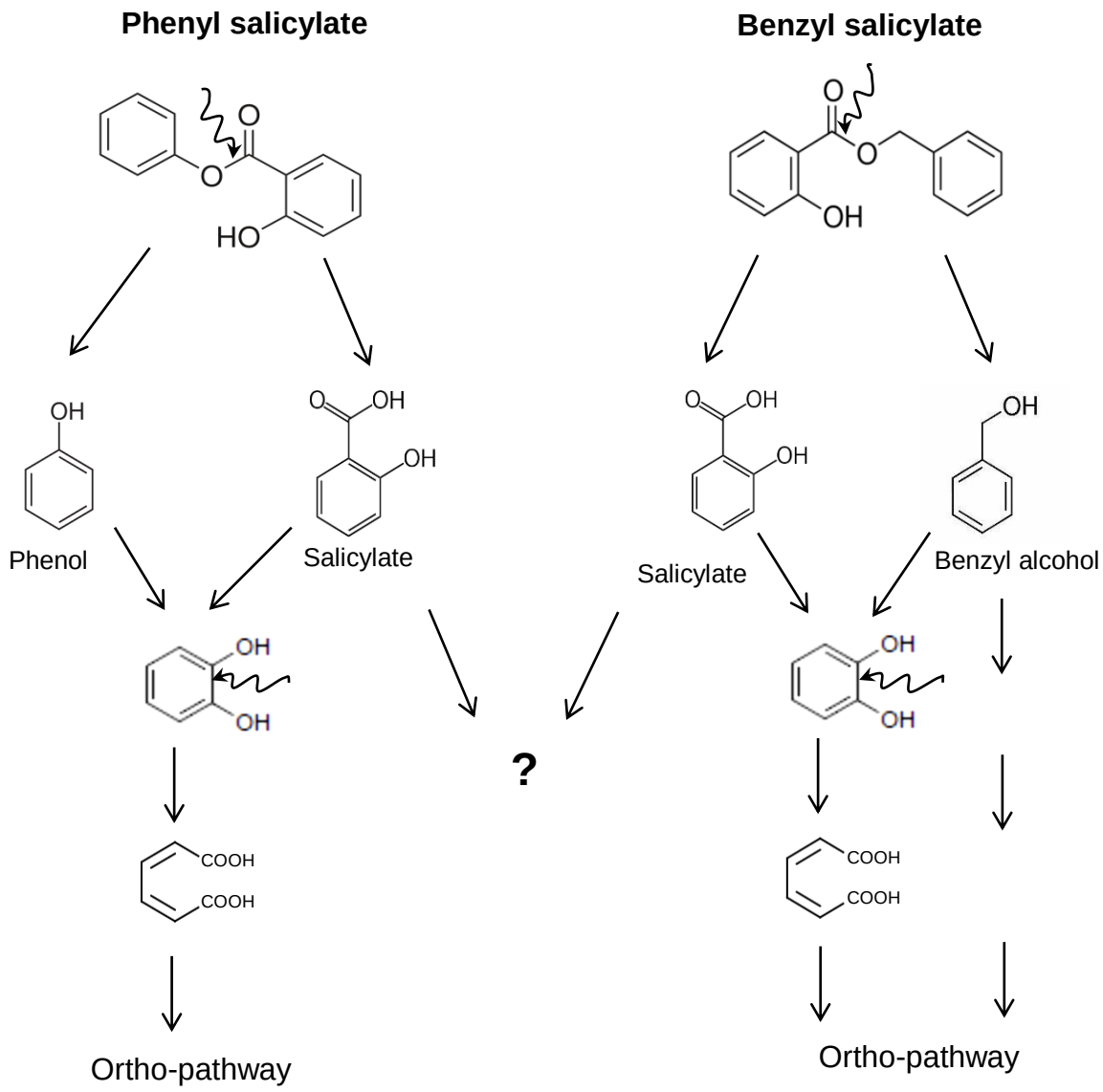

Figure 4.1: Possible catabolism of phenyl salicylate and benzyl salicylate by *Fusarium* sp. strain VM1 and *Trichosporon* sp. strain VM2

CHAPTER 5: CONCLUSION

The microbiological analysis of the newly isolated strains VM1 and VM2 indicates these are members of the genus *Fusarium* and *Trichosporon*, respectively. Although analysis of the ITS1-5.8S rRNA-ITS region demonstrated that the isolated fungal strain VM1 is closely related to *F. oxysporum* and that strain VM2 clusters with *T. terricola*, it is not yet possible to assign the isolates to species level. The ability of *Fusarium* sp. strain VM1 to utilize phenyl salicylate and *Trichosporon* sp. VM2 to utilize benzyl salicylate – diaryl ester biocides exhibiting endocrine-disrupting properties – as sole carbon and energy source confirms that such diaryl ester compounds are potential substrates for fungi present in South African soil environments. The possible catabolic pathway identified for phenyl salicylate and benzyl salicylate would be initiated by hydrolysis of the ester-linkage. The hydrolysis products would then be channelled into the ortho-pathway. Although there is only limited information pertaining to the catabolism of salicylate esters by fungi, this study provides evidence that members the genera of *Fusarium* and *Trichosporon* can aid in the removal of similar organic pollutants in soil environments. Additional analysis would be required to verify the involvement of other expected catabolic enzymes of the proposed pathway and to confirm the pathway intermediates.

REFERENCES

Aleksieva K., Ivanova D., Godjevargova T. and Atanasov B. 2002. Degradation of some phenol derivatives by *Trichosporon cutaneum* R57. *Process Biochemistry* **37,** 1215–1219.

Anderson J.J. and Dagley S. 1980. Catabolism of aromatic acids in *Trichosporon cutaneum*. *Journal of Bacteriology* **141,** 534–543.

Atlas R.M. and Cerniglia C.E. 1995 Bioremediation of petroleum pollutants. *Bioscience* **45,** 332–338.

Baek K., Yoon B., Oh H. and Kim H. 2006. Biodegradation of aliphatic and aromatic hydrocarbons by *Nocardia* sp. H17-1. *Geomicrobiology Journal* **23,** 253–259.

Batran M. 2014. Persistent organic pollutants (POPS): environment persistence and bioaccumulation potential. *Naval Academy Scientific Bulletin* **17,** 115–122.

Belsito D., Bickers D., Bruze M., Calow P., Gram H., Hanifin J.M., Rogers A.E., Saurge J.H., Sipes I.G. and Tagami H. 2007. A toxicology and dermatology assessment of salicylate when used in fragrance ingredients. *Journal Food and Chemical Toxicology* **45,** 316– 318.

Block S.S. 2001. Disinfection, sterilization and preservation 5TH Ed. Lippincott Williams and Walkings. USA.

Boethling R.S. and Alexander M. 1979. Effect of concentration of organic chemicals on their biodegradation by natural microbial communities. *Applied and Environmental Microbiology* **37,** 1211–1216.

Boopathy R. 2000. Factors limiting bioremediation technologies. *Bioresource Technology* **74,** 63–67.

Bracharz F., Beukhout T., Mehlmer N. and Brück T. 2017. Opportunities and challengers in the development of Cutaneotrichosporon oleaginosus ATCC 20509 as a new cell factory for custom tailored microbial oils. *Microbial Cell Factories* **16,** 178–188.

Bradford M.M. 1976. A rapid and sensitive methid for the quantification of microgram quantities of protein utilizing the principle of protein-dye binding. *Analytical Chemistry* **72,** 248–254.

Brieger L. 1878. Ueber die flüchtigen Bestandtheile der menschlichen Excremente (On the volatile components of human excrement). *Journal für Praktische Chemie*, **17,** 124–138.

Cain R.B., Bilton R.F. and Darrah J.A. 1968. The metabolism of aromatic acids by microganisms: metabolic pathways in the fungi. *Biochemistry Journal* **108,** 797–828.

Caliman F.A. and Gavrilescu M. 2009. Pharmaceuticals, personal care products and endocrine disrupting agents in the environment – a review. *Clean* **37,** 277–303.

Camacho-Muńoz D., Martin J., Jantos J.L., Aparicio I. and Alonso E. 2010. Occurrence, temporal evaluation and risk assessment of pharmaceutical active compounds in Donana Park (Spain). *Journal of Hazardous Material* **183,** 602–608.

Cameron G.W., Jordan K.N., Holt P.J., Baker P.B., Lowe C.R. and Bruce N.C. 1994. Identification of a heroin esterase in *Rhodococcus* sp. strain H1. *Applied Environmental Microbiology* **60,** 3881–3883.

Carey J.H. 1994. Transformation processes of contaminants in rivers*. Hydrological, Chemical and Biological Processes of Transformation and Transport of Contaminants in Aquatic Environments* **219,** 41–50.

Cerniglia C.E. 1993. Biodegradation of polycyclic aromatic hydrocarbons. *Current Opinion in Biotechnology* **4,** 331–338.

Cerniglia C.E., Sutherland J.B. and Crow S.A. 1992. Fungal metabolism of aromatic hydrocarbons. I. Microbial Degradation of Natural Products (Winkelmann G. ed.). *VCH Verlagsgesellschaft.* Weinheim, Germany. 193–217.

Chang S. and Han C. D. 1996. Effect of bulky pendent side groups on the structure of mesophase in a thermotropic mainchain liquid-crystall polymer. *Macromolecules* **29,** 2103–2111.

Charles A.K. and Darbrea P.D. 2009. Oestrogenic activity of benzyl salicylate, benzyl benzoate and butylphenylmethylpropional (Lilial) in MCF7 human breast cancer cells in vitro. *Journal of Applied Toxicology* **29,** 422–434.

Chase M.W. and Reveal J.L. 2009. A phylogenetic classification of the land plants to accompany APG III. *Botannical Journal of the Linnean Society* **161,** 122–127.

Christen V., Hickmann S., Rechenberg B. and Fenta K. 2010. Highly active human pharmaceuticals in aquatic systems: a concept for their identification based on their mode of action. *Aquatic Toxicology* **96,** 167–181.

Clauβen M. and Schmidt S. 1998. Biodegradation of phenol and *p*-cresol by the hyphomycete *Scedosporium apiospermum. Research in Microbiology* **149.** 399–406.

Clauβen M. and Schmidt S. 1999. Biodegradation of phenyl benzoate and some of its derivatives by *Scedosporium apiospermum*. *Research in Microbiology* **150,** 413–420.

Colombo J.C., Cabello M. and Arambarri A.M. 1996. Biodegradation of aliphatic and aromatic hydrocarbons by natural soil microflora and pure culture of imperfect and lignolitic fungi. *Environmental Pollution* **94,** 355–362.

Connell D.W. 1990. General characteristics of organic compounds which exhibit bioaccumulation. In: Connell, D. W. (ed.) Bioaccumulation of xenobiontic compounds. *CRC Press*. 47–57.

Cookson J.T. 1995. Bioremediation engineering: design and application, **2nd ed.** *McGraw-Hill*. New York.

Cox H.H.J., Houtman J.H.M., Doddema H.J. and Harder W. 1993. Enrichment of fungi and degradation of styrene in biofilters. *Biotechnology Letters 15,* 737–742.

Daane L.L., Harjono I., Zylstra G.J. and Häggblom M.M. 2001. Isolation and characterization of polycyclic aromatic hydrocarbon-degrading bacteria associated with the rhizosphere of salt marsh plants. *Applied and Environmental Microbiology* **1,** 2683–2691.

Dąbrowska D., Kot-Wasik A. and Namieśnik J. 2004. The importance of degradation in the fate of selected organic compounds in the environment part II: photodegradation and biodegradation. *Polish Journal of Environmental Studies* **13,** 617–626.

Dagley S. 1971. Catabolism of aromatic compounds by micro-organisms. *Advances in Microbial Physiology* **6,** 1– 46.

D'Annibale A., Quaratino D., Federici F. and Fenice M. 2006. Effect of agitation and aeration on the reduction of pollutant load of olive mill wastewater by the white-rot fungus *Panus tigrinus*. *Biochemical Engineering Journal* ***29,*** 243–249.

Das N. and Chandran P. 2010. Microbial degradation of petroleum hydrocarbon contaminants: an overview. *Biotechnology Research International* **2011,** 1–13.

Davoren M., Ní-Shúilleabháin S., Hartl M.G.J., Sheehan D., O'Brien N.M. and O'Halloran J. 2005. Assessing the potential of fish cell lines as tools for the cytotoxicity testing of estuarine sediment aqueous elutriates. *Toxicology in Vitro* **19,** 421–431.

De Castro-Català N., Kuzmanovic M., Roig N., Sierra J., Ginebreda A., Barceló D., Pérez S., Petrovic M., Picó Y., Schuhmacher M. and Muñoz I. 2016. Ecotoxicity of sediments in rivers: invertebrate community, toxicity bioassays and the toxic unit approach as complementary assessment tools. *Science of the Total Environment* **540,** 297–306.

Dearing M.D., Mangione A.M., and Karasov W.H. 2000. Diet breadth of mammalian herbivores: nutrient versus detoxification constraints. *Oecologia* **123,** 397–405.

Department of Health and Human Services. 2015. Medical management guidelines for phenol. *Agency for Toxic Substances and Disease Registry*. United States.

Dìaz E. 2004. Bacterial degradation of aromatic pollutants: a paradigm of metabolic versatility. *International Microbiology* **7,** 173–180.

Dix N.J. and Webster J. 1995. Fungi of Soil and Rhizosphere. *Fungal Ecology* **1,** 172–202.

Dodge A.G. and Wackett L.P. 2005. Metabolism of bismuth subsalicylate and intracellular accumulation of bismuth by *Fusarium* sp. strain BI. *Applied and Environmental Microbiology* **71,** 876–882.

Dongwei W., Yanghon P., Chao Z. and Feng Y. 2009. Measurement and correlation of solid-liquid equilibria of Phenyl salicylate with C4 alcohol. *Chinese Journal of Chemical Engineering* **17,** 140–144.

Dorn E. and Knackmuss H. 1978a. Chemical structure and biodegradability of halogenated aromatic compounds. Two catechol-1,2-dioxygenases from a 3-chlorobenzoate-grown *Pseudomonad*. *Biochemistry Journal* **174,** 73–84.

Dorn E. and Knackmuss H. 1978b. Chemical structure and biodegradability of halogenated aromatic compounds. Substituent effects on 1,2-dioxygenation of catechol. *Biochemistry Journal* **174,** 85–94.

EFSA CEF Panel. 2013. Scientific opinion on the toxicological evaluation of phenol. *EFSA Journal* **11,** 3189–3233.

El-Naas M.H., Al-Muhtaseb S.A. and Makhlouf S. 2009. Biodegradation of phenol by *Pseudomonas putida* immobilized in polyvinyl alcohol (PVA) gel. *Journal of Hazardous Material* **164,** 720–725.

Farré M., Pérez S., Kantiani L. and Barcelo M. 2008. Fate and toxicity of emerging pollutants, their metabolites and transformation products in the aquatic environment. *Trends in Analytical Chemistry* **27,** 991–1007.

Filonov A.E., Karpov A.V., Kosheleva I.A., Puntus I.F., Balashova N.V. and Boronin A.M. 2000. The efficiency of salicylate utilization by *Pseudomonas putida* strains catabolizing naphthalene via different biochemical pathways. *Process Biochemistry* **35,** 983–987.

Fimiani M., Casini L. and Bocci S. 1990. Contact dermatitis from phenyl salicylate in a galenic cream. *Contact Dermatitis* **22,** 239–250.

Fishbeck W.A., Langer R.R. and Kociba R.J. 1975. Elevated urinary phenol levels not related to benzene exposure. *American Industrial Hygiene Association Journal* **36,** 820–824.

Gaal A. and Neujahr H.Y. 1980. *cis,cis*-Muconate cyclase from *Trichosporon cutaneum. Biochemical Journal* **191,** 37-43.

Ghosal D., Ghosh S., Dutta T.K. and Ahn Y. 2016. Current state of knowledge in microbial degradation of polycyclic aromatic hydrocarbons (PAHs): a review. *Frontiers in Microbiology* **7,** 1–27.

Gibson D.T. 1968. Microbial degradation aromatic compounds. *Science* **161,** (3846), 1093–1097.

Golovleva L.A., Aharonson N., Greenhalgh R., Sethunathan N. and Vonk J.W. 1990. The role and limitations of microorganisms in the conversion of xenobiotics. *Pure Applied Chemistry* **62,** 351–364.

Göttsching A. and Schmidt S. 2007. Productive degradation of the biocide benzylbenzoate by *Acinetobacter* sp. strain AG1 isolated from the River Elbe. *Research in Microbiology* **158,** 251–257.

Harwood C.S. and Parales R.E. 1996. The β-ketoadipate pathway and biology of self-identity. *Annual Review of Microbiology* **50,** 553–590.

Hasegawa Y., Okamoto T., Obata H. and Tokuyama T. 1990. Utilization of aromatic compounds by *Trichosporon cutaneum* KUY-6A. *Journal of fermentation and bioengineering* **69,** 122–124.

Hashimotoa Y., Kawaguchib M., Miyazakib K. and Nakamura M. 2003. Estrogenic activity of tissue conditioners in vitro. *Dental Materials* **19,** 341–346.

Hassan R., El-Kadi S. and Sand M. 2015. Effect of some organic acids on some fungal growth and their toxins production. *International journal of advances in Biology* **2,** 1–22.

Have R. and Teunissen P.J. 2001. Oxidative mechanisms involved in lignin degradation by white-rot fungi. *Chemistry Reviews* **101,** 3397-3413.

Hedgespeth M.L., Sapozhnikova Y., Pennington P., Allan Clum A., Fairey A., and Wirth E. 2012. Pharmaceuticals and Personal Care Products (PPCPs) in treated wastewater discharges into Charleston Harbour, South Carolina. *Science of the Total Environment* **437,** 1–9.

Hegeman G.D. 1966. Synthesis of the enzymes of the mandelate pathway by *Pseudomonas putida*: isolation and properties of constitutive mutants. *Journal of Bacteriology* **91,** 1161–1167.

Henderson M.E.K. 1960. The influence of trace elements on the metabolism of aromatic compounds by soil fungi. *Journal of General Microbiology* **23,** 307–314.

Henderson M.E.K. 1961a. Isolation, identification and growth of some soil hyphomycetes and yeast-like fungi which utilize aromatic compounds related to lignin. *Journal of General Microbiology* **26,** 149–160.

Henderson M.E.K. 1961b. The metabolism of aromatic compounds related to lignin by some hyphomycetes and yeast-like fungi of soil. *Journal of General Microbiology* **26,** 155–165.

Henderson M.E.K. and Farmer V.C. 1955. Utilization by soil fungi of *p*-hydroxybenzaldehyde, ferulic acid, syringaldehyde and vanillin. *Journal of General Microbiology* **12,** 37–49.

Hennequin C., Abachin E., Symoens F., Lavarde V., Reboux G., Nolard N. and Berche P. 1999. Identification of *Fusarium* species involved inhuman infections by 28S rRNA gene sequencing. *Journal of Clinical Microbiology* **37,** 3586–3589.

Hofrichter M. and Scheibner K. 1993. Utilization of aromatic compounds by the *Penicillium* strain Bi 7/2. *Journal of Basic Microbiology* **33,** 163–173.

Holland H.L., Bergen E.J., Chenchaiah P.C., Khan S.H., Munoz B., Ninniss R.W. and Richards D. 1987. Side chain hydroxylation of aromatic compounds by fungi: products and stereochemistry. *Canadian Journal of Chemistry* **65,** 502–507.

Hwang H., Hodson R.E. and Lee R.F. 1987. Photolysis of phenol and chlorophenols in estuarine water. *ACS Symposium Series*: Washington DC.

Ishiyama D., Vujaklija D. and Davies J. 2004. Novel pathway of salicylate degradation by *Streptomyces* sp. strain WA46. *Applied and Environmental Microbiology* **73,** 1297–1306.

Iqbal M.J. and Chaudhry M. 2008. Thermodynamic studies on the interactions of phenyl salicylate in protic solvents at different temperatures. *Journal of Molecular Liquids* **143,** 75–80.

Janda J.M. and Abbott S.L. 2007. 16S rRNA gene sequence for bacterial identification in the diagnostic laboratory: pluses, perils and pitfalls. *Journal of Clinical Microbiology* **45,** 2761–2764.

Jones K.H., Trudgill P.W. and Hopper D. 1993. Metabolism of *p*-cresol by the fungus *Aspergillus fumigatus*. *Applied Environmental Microbiology* **59,** 1125–1130.

Jury M.R. 2013. Climatic trends in southern Africa. *South African Journal of Science* **109,** 1–11.

Kamra D.N. 2005. Rumen microbial ecosystem. *Current Science* **89,** 125–135.

Karegoudar T.B. and Kim C.K. 2000. Microbial degradation of monohydroxybenzoic acids. *The Journal of Microbiology* **38,** 53–61.

Kaschabek S.R., Kasberg T., Müller D., Mars A.E. Janssen D.B. and Reineke W. 1998. Degradation of chloroaromatics: purification and characterization of a novel type of chlorocatechol-2,3-dioxygenase of *Pseudomonas putida* GJ31. *Journal of Bacteriology* **180,** 296–302.

Kawabe T. and Morita H. 1994. Production of benzaldehyde and benzyl alcohol by mushroom *Polyporus tuberaster* K2606. *Journal of Agricultural and Food Chemistry* **42,** 1–9.

Khan R.I., Onodera R., Amin M.R. and Mohammed N. 2002. Aromatic amino acid biosynthesis and production of related compounds from *p*-hydroxyphenylpyruvic acid by rumen bacteria, protozoa and their mixture. *Amino acids* **22,** 167–177.

Kirk O., Borchert T.V. and Fuglsang C.C. 2002. Industrial enzyme applications. *Current Opinion in Biotechnology* **13,** 345–351.

Kirk T.K. and Farrell R.L. 1987. Enzymatic “combustion”: the microbial degradation of lignin. *Annual Reviews of Microbiology* **41,** 465–505.

Klittich C.J.R., Leslie J.F., Nelson P.E. and Marasas W.F.O. 1997. *Fusarium thapsinum* (*Gibberella thapsina*): A new species in section Liseola from sorghum. *Mycologia* **89,** 643–652.

Kohl K.D., Weiss R.B., Cox J., Dale C. and Dearing M.D. 2014. Gut microbes of mammalian herbivores facilitate intake of plant toxins. *Ecology Letter* **1,** 1–9.

Kristensen D.M., Hass U., Lesne L. and Lottrup G. 2010. Intrauterine exposure to mild analgesics is a risk factor for development of male reproductive disorders in human and rat. *Human Reproduction* **1,** 3231–3323.

Krücke B., Zaschke H., Kostromin S.G. and Shibaen V.P. 1985. Thermotrope liquid-crystalline polymers. *Acta Polymer* **36,** 639–643.

Kunz P.Y., Galicia H.F. and Fent K. 2006. Comparison of in Vitro and in Vivo estrogenic activity of UV filters in fish. *Toxicological Science* **90,** 349–361.

Kurane R., Suzuki T. and Takahara Y. 1980. Induction of enzymes involved in phthalate esters metabolism in *Nocardia erythropolis* and enzymatic hydrolysis of phthalate esters by commercial lipases. *Agricultural and Biological Chemistry* **44,** 529–536.

Lapczynski A., Jones L., McGinty D., Bhatia S.P., Letizia C.S. and Api A.M. 2007. Fragrance material review on phenyl salicylate. *Food Chemical Toxicology* **45,** 472–476.

Larone D.H. 1995. Medically important fungi – a guide to identification, **3rd ed.** *ASM Press, Washington DC.*

Law A.M.J. and Aitken M.D. 2003. Bacterial chemotaxis to naphthalene desorbing from a non-aqueous liquid. *Applied and Environmental Microbiology* **69,** 5968–5973.

Leahy J.G. and Colwell R.R. 1990. Microbial degradation of hydrocarbons in the environment. *Microbiological Review* **54,** 305–315.

Lebel M., Ferron L., Masson M., Pichette J. and Carrier C. 1998. Benzyl alcohol metabolism and elimination in neonates. *Development Pharmacology and Therapeutics* **11,** 347–356.

Leonowicz A., Matuszewska A., Luterek J., Ziegenhagen D., Wojtas-Wasilewska M., Cho N.S., Hofrichter M. and Rogalski J. 1999. Biodegradation of lignin by white rot fungi. *Fungal Genetics and Biology* **27,** 175–185.

Lepper P., Soroklin N., Atkinson C., Rule K. and Hope S. J. 2007. Proposed EQS for water framework directive Annex VII substances: phenol. *Science Report* **12,** 1–77.

Lotufo G.R. 1998. Bioaccumulation of sediment-associated fluoranthene in benthic copepods: uptake, elimination and biotransformation. *Aquatic Toxicology* **44,** 1–15.

Lyman W. J., Reehl W.F. and Rosenblatt D.H. 1990. Handbook of chemical property estimation methods. *McGraw-Hill.* New York.

Mach H., Middaugh R. and Lewis R.V. 1992. Detection of proteins and phenol in DNA samples with second-derivative absorption spectroscopy. *Analytical Biochemistry* **200,** 20–26.

Mackay D. and Fraser M. 2000. Bioaccumulation of persistent organic chemicals: mechanism and model. *Environmental Pollution* **110,** 375–391.

Maddela N.R., Scalvenzi L., Pérez M., Montero C. and Gooty J.M. 2015. Efficiency of indigenous filamentous fungi for biodegradation of petroleum hydrocarbons in medium and soil: laboratory study from Ecuador. *Bulletin of Environmental Contamination and Toxicology* **95,** 385–394.

Maloney S.E., Maule A. and Smith, A.R.W. 1988. Microbial transformation of the pyrethroid insecticides: permethrin, deltamethrin, fastac, fenvalerate, and euvalinate. *Applied Environmental Microbiology* **54,** 2874–2876.

Margesin R. and Schinner F. 2001. Biodegradation and Bioremediation of hydrocarbons in extreme environment. *Applied Microbiology Biotechnology* **56,** 650–663.

Masters K. and Bräse S. 2012. Xanthones from fungi, lichens and bacteria: the natural products and their synthesis. *Chemistry Review* **112,** 3717–3776.

McIlwain H. 1948. Preparation of cell-free bacterial extracts with powdered alumina. *Journal of General Microbiology* **2,** 288–291.

Meagher R.B. and Ornston L.N. 1973. Relationships among enzymes of the β-ketoadipate pathway. I. Properties of *cis,cis*-muconate-lactonizing enzyme and muconolactone isomerase from *Pseudomonas putida. Biochemistry* **12,** 3523–3530.

Menzie C.A., Potocki B.B. and Santodonato J. 1992. Exposure to carcinogenic PAHs in the environment. *Environmental Science and Technology* **26,** 1278–1284.

Middelhoven W.J. 1993. Catabolism of benzene compounds by ascomycetous and basidomycetous yeasts and yeastlike fungi – a literature review and an experimental approach. *Antonie van Leeuwenhoek* **63**, 122–144.

Mill T. and Mabey W. 1988. Hydrolysis of organic chemicals. *The Handbook of Environmental Chemistry* **2,** 71–111.

Mill T.M. 1989. Structure-activity relationships for photooxidation processes in environment. *Environmental Toxicology and Chemistry* **8,** 31–43.

Mineki S., Suzuki K., Iwata K., Nakajima D. and Goto S. 2015. Degradation of polyaromatic hydrocarbons by fungi isolated from soil in Japan. *Polycyclic Aromatic Compounds* **35,** 102–108.

Moore B.D. and Foley W.J. 2005. Trees used by koalas in a chemically complex landscape. *Nature* **435,** 488–490.

Nair B. 2001. Final report of the safety and assessment of benzyl alcohol, benzoic acid and sodium benzoate. *International Journal of Toxicology* **20,** 23–50.

Ndlela L.L. and Schmidt S. 2016. Evaluation of wild herbivore faeces from South Africa as a potential source of hydrolytically active microorganisms. *SpringerPlus* **5,** 118–129.

Nelson P.E., Dignani M.C. and Anaissie E.J. 1994. Taxonomy, biology and clinical aspects of *Fusarium* species. *Clinical Microbiology Review* **7,** 452–479.

Nielsen S.B., Lapierre A., Andersen J.U., Pedersen U.V., Tomita S. and Andersen L.H. 2001. Absorption spectrum of the green fluorescent protein chromophore anion in vacuo. *Physical Review Letters* **87,** 228102.

Nordström F.L. and Rasmuson A.C. 2006. Solubility and melting properties of salicylic acid. *Journal of Chemical and Engineering Data* **51,** 1668–1671.

O'Donnell K. 1992. Ribosomal DNA internal transcribed spacers are highly divergent in the phytopathogenic ascomycete *Fusarium sambucinum* (*Gibberella pulicaris*). *Genetics* **22,** 213–220.

Odenyo A.A., Mackie R.I. Stahl D.A. and White B.A. 1994. The use of 16S rRNA probes to study competition between rumen fibrolytic bacteria: development of probe for *Ruminococcus* species and evidence for bacteriocin production. *Applied Environmental Microbiology* **60,** 3688–3696.

Ornston L.N. and Stanier R.Y. 1966. The conversion of catechol and protocatechuate to β-ketoadipate by *Pseudomonas putida*. *Journal of Biological Chemistry* **241,** 3776–3786.

Ortega- Calvo J.J., Birman I. and Alexander M. 1995. Effect of varying the rate of partitioning of phenanthrene in non-aqueous-phase liquids on biodegradation in soil slurries. *Environmental Science and Technology* **29,** 2222–2225.

Panagiotou G., Pachidou F., Petroutsos D., Olsson L. and Christakopoulos P. 2008. Fermentation characteristics of *Fusarium oxysporum* grown on acetate. *Bioresource Technology* **99,** 7397–7401.

Park J.Y., Hong J.W. and Gadd G.M. 2009. Phenol degradation by *Fusarium oxysporum* GJ4 is affected by toxic catalytic polymerization mediated by copper oxide. *Chemosphere*, **75,** 765–771.

Pawar R.M. 2015. The effect of soil pH on bioremediation of polycyclic aromatic hydrocarbons (PAH's). *Journal of Bioremediation and Biodegradation*, **6,** 3–17.

Pèrez-Pantoja D., De la Iglesia R., Pieper D.H. and Gonzàlez B. 2008. Metabolic reconstruction of aromatic compounds degradation from the genome of the amazing pollutant-degrading bacterium *Cupriavidus necator* JMP134. *FEMS Microbiology Reviews* **32,** 736–794.

Pinedo-Rivilla C., Aleu J. and Collado I.G. 2009. Pollutants biodegradation by fungi. *Current Organic Chemistry* **13,** 1194–1214.

Piscitelli S.C., Thibault A., Figg W.D., Tompkins A., Headlee D., Lieberman R., Samid D. and Myers C.E. 1995. Disposition of phenylbutyrate and its metabolites,

phenylacetate and phenylacetylgutamine. *Journal of Clinical Pharmacology* **35,** 368–373.

Prenafeta-Boldú F.X., Summerbell R., and de Hoog G.S. 2006. Fungi growing on aromatic hydrocarbons: biotechnology's unexpected encounter with biohazard?. *FEMS Microbiology Reviews* **30,** 109–130.

Price C.T.D., Lee I.R. and Gustafson J.E. 2000. The effect of salicylate on bacteria. *International Journal of Biochemistry and Cell Biology* **32,** 1029–1043.

Powlowski J.B., Ingerbrand J. and Dagley S. 1985. Enzymology of the beta-ketoadipate pathway in *Trichosporon cutaneum*. *Journal of Bacteriology* **163,** 1136–1141.

Rabe F., Ajami Z., Doehleman G. and Kahmann R. 2013. Degradation of the plant defence hormone salicylic acid by the biotrophic fungus *Ustilago maydis*. *Molecular Microbiology* **89,**179–188.

Radulović N., Dekić M., Radić Z.R. and Palić R. 2011. Chemical composition and antimicrobial activity of the essential oils of *Geranium columbinum* L. and *G. lucidum L.* (*Geraniaceae*). *Turkish Journal of Chemistry* **35,** 499–512.

Reich T., Schmidt S. and Fortnagel P. 1999. Metabolism of phenyl benzoate by *Pseudomonas* sp. strain TR3. *FEMS Microbiology Letters* **176,** 477–482.

Rodriguez, J., Ferraz A., Nogueira R.F., Ferrer I., Esposito E. and Duran N. 1997. Lignin biodegradation by the ascomycete *Chrysonilia sitophila*. *Applied Biochemistry and Biotechnology* **62,** 233–242.

Rumpel C., Seraphin A. and Kögel-Knabner I. 2005. Effect of base hydrolysis on the chemical composition of organic matter of an acid forest soil. *Organic Geochemistry* **36,** 239–249.

Sampedro I., D'Annibale, A., Ocampo J.A., Stazi, S.R. and Garcia-Romera I. 2007. Solid-state cultures of *Fusarium oxysporum* transform aromatic components of olive-mill dry residue and reduce its phytotoxicity. *Bioresource Technology* **98,** 3547–3554.

Santos V.L. and Linardi V.R. 2004. Biodegradation of phenol by filamentous fungi isolated from industrial effluents – identification and degradation potential. *Process Biochemistry* **39,** 1001–1006.

Saremi H. and Saremi H. 2013. Isolation of the most common *Fusarium* species and the effect of soil solarisation on main pathogenic species in different climatic zones of Iran. *European Journal of Plant Pathology* **137,** 585–596.

Scheringer M., Strempel S., Hukari S., Ng C.A., Blepp M. and Hungerbuhler K. 2012. How many persistent organic pollutants should we expect?. *Atmospheric Pollution Research* **3,** 383–391.

Schmidt S. 2002. Biodegradation of diaryl esters: bacterial and fungal catabolism of phenyl benzoate and some of its derivatives. *Biotransformations: Bioremediation Technology for Health and Environmental Protection* **1,** 349–364.

Schmidt S. and Kirby G.W. 2001. Dioxygenative cleavage of C-methylated hydroquinones and 2,6-dichlorohydroquinone by *Pseudomonas* sp. HH35. *Biochimica et Biophysica Acta* **1568,** 83–89.

Schultz T.W. 1987. Relative toxicity of para-substituted phenols: log K_{ow} and pKa-dependent structure-activity relationships. *Bulletin of Environmental Contamination and Toxicology* **38,** 994–999.

Seo J., Keum Y. and Li Q. X. 2009. Bacterial degradation of aromatic compounds. *International Journal of Environmental Research and Public Health* **6,** 278–309.

Sharifi M. and Connell D.W. 2003. Development of QSARS for dietary accumulation of PP'DDT and chlorobenzenes with goldfish (*Carassius auratus*). *Australasian Journal of Ecotoxicology* **9,** 55–60.

Sikkema J., De Bont J.A.M. and Poolman B. 1995. Mechanisms of membrane toxicity of hydrocarbons. *Microbiological reviews* **51,** 201–222.

Silva T.R., Valdman E., Valdman B. and Leite S.G.F. 2007. Salicylic acid degradation from aqueous solutions using *Pseudomonas fluorescens* HK44: parameters studies and applications. *Brazilian Journal of Microbiology* **38,** 39–44.

Song Y. 2009. Characterization of aromatic hydrocarbon degrading bacteria isolated from pine litter. *Korean Journal of Microbiology and Biotechnology* **37,** 333–339.

Spencer W.F. and Ciath M.M. 1973. Pesticide volatization as related to water loss of soil. *Journal of Environmental Quality* **2,** 284–289.

Spencer W.F., Farmer W.J. and Jury W.A. 2009. Review: behaviour of organic chemicals at soil, air, water interfaces as related to predicting the transport and volatilization of organic pollutants. *Environmental Toxicology and Chemistry* **1,** 1–17.

Spurr A.R. 1969. A low-viscosity epoxy resin embedding medium for electron microscopy. *Journal of Ultrastructure Research* **26,** 31–43.

Stanier R.Y. and Ornston L.N. 1973. The beta-ketoadipate pathway. Advances Microbial Physiology **9,** 89–151.

Steen W.C. and Karickhoff S.W. 1981. Biosorption of hydrophobic organic pollutants by mixed microbial populations. *Chemosphere* **10,** 27–32.

Steward C.C., Dixon R.B., Chen Y.P. and Lovell C.R. 1992. Bacterial numbers and activity, microalgal biomass and productivity and meiofaunal distribution in sediments naturally contaminated with biogenic bromophenols. *Marine Ecology Progress Series* **90,** 61–72.

Stömer K. 1908. Über die Wirkung von Schwefelkohlenstoff und ähnlicher Stoffe auf den Boden (On the action of carbon disulphide and similar substances on the soil). *Bakteriol. Parasitenk. Infekt. Abt*. **II, 20,** 282–286.

Su G., Wei Y. and Guo M. 2011. Direct colorimetric detection of hydrogen peroxide using 4-nitrophenyl boronic acid or its pinacol ester. *American Journal of Analytical Chemistry* **2,** 879–884.

Sugita T., Takashima M., Nakase T., Ichikawa T., Shinoda T. and Nishikawa A. 2002. A basidiomycetous anamorphic yeast, *Trichosporon terricola* sp. nov, isolated from soil. *Journal of General and Applied Microbiology* **48,** 293–297.

Sulaiman F.M., Yaacob S.S., Lan T.M. and Muhammad T.S.T. 2008. Chemical components of the essential oils from three species of Malaysian *Plumeria L.* and their effects on the growth of selected microorganism. *Journal of Bioscience* **19,** 1–7.

Sutton D.A., Fothergill A.W. and Rinaldi G. 1998. Guide to clinically significant fungi, **1st ed.** *Williams and Wilkins,* Baltimore.

Sylvia D.M. 2005. Principles and applications of soil microbiology, **2nd ed.** Pearson Prentice Hall. New Jersey.

Taj-Aldeen S.J., Al-Ansari N., Shafei S.E., Meis J.F., Curfs-Breuker I., Theelen B. and Boekhout T. 2009. Molecular identification and susceptibility of *Trichosporon* species isolated from clinical specimens in Qatar: Isolation of *Trichosporon dohaense*. *Journal of Clinical Microbiology* **47,** 1791–1799.

Tamura K., Stecher G., Peterson D., Filipski A. and Kumar S. 2016. MEGA7: Molecular Evolutionary Genetics Analysis Version 7.0. *Molecular Biology and Evolution* **30,** 2129–2725.

Tang Y.J., Qi L. and Krieger-Brockett B. 2005. Evaluating factors that influence microbial phenanthrene biodegradation rates by regression with categorical variables. *Chemosphere* **59,** 729–741.

Teixeira L.M., Coelho L. and Tebaldi N.D. 2017. Characterization of *Fusarium oxysporum* isolates and resistance of passion fruit genotypes to fusariosis. *Revista Brasileira de Fruticultura* **39,** 415–426.

Ungar G., Damgaard E. and Wong W.K. 1952. Determination of salicylic acid and related substances in serum by ultraviolet spectroscopy. *Experimental Biology and Medicine* **80,** 45–47.

van den Brink H.J.M., van Gorcom R.F.M., van den Hondel C.A.M.J.J. and Punt P.J. 1998. Cytochrome P450 enzyme systems in fungi. *Fungal Genetics and Biology* **23,** 1–17.

Van Hamme J.D., Singh A. and Ward O.P. 2003. Recent advances in petroleum microbiology. *Microbiology and Molecular Biology Reviews* **67,** 503–549.

Vione D., Picatonotto T. and Carlotti M.E. 2003. Photodegradation of phenol and salicylic acid by coated rutile-based pigments A: new approach for the assessment of sunscreen treatment efficiency. *International Journal of Cosmetic Science* **54,** 513–524.

Wackett L.P. and Ellis L.B. 1999. Predicting biodegradation. *Environmental Microbiology* **1,** 119–124.

Wackett L.P., Sadowsky M.J., Newman L.M., Hur H.G. and Li S. 1994. Metabolism of polyhalgonated compounds by a genetically engineered bacterium. *Nature* **368,** 627-629.

Wang X., Guo X., Yang Y., Tao S. and Xing B. 2011. Sorption mechanisms of phenanthrene, lindane, and atrazine with various humic acid fractions from a single soil sample. *Environmental Science and Technology* **45,** 2124–2130.

Wang Y., Suidan M.T., Pfeffer J.T. and Najm I. 1988. Effect of some alkyl on methanogenic degradation of phenol. *Applied and Environmental Microbiology* **54,** 1277–1279.

Watson M.D., Fechtenkotter A. and Mullen K. 2001. Big is beautiful - aromaticity revisited from the viewpoint of macromolecular and supramolecular benzene chemistry. *Chemical Review* **101,** 1267–1300.

White T.J., Bruns T., Lee S. and Taylor J. 1990. Amplification and direct sequencing of fungal ribosomal RNA genes for phylogenetics. In: Innis M. A., Gelfand D.H., Sninsky J.J. and White T.J. (eds), PCR protocols: a guide to methods and applications. *Academic Press*. San Diego. 315–322.

World Health Organization & International Programme on Chemical Safety. 1994. Phenol: health and safety guide. *World Health Organization*: Geneva.

Wright J.D. 1993. Fungal degradation of benzoic acid and related compounds. *World Journal of Microbiology and Biotechnology* **9,** 9–16.

Wu C.H., Liu X., Wei D., Fan J. and Wang L. 2001. Photochemical degradation of phenol in water. *Water Research* **35,** 3927–3938.

Wu R.S.S., Richardson B.J. and Lam P.K.S. 2000. Chemistry of organic pollutants, including agrochemicals. *Environmental and Ecological Chemistry* **3,** 1–10.

Yang H.M. and Li C.C. 2006. Kinetics for synthesizing benzyl salicylate by third-liquid phase-transfer catalysis. *Journal of Molecular Catalysis A: Chemical* **246,** 255–262.

Ying G. and Kookana R. 2003. Degradation of five selected endocrine-disrupting chemicals in seawater and marine sediment. *Environmental Science Technology* **37,** 1256–1260.

Zepp R.G. and Schlotzhauer P.F. 1983. Influence of algae on photolysis rates of chemicals in water, *Environmental Science and Technology* **17,** 462–473.

Zhang T., Wang N., Liu H., Zhang Y. and Yu L. 2016. Soil pH is a key determinant of soil fungal community composition in the Ny-Alesund region, Svalbard (High Artic). *Frontiers in Microbiology* **7**, 227–238.

Zhanga Z., Jia C., Hua Y., Suna L., Jiao J., Zhaoa L., Zhuc D., Li J., TiancnY., Baic H., Li R. and Hua J. 2012. The estrogenic potential of salicylate esters and their possible risks in foods and cosmetics. *Toxicology Letters* **209,** 146–153.

APPENDIX A

Appendix I: Contig sequence (563 bases) for strain VM1 ITS1-5.8S rRNA-ITS2 region

5′-TGATATGCTTAAGTTCAGCGGGTATTCCTACCTGATCCGAGGTCAACATTCAGAAGTTG
GGGGTTTAACGGCTTGGCCGCGCCGCGTACCAGTTGCGAGGGTTTTACTACTACGCAATGGA
AGCTGCAGCGAGACCGCCACTGTATTTCGGGGCCGGCTTGCCGTGAGGCTCGCCGATCCCCA
ACACCAAACCCGGGGGCTTGAGGGTTGAAATGACGCTCGAACAGGCATGCCCGCCAGAATAC
TGGCGGGCGCAATGTGCGTTCAAAGATTCGATGATTCACTGAATTCTGCAATTCACATTACT
TATCGCATTTTGCTGCGTTCTTCATCGATGCCAGAACCAAGAGATCCGTTGTTGAAAGTTTT
GATTTATTTATGGTTTTACTCAGAAGTTACATATAGAAACAGAGTTTAGGGGTCCTCTGGCG
GGCCGTTCCGTTTTACCGGGAGCGGGCTGATCCGCCGAGGCAACAATTGGTATGTTCACAGG
GGTTTGGGAGTTGTAAACTCGGTAATGATCCCTCCGCTGGTTCACCAACGGAGACCTTGTTA
CGACTTTT-3′

Appendix II: Contig sequence (521 bases) for strain VM2 ITS1-5.8S rRNA-ITS2 region

5′-TTGGAAGTAAAAGTCGTAACAAGGTTTCCGTAGGTGACCCTGCGGAAGGATCATTAGTG
AATTGCTCTCTGAACGTTAACGATATCCATCTACACCTGTGAACTGTTGATAGACTTCGGTC
AGTTACTTTTACAAACATTGTGTAATGAACGTCATGTTATTATAACAAAAATAACTTTCAAC
AACGGATCTCTTGGCTCTCGCATCGATGAAGAACGCAGCGAAATGCGATAAGTAATGTGAAT
TGCAGAATTCAGTGAATCATCGAATCTTTGAACGCAACTTGCGCTCTCTGGTATTCCGGAGA
GCATGCCTGTTTGAGTATCATGAAATCTCAACCATTAGGGTTTCTTAATGGCTCGGATTTGA
GTGATGGCAGTTCGCCTGCCTCGCTTTAAAAGAGTTAGCGTGTTTAACTTGTCGATCTGGCG
TAATAAGTTTCGCTGGTGTAGACTTGGGAAGTGCGCTTCTAATCGTCTTCGGACAATTCTGA
ACTCTGTCTCAATCCAGTTAGGACACAG-3′

Appendix III: Calibration curve for protein concentration

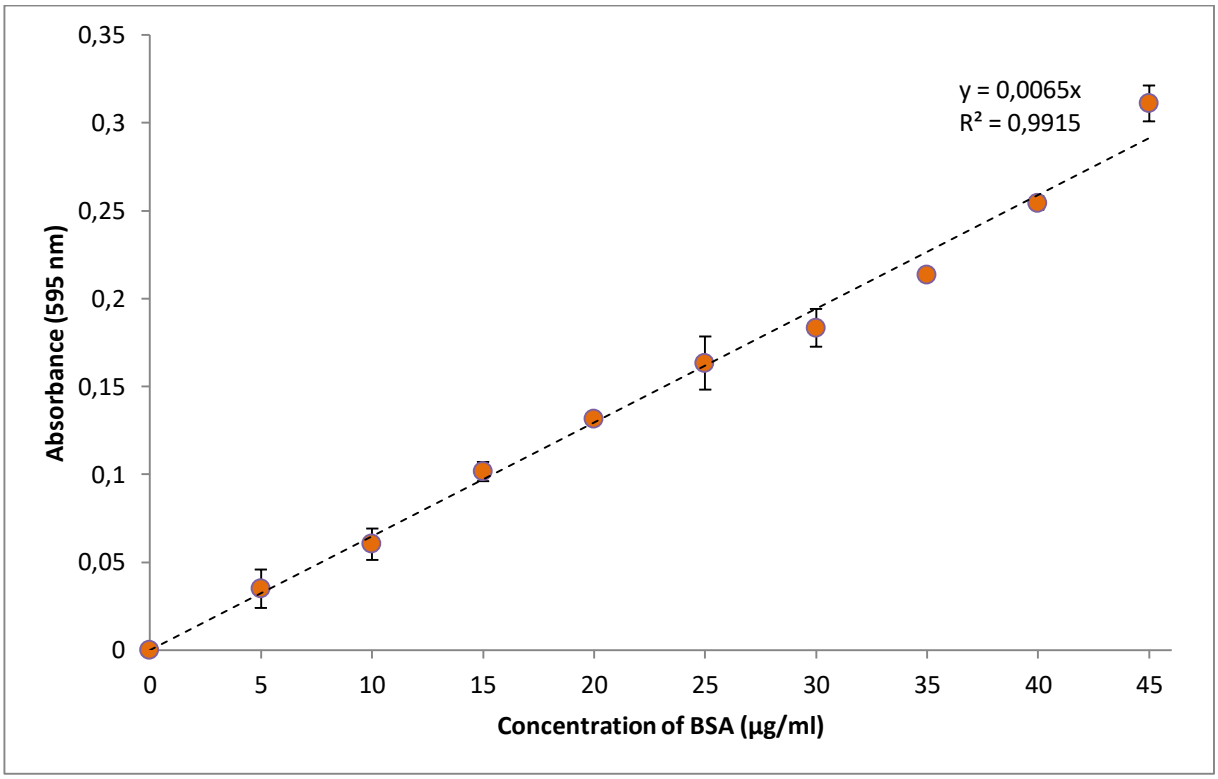

Figure A1: Standard curve for the quantification of protein in crude extracts using Bovine Serum Albumin in 20 mM phosphate buffer (pH 7.4) at 595nm.